

THE ROLE OF IRON OXYHYDROXIDES IN PHOSPHORUS CHEMISTRY  
OF SOME EAST TEXAS FOREST SOILS

A Dissertation

by

AMIR HASS

Submitted to the Office of Graduate Studies of  
Texas A&M University  
in partial fulfillment of the requirements for the degree of

DOCTOR OF PHILOSOPHY

August 2005

Major Subject: Forestry

THE ROLE OF IRON OXYHYDROXIDES IN PHOSPHORUS CHEMISTRY  
OF SOME EAST TEXAS FOREST SOILS

A Dissertation

by

AMIR HASS

Submitted to the Office of Graduate Studies of  
Texas A&M University  
in partial fulfillment of the requirements for the degree of

DOCTOR OF PHILOSOPHY

Approved by:

Chair of Committee, Michael G. Messina

Committee Members, Richard F. Fisher

Frank M. Hons

Richard H. Loeppert, Jr.

Charles T. Smith, Jr.

Head of Department, Charles T. Smith, Jr.

August 2005

Major Subject: Forestry

## ABSTRACT

The Role of Iron Oxyhydroxides in Phosphorus Chemistry of Some East Texas Forest  
Soils. (August 2005)

Amir Hass, B.S., The Hebrew University of Jerusalem;

M.S., The Hebrew University of Jerusalem

Chair of Advisory Committee: Dr. Michael G. Messina

Forest soil phosphorus (P) chemical behavior was evaluated in some mid-rotation fertilized loblolly pine (*Pinus taeda* L.) plantations in East Texas, that differed in their site drainage characteristics. Forest floor mass and carbon content in the forest floor were determined. Total P ( $P_T$ ) in the forest floor, and total and Mehlich-1 P and citrate-dithionite (CD) and acid ammonium-oxalate (AAO) extractable P, Al, Fe, and Mn within the mineral soil upper 100 cm were determined. Colorimetric determination of AAO- and CD-extractable P by the molybdenum blue ascorbic acid method, without the use of pre-digestion, was assessed by an automated continuous flow injection system. Phosphorus distribution between different operationally defined solid phases and its relationships with CD and AAO extractable Mn, Al, Fe among depth, site, drainage class and treatment were evaluated. Soil P forms were highly correlated with iron oxides across sites, drainage classes, treatments, and depth intervals with significant differences in P content and distribution in the soil profile and solid phases among drainage classes. Soil P distribution patterns differed among drainage classes, yet it followed the distribution of the iron oxides. Iron oxide's role as a sink for soil P was higher in the well-drained compared to the poorly drained sites. Amorphous phases of iron oxides were higher in the poorly drained sites and dominated the role of iron oxides as a sink for P under the poor drainage conditions. Fertilization resulted in significantly higher forest floor mass, P content in the forest floor, and total P ( $P_T$ ) and CD-extractable P ( $P_d$ ) in the soils' upper 10 cm. The treatment effect on P in the forest floor, and on  $P_T$  and  $P_d$  in the upper 10 cm of the mineral soil was equivalent to 6, 19, and 11% of the applied P,

respectively. AAO-extractable P was highly correlated with Mehlich-1 P in the fertilized plots. Treatment and site drainage class effects on P accumulation in the different solid phases in the mineral soil and in the forest floor and the potential contribution of these pools to P availability in subsequent rotations, following clearcutting, are discussed.

## DEDICATION

To my father, Uzi Hass

## ACKNOWLEDGEMENTS

I would like to thank my major advisor, Dr. Mike Messina, and our lab manager, Mr. Tim Rogers, for providing me with a very challenging working environment. Many thanks to Dr. Richard Loeppert for enabling me to use his lab to conduct some of my experiments.

I also would like to thank Dr. Frank Hons, Dr. Richard Fisher and Dr. Tat Smith for serving on my advisory committee and for their contribution to my dissertation.

I am mostly grateful to my wife, Pnina, and my sons, Bar and Rotem. This work, as most of my life aspects, could not be accomplished without Pnina's emotional, spiritual, mental, and practical and physical support, or without the joy and strength I gain from her companionship.

## TABLE OF CONTENTS

	Page
INTRODUCTION.....	1
COLORIMETRIC DETERMINATION OF SOIL PHOSPHATE IN ACID AMMONIUM-OXALATE AND CITRATE-DITHIONITE SOIL EXTRACTS WITHOUT PREDIGESTION STEP .....	4
Overview .....	4
Introduction .....	5
Materials and Methods.....	7
Soil and standard reference material .....	7
Phosphorus determination .....	9
Citrate-Dithionite (CD) extraction .....	9
Effect of CD background solution on P color reaction (peak) development .....	10
Analytical performance .....	10
Accuracy and precision .....	10
Minimum Detection Limit (MDL) .....	11
Acid Ammonium-Oxalate (AAO) extraction.....	11
Effect of AAO background solution on P color reaction (peak) development .....	11
Analytical performance .....	12
Phosphorus behavior during AAO extraction procedure .....	12
Results .....	13
Citrate dithionite extractable P .....	13
CD background solution influence on the colorimetric reaction development - peak shape .....	13
CD analytical performance.....	16
Acid ammonium-oxalate extractable P .....	17
AAO background solution influence on colorimetric reaction development - peak shape .....	17
AAO analytical performance .....	20
P behavior during AAO extraction.....	21
Discussion .....	24
Conclusions .....	27
PHOSPHORUS DISTRIBUTION IN THE PROFILE OF TWO EAST TEXAS FOREST SOILS OF DIFFERENT SITE DRAINAGE CHARACTERISTICS .....	28
Overview .....	28
Introduction .....	29
Materials and Methods.....	30
Study sites .....	30
Soil sampling and handling.....	32

	Page
Chemical and physical analysis .....	33
Statistical analysis .....	34
Results .....	35
Discussion .....	43
Conclusions .....	47
<b>PHOSPHORUS RETENTION IN FERTILIZED FOREST SOILS OF DIFFERENT DRAINAGE CLASSES: THE ROLE OF IRON OXIDES AND THE POTENTIAL INFLUENCE ON PHOSPHORUS AVAILABILITY IN SUBSEQUENT ROTATIONS .....</b>	<b>48</b>
Overview .....	48
Introduction .....	49
Materials and Methods .....	51
Study sites .....	51
Forest floor and mineral soil sampling and preparation .....	51
Soil and forest floor analysis .....	53
Statistical analysis .....	55
Results .....	55
Phosphorus in the mineral soil .....	55
Phosphorus in the forest floor .....	67
Treatment effect on forest floor and on upper 10-cm mineral soil P contents .....	69
Discussion .....	71
Conclusions .....	74
SUMMARY .....	76
REFERENCES .....	78
VITA .....	89



## LIST OF TABLES

	Page
Table 1. Selected properties of the forest soils used in the study.....	8
Table 2. Analytical performance of the continuous flow injection analyzer in the colorimetric determination of citrate-dithionite (CD) extractable P in 4x-diluted aliquots.....	16
Table 3. Analytical performances of the continuous flow injection analyzer in the colorimetric determination of acid ammonium-oxalate (AAO) extractable P in 8x diluted aliquots. ....	21
Table 4. Recovery (%) of phosphorus-spiked acid ammonium-oxalate (AAO) extraction solution during the AAO extraction of San-Joaquin SRM-2709 and the two forest soils used in this study.....	24
Table 5. Selected chemical and physical properties of the soils included in the study.....	31
Table 6. Total P ( $P_T$ ) and citrate-dithionite (subscript d) and acid ammonium-oxalate (subscript ox) extractable Al, Fe, Mn, and P in the soil profile of site 11 and site 33.....	36
Table 7. Relationships between total phosphorus and selected soil properties at sites 11 and 33.....	39
Table 8. Soils taxonomic class, drainage class, and A horizon characteristics in the study sites.....	52
Table 9. Mehlich 1 (M-1) P, total phosphorus ( $P_T$ ) and acid ammonium-oxalate ( $P_{ox}$ ) and citrate dithionite ( $P_d$ ) extractable P (as % of $P_T$ ) in the soil profile of the experimental plots. ....	56
Table 10. Correlation coefficients of analysis between acid ammonium-oxalate extractable P and Mehlich-1 extractable-P in the soil 0-20 cm layers (n=10).....	67
Table 11. Forest floor mass and phosphorus concentration and content in the forest floor in the experimental plots.....	68
Table 12. Fertilization treatment effect on forest floor mass and total phosphorus ( $P_T$ ) content in the forest floor, and on $P_T$ and $P_d$ content in the soil upper 10-cm eight years after application.....	70

## LIST OF FIGURES

	Page
Fig. 1. Phosphorus peaks from standard solutions made in two (A) and four (B) times dilution of citrate-dithionite extraction blanks as background solution, obtained by a continuous Flow Injection Analyzer.....	14
Fig. 2. Three replicate peaks of 0.100, 0.200, and 0.300 mg P L <sup>-1</sup> standard solutions made in background solution of 2x (A) and 10x (B) dilution of acid ammonium-oxalate extraction solution as obtained by the continuous flow injection analyzer .....	18
Fig. 3. SRM-2709, soil 1 and soil 2 acid ammonium-oxalate (AAO) extractable Fe and P at different times during the AAO 120-min extraction procedure .....	22
Fig. 4. Relationships between the acid ammonium-oxalate (AAO) extractable Fe and P in SRM-2709 and the two forest soils used in the study .....	23
Fig. 5. A USA map with the location of study sites 11 and 33 in East Texas (enlarged) .....	32
Fig. 6. Representative core soil profile (0-100 cm) from site 11 (A) and site 33 (B).....	35
Fig. 7. Distribution of citrate-dithionite (CD) extractable iron (Fe <sub>d</sub> ), acid ammonium-oxalate (AAO) extractable phosphorus (P <sub>ox</sub> ), P associated with crystalline iron oxides (P <sub>d-ox</sub> ), organic P (P <sub>T-d</sub> ), and clay content in the soil profile of site 11 (A) and site 33 (B) .....	37
Fig. 8. Relationships between total phosphorus and citrate-dithionite extractable iron (Fe <sub>d</sub> ), aluminum (Al <sub>d</sub> ), and manganese (Mn <sub>d</sub> ) on sites 11 and 33 .....	38
Fig. 9. Relationships between total phosphorus and acid ammonium-oxalate extractable iron (Fe <sub>ox</sub> ) and aluminum (Al <sub>ox</sub> ) on site 11 and site 33 .....	40
Fig. 10. Relationships between citrate-dithionite extractable phosphorus (P <sub>d</sub> ) and iron (Fe <sub>d</sub> ) in the soils of sites 11 and 33. Data from all depth intervals are included. ....	41
Fig. 11. Distributions of the mole ratio (P <sub>d</sub> /Fe <sub>d</sub> ) between citrate-dithionite extractable phosphorus (P <sub>d</sub> ) and iron (Fe <sub>d</sub> ) in the soil profile of sites 11 and 33 .....	42
Fig. 12. Distributions of the Fe <sub>ox</sub> /Fe <sub>d</sub> and of P <sub>ox</sub> /P <sub>d</sub> ratios in the soils profiles .....	42
Fig. 13. Phosphorus (P) distribution in the profiles of the different experimental plots .....	58
Fig. 14. Distribution of total phosphorus (P <sub>T</sub> ) and P <sub>d</sub> /P <sub>T</sub> ratio in the control plots (Cont) and P-fertilized plots (Fert) in the soil profile in site 20 and site 9 .....	60

	Page
Fig. 15. Distribution of % clay and % base saturation (base sat.) in the soil profile in site 20 and site 9.....	61
Fig. 16. Citrate-dithionite extractable P ( $P_d$ ) distribution in the profile of soil from different drainage classes .....	63
Fig. 17. Distribution of citrate-dithionite extractable phosphorus ( $P_d$ ) in site 22 and site 11, well-drained site with high clay and iron oxide contents .....	64
Fig. 18. Relationships of total phosphorus ( $P_T$ ) and citrate-dithionite (CD) extractable P ( $P_d$ ) with CD extractable iron ( $Fe_d$ ), (A and C, respectively) and with aluminum ( $Al_d$ ), (B, and D, respectively) .....	65
Fig. 19. Relationships of total phosphorus ( $P_T$ ) and acid ammonium-oxalate (AAO) extractable P ( $P_{ox}$ ), with AAO extractable iron ( $Fe_{ox}$ ), (A and C, respectively) and with AAO extractable aluminum ( $Al_{ox}$ ), (B and D).....	66
Fig. 20. Average phosphorus (P) concentration (A) and content (B) in the forest floor of the control and the fertilized plots (n=7).....	68

## INTRODUCTION

Most (75 %) pine stands in the southeastern USA grow on highly weathered, nutrient-deficient Ultisols (Miller, 1983; Schultz, 1997; Walker and Oswald, 2000). Intensive forest management practices, such as fertilization, mechanical site preparation, and herbicide application have been shown to increase stand productivity (Jokela et al., 2004; Albaugh et al., 2004; Sayer et al. 2004). Fertilization, mainly with nitrogen (N) and phosphorus (P) has become a common practice in the region (Wells and Allen, 1985; Jokela et al., 1988; Nyland, 1996; Ngono and Fisher, 2001). Phosphorus, primarily as superphosphate, triple superphosphate (TSP) or diammonium phosphate, is usually applied at stand establishment at a rate of 50-100 kg P ha<sup>-1</sup> (Ballard, 1980; Comerford et al., 1983; Binkley, 1986).

Site fertility, expressed as site index (SI), is closely related to depth to the subsoil diagnostic horizon, subsoil characteristics (mostly physical), drainage conditions, and annual precipitation (Coile, 1952; Ralston, 1964; Covell and McClurkin, 1967; Carmean, 1975; Schonau, 1988; Louw and Scholes, 2002; Sanchez-Rodrigues et al., 2002). Soil moisture content, besides its physiological functions, seems to control the effective rooting volume of soil, and the soil resources that are available for tree roots (Coile, 1952; Pritchett, 1979; Stone and Kalisz, 1991; Barnes et al., 1998). Similarly to SI, stand response to P fertilization is inversely related to site drainage conditions, with better response on sites with poorer drainage (Wells et al., 1973; Kushla and Fisher, 1980; Jokela et al., 1988; Jokela and Long, 2000). Borders and Bailey (2001) recently showed N and P fertilization and herbicide application to increase loblolly pine (*Pinus taeda* L.) productivity in Georgia by up to three-fold, where the highest results were obtained on a poorly drained site. Furthermore, P fertilization was shown to have a

---

This dissertation follows the style of Soil Science Society of America Journal.

positive residual effect on subsequent rotations (Gentle et al., 1986; Gresham, 2002; Turner et al., 2002). Turner et al. (2002) found P fertilization to positively influence stand growth in the next two consecutive rotations. Higher growth response to fertilization was evident 50 years after application.

Fertilization was also found to affect forest floor litter dynamics. Increases in litter mass and in its N and P content after fertilization were observed (Wienand and Stock, 1995; Comerford et al., 2002; Butnor et al., 2003; Franklin et al., 2003). An increase in litterfall and a decrease in litter decomposition are the two main mechanisms that accounted for the observed differences, with the former being more dominant early in the rotation (Wienand and Stock, 1995; Franklin et al., 2003). Based on nutrient release dynamics from the litter, the mineral soil, rather than the decomposed organic matter, was suggested as the main source for plant-available N and P at mid-rotation (Gurlevik et al., 2003). The accumulation of litter mass and its P content, with concurrently decreasing decomposition rates after P fertilization, was suggested to further intensify environmental problems of P accumulation in forest floor (Wienand and Stock, 1995). However, the accumulated litter P in fertilized stands was suggested to account for the residual effect of P fertilization in subsequent rotations (Polglase et al., 1992; Comerford et al., 2002).

Free iron oxyhydroxides and organic matter are two major soil components in Ultisols that seem to contribute to soil chemical characteristics (Juo, 1980; Parfitt, 1980; USDA Soil Conservation Service, 1983; Fisher and Binkley, 2000). These two soil components also interact with each other, mutually affecting their respective stabilities and chemical characteristics (Martin and Haider, 1986; Schwertmann, 1988; Oades, 1989). High temperatures and soil moisture content, high content of decomposable organic matter, and low pH all favor reducing conditions (Liu et al., 1997). Such conditions inhibit the formation of stable oxides and result in high proportion of amorphous oxides (Ponnamperuma, 1972; Sanyal and De Datta, 1991). Crystalline and amorphous oxyhydroxides, respectively, tend to have 10 and 100 times more P sorption capacity than the 1:1 clay minerals (mainly kaolinite) that dominate Ultisols (Fox, 1980).

However, the newly formed soil oxyhydroxides are more susceptible to the frequent reducing conditions that prevail under waterlogged conditions. Under such conditions, redissolution of the oxyhydroxides will occur which would release the P retained via adsorption and co-precipitation. The alternating reducing-oxidizing conditions result in discontinuance of mineral aging, in a high proportion of reactive amorphous oxides and increased concentrations of plant-available P (McKee, 1970; Simonson, 1970; Ponnampetuma, 1972; Breemen, 1988a; Lindsay et al., 1989; Sanyal and De Datta, 1991; Willett, 1989). Hence, the positive growth response to P fertilizer on poorly drained soils as opposed to the moderate to no response on well-drained soils (Wells et al., 1973; Kushla and Fisher, 1980; Pritchett and Comerford, 1982) might be related to the influence of the drainage conditions on the chemistry of both indigenous and applied P, mainly through the changes in oxide mineralogy induced by the alternating reducing environment. Furthermore, a buildup of P associated with iron oxides during the rotation and the subsequent alternation of the site moisture characteristics in the first few years following clearcutting may result in P chemical redistribution to more plant-available forms. This may contribute to the P fertilization residual effects in subsequent rotations.

Following this hypothesis, the main goal of my work is to study the relationships between P and oxyhydroxides in loblolly pine forest soils in East Texas. The first section of this dissertation explores and evaluates the methodology for the colorimetric determination of the citrate-dithionite and acid-ammonium-oxalate extractable inorganic P; the second section discusses P distribution in the soil profile and between solid phases of two East Texas forest soils of contrasting drainage conditions; the following section discusses the role of iron oxide in P retention in some P-fertilized East Texas forest soils and its potential influence on available P in subsequent rotations.

COLORIMETRIC DETERMINATION OF SOIL PHOSPHATE IN ACID  
AMMONIUM-OXALATE AND CITRATE-DITHIONITE SOIL EXTRACTS  
WITHOUT THE PREDIGESTION STEP

### Overview

Colorimetric determination of soil phosphorus (P) extracted without digestion by the acid ammonium-oxalate and citrate-dithionite procedures was evaluated by the molybdenum blue ascorbic acid method in an automated continuous flow injection system. Speciation of the inorganic and organic forms of the extractable P is vital information, yet is lost by the predigestion procedure commonly used prior to the colorimetric reaction to overcome oxalate and citrate interferences. In this study the analytical performance of the colorimetric method in the presence of oxalate and citrate was assessed using non-digested blanks and soil extracts at a wide range of dilution rates. The acid ammonium-oxalate extraction procedure for soil P was also evaluated with respect to P solubility and possible resorption during the extraction. Four and eight times dilution of the citrate-dithionite and the acid ammonium-oxalate extracts, respectively, were needed to produce smooth bell-shaped peaks during the colorimetric reaction. The above dilution rates result in 51 and 34  $\mu\text{M}$  citrate and oxalate in the analytes, respectively. High precision of  $1.7 \pm 1.3$  and  $2.9 \pm 3.7$  %, and recoveries of  $105.7 \pm 1.0$  and  $99.8 \pm 3.8$  % for spiked samples, were found in the citrate-dithionite and the acid ammonium-oxalate extractions, respectively. Phosphorus minimum detection limits (MDL) were determined to be  $8.6 \mu\text{g L}^{-1}$ , and  $2.3 \mu\text{g L}^{-1}$ , respectively. Considering the dilution factors and the solution:soil ratios, the above MDL results in MDL of  $6.9 \text{ mg P kg}^{-1}$  and  $1.1 \text{ mg P kg}^{-1}$  soil in the citrate-dithionite and the acid ammonium-oxalate extraction procedure, respectively. Phosphorus solubility during the acid ammonium-oxalate extraction followed the same trend as that of Fe. Spiked

extraction solution showed  $100.8 \pm 1.3$  % recovery, implying that no sorption (and hence resorption) occurred during the extraction. The ability to differentiate between organic and inorganic species, in the above selective extractions for soil iron oxides, enabled a more detailed insight into the complex relationships of soil P within the Al and Fe organo-mineral complex in soil environments.

## **Introduction**

Phosphorus is an important element in both terrestrial and estuarial environments. It can be limiting in both agricultural and natural ecosystems, yet pose a threat to nutrient balance in water bodies, mainly from runoff from intensively managed agricultural systems, grazed areas, and organic waste disposal watersheds (Sharpley et al., 2003; Condon, 2004). Soil P availability for plant uptake and for lateral or vertical movement in the soil is dictated by its composition and its chemical interaction within the soil solid and liquid phases. Hence, understanding P chemistry in the soil environment is essential in predicting and controlling human influences on P in terrestrial and estuarial environments.

Minerals of iron oxides have marked effects on the behavior of native and applied P in soil (Barberis et al., 1996; Torrent, 1997). Stability of the iron oxide minerals, their occurrence, and physico-chemical characteristics depend on the solution composition at the solid-solution interface, especially characteristics such as pH, and dissolved organic acid content and composition (Furrer and Stumm, 1986; Miller et al., 1986; Zinder et al., 1986). Rhizosphere pH manipulation and active exudation of organic acids such as oxalate and citrate are processes used by soil biota in acquiring P (Graustein et al., 1977; Hinsinger, 2001; Miyasaka and Habte, 2001; Ryan et al., 2001; Grierson et al., 2004), and are used in simulating plant availability and mobility of P (Geelhoed et al., 1999; Drouillon and Merckx, 2003). The fact that iron oxides are an important pool of soil P and are sensitive to rhizosphere environmental changes (e.g., pH, organic anion) induced by biota suggests that these minerals play an important role in controlling soil P mobility and availability. Hence, the use of selective extractions for iron oxide minerals will help characterize the drivers and mechanisms controlling soil P



behavior. Guo and Yost (1999) showed that acid ammonium-oxalate extraction, a well-established extraction procedure for characterizing the amorphous phases of iron oxides (Schwertmann, 1973; Loeppert and Inskeep, 1996), successfully characterized the available P pool in weathered soils. The acidity and composition of acid ammonium-oxalate makes it useful for mimicking rhizosphere processes, identifying the available P pool, and in identifying the solid phase from which P is released in weathered soils. Yet, the presence of the organic anion (i.e., oxalate) in the acid ammonium-oxalate extraction solution poses analytical difficulties when determining P, and more so when trying to differentiate between the two important extractable species; i.e., inorganic and organic P. Since plants take up P in its inorganic form, such a distinction is desirable.

The “molybdenum blue” method (Murphy and Riley, 1962) is an accepted (Zimmermann and Keefe, 1997) and widely used method for determining P in water samples. With this method, orthophosphate is detected through its complexation with molybdate and subsequent reduction of the phosphomolybdate complex, mostly in the presence of ascorbic acid, to produce the spectrophotometrically detectable “molybdenum blue”, at wavelengths of 660 or 880 nm. The selectivity of the method for the inorganic form enables a distinction between the organic and inorganic soluble P by analyzing a non-digested (for inorganic form) and a digested sample (for total P), usually by persulfate digestion (Standard Methods, 1995a). The difference between the two values is the organic P.

Organic acids interfere with the color development reaction in the molybdenum blue method. Organic anions, such as oxalate and citrate are components of most iron oxide selective-extraction procedures; i.e., oxalate in the acid ammonium-oxalate method for amorphous iron oxide phases, and citrate in the citrate (bicarbonate) dithionite method for total soil iron oxides (Mehra and Jackson, 1960; Parfitt and Childs, 1988; Loeppert and Inskeep, 1996). Oxalate, for example, is known to destroy the phosphomolybdic complex and as such is used in determining silica (Si) in water (Campbell and Thomas, 1970). To overcome the organic anion interference in the development of the colorimetric reaction, in the aforementioned methods, an increase in

molybdate concentration (Owens et al., 1977; Wolf and Baker, 1990; Ruiz et al., 1997; Drouillon and Merckx, 2003), predigestion of the dissolved organic materials by dry combustion (Guo and Yost, 1999), wet digestion by peroxide (Chang and Jackson 1957) or persulfate (Bowman et. al., 1998), mixture of strong acids (i.e.-  $\text{H}_2\text{SO}_4$ ,  $\text{HClO}_4$  and  $\text{HNO}_3$ ; Zhang et al., 2003) and dilution of the extract solution (Yuan and Lavkulich, 1995) have been employed. Alternatively, the acid ammonium-oxalate extractable P could be determined with an ICP (Pautler and Sims, 2000; Sims et al., 2002; D'Angelo et al., 2003; Koopmans et al., 2004), which is inherently incapable of differentiating between different soluble species of the element.

Sample predigestion, although overcoming the organic anion interferences, converts all soluble P into inorganic form in the process, resulting in loss of vital information about P speciation into organic and inorganic forms. Furthermore, the sensitivity of the molybdenum blue method to reactant stoichiometry, the medium pH, color developers, and P concentrations (Fiske and Subbarow, 1925; Jackson, 1958; Towns, 1986; Broberg and Pettersson, 1988; McKelvie et al., 1995) subject any manipulation of the reaction conditions to possible analytical problems.

This study examined the performance of the acid ammonium-oxalate extraction for extracting soil P. The analytical performance of molybdenum blue, by the ascorbic acid method was also evaluated in detecting acid ammonium-oxalate and citrate dithionite extractable P using a continuous flow injection system and applied minimal manipulations of the analytical procedure.

## **Materials and Methods**

### Soil and standard reference material

National Institute of Standards and Technology (NIST) Standard Reference Material (SRM) 2709 - San Joaquin soil (Abruptic Durixeralf) and two East Texas forest soils differing markedly in their moisture regime and content of total P and iron oxides were used in this study (Table 1). About 1.5-kg composited samples of the upper 10 cm of two forest soils were collected during January 2004. The samples were air dried and ground to pass a 2-mm sieve. Subsamples were further ground using a porcelain mortar

and pestle to pass a 150- $\mu\text{m}$  sieve. The finely ground samples were stored at 4° C and used later to determine soil carbon (C), citrate-dithionite (CD) and acid ammonium-oxalate (AAO) extractable iron and P, and total P. Soil pH and texture were determined on <2-mm samples.

Table 1. Selected properties of the forest soils used in the study.

Soil	Taxonomic Class	pH	Carbon	Soil Texture			Fe <sub>d</sub> <sup>#</sup>	Fe <sub>ox</sub> <sup>*</sup>	P	
				Sand	Silt	Clay			Total	P <sub>d</sub> <sup>**</sup>
				g kg <sup>-1</sup>					mg kg <sup>-1</sup>	
Soil 1	Typic Hapludults	6.2	28	58	24	18	99193	2024	515	308
Soil 2	Aquic Glossudalfs	5.8	13	63	26	11	1162	467	64	18

<sup>#</sup>citrate-dithionite extractable Fe; <sup>\*</sup> acid ammonium-oxalate extractable Fe; <sup>\*\*</sup> citrate-dithionite extractable P.

Soil pH was measured in distilled water at a 1:2 soil:solution ratio using a combination glass electrode. Soil texture was determined by the hydrometer method (Day, 1965) and soil C by an NC analyzer (Thermo Finnigan, Flash EA 1112 series, Milano, Italy). Total P was determined by the perchloric acid ( $\text{HClO}_4$ ) digestion method following Kuo (1996). A 0.2-g sample (<150  $\mu\text{m}$  seive) was placed in a 75-ml Pyrex tube and predigested overnight at room temperature in a perchloric hood with 2 ml of concentrated  $\text{HNO}_3$ . Subsequently, 3 ml of  $\text{HClO}_4$  were added and the tubes were heated on a digestion block to 130° C until visual organic matter digestion, followed by heating to 203° C until white fumes formed. After cooling to room temperature the solution was adjusted to volume (75 ml) with deionized water (DIW), mixed, and an aliquot taken for analysis. AAO and CD extractions followed the procedures of Loeppert and Inskeep (1996) and are described in detail below. Iron in the CD ( $\text{Fe}_d$ ) and in the AAO ( $\text{Fe}_{ox}$ ) extractions was determined by flame atomic absorbance (flame AA)

(Varian SpectraAA 220 FS, Mulgrave, Victoria Australia) at 248.3 nm wavelength in air/acetylene flame at 0-4 mg Fe L<sup>-1</sup> range using CertiPUR™ 1000 mg Fe L<sup>-1</sup> standard solution (EMD Chemicas Inc., Gibbstown NJ, USA) with the relevant blanks and dilution rates as background for the calibration solution. Total P was determined colorimetrically by the ascorbic acid method using a continuous Flow Injection Analyzer (FIA) as described below. Total P, Fe<sub>d</sub>, Fe<sub>ox</sub> and CD extractable P were determined on the SRM-2709 and were 568±22, 12,726±951, 2,543±25 and 374± 7.3 mg kg<sup>-1</sup>, respectively.

#### Phosphorus determination

Phosphorus was determined by the molybdenum blue ascorbic acid method according to the “Total phosphorus, USEPA by Flow Injection Analysis Cartridge part #A001558” method using an ALPKEM FS3000 continuous flow injection system (OI Analytical, College Station, TX). Analysis involved a sample loop of 200 µl, cycle duration of 90 sec at 37° C, 5-mm path length flowcell, 660-nm optical filter and peak height as a quantitative parameter. Linear standard curves were constructed using blank solutions, at the relevant dilution level, as background solution. A 995-mg P L<sup>-1</sup> stock solution was used for the standards (Phosphorus Atomic Absorption Standard Solution, Sigma-Aldrich, Steinheim, Germany). All glassware was soaked in 20 % HCl for 24 h followed by thorough rinsing with deionized water (DIW) prior to analysis.

#### Citrate-Dithionite (CD) extraction

Three samples of SRM-2709 were extracted using the CD procedure following Loeppert and Inskeep (1996). A 0.25-g sample (<150 µm) was placed in a 50-ml polypropylene centrifuge tube, to which addition of 0.25 g Na-Dithionite (S310, Fisher Scientific, Pittsburgh, PA) and 3.0 g of Na-Citrate (S279, Fisher Scientific, Pittsburgh, PA) was followed by an addition of 15 ml DIW. The tubes were then sealed, hand mixed and placed horizontally on a reciprocating shaker for sixteen hours at 160 cy/min at room temperature. Following the shaking step the solutions were quantitatively transferred to 50-ml volumetric flasks, diluted to volume with DIW, hand mixed, filtered through a paper filter (Q5 Fisher Scientific, Pittsburgh, PA) and left exposed to the

ambient air for about 20 min. Eight blank solutions were made and carried out throughout the extraction procedure. Filtrates were analyzed within 24 h following the extraction. All reagents used were of analytical grade.

#### *Effect of CD background solution on P color reaction (peak) development*

To evaluate the influence of the CD extraction solution on the colorimetric determination of P we used P standard solutions of 0.800, 0.320 and 0.160 mg L<sup>-1</sup> made in 2x dilution of CD blank (corresponding to 0.102 M citrate). Subsequent dilutions were made using DIW to end up with four (4BD), ten (10BD), and a hundred (100BD) times dilutions of the original CD blank (corresponding to 0.051, 0.020 and 0.002 M citrate, respectively). The different standard solutions were then analyzed for P in the FIA and the absorbance peaks were monitored and evaluated.

#### *Analytical performance*

The analytical performance (i.e., accuracy, precision and minimum detection limit) of the ascorbic acid method, using the FIA system to determine P in CD extracting solution was determined using the 4BD; the minimal dilution rate where no interference in the peak bell-shape curve development was noted.

#### *Accuracy and precision*

The extract of each of the three replicates of the SRM-2709 were split in half. One half was diluted four times, the other was spiked with P by adding 2 ml of the subsample to a 15-ml Pyrex tube, to which 6 ml of DIW and 1 ml of 10 mg P L<sup>-1</sup> stock solution (made in 4BD background solution) were added to make a spiked sample with 1.11 mg P L<sup>-1</sup>. All subsamples were thoroughly mixed. Each of the three non-spiked subsamples were read three times and each of the spiked subsamples were read seven times (except SRM-2709-A that was read four times). Accuracy, computed as percent recovery (% R) was evaluated from the recovery of the P-spiked samples and from the standards, measured as unknowns. The higher dilution rate in the spiked sample (2:7) than in the non-spiked sample (2:6) was taken into consideration in the recovery calculations. Precision was evaluated by the percent relative standard deviation (% RSD) computed from the series of measurements for each of the samples and standards.

### *Minimum Detection Limit (MDL)*

Each of the standard solutions (0.400, 0.160, and 0.080 mg P L<sup>-1</sup>) were measured 11 times as unknown and the results were used to determine the MDL using two procedures: a) extrapolation of the linear regression line, obtained by plotting the standard deviation of the standard solutions as a function of its concentration to zero (i.e., the “b” value of the linear regression equation); and b) by multiplying the standard deviation obtained for the 0.080 mg P L<sup>-1</sup> standard solution by the student’s t value (df = 10), at 99 % confidence level ( $t_{10, 0.01} = 2.764$ ) (Zimmermann and Keefe, 1997).

### Acid Ammonium-Oxalate (AAO) extraction

Two replicates of SRM-2709 and of soil 1 and soil 2 were extracted by the AAO method following Loeppert and Inskeep (1996). A 0.25-g sample of <150 µm were placed in a 50-ml polypropylene centrifuge tube to which 15 ml of pH 3.00 AAO extraction solution were added. Tubes were placed in a tube rack, covered and sealed tightly with aluminum foil and placed horizontally on an orbital shaker for two hours at 300 cy/min. Following the shaking step the tubes were centrifuged for 10 min at 10,000 rpm, filtered through 0.2-µm mixed cellulose ester membrane to a 30-ml polypropylene scintillation tube and kept refrigerated for further analysis. The AAO extraction solutions were prepared daily, as described by Loeppert and Inskeep (1996) using analytical-grade reagent. The extraction procedure was done in the dark and all analyses were completed within 24 h following the extraction.

### *Effect of AAO background solution on P color reaction (peak) development*

Standard solutions of 0.100, 0.200, and 0.300 mg P L<sup>-1</sup> were made in background solution of two (2BD), four (4BD) and ten (10BD) times dilution of AAO blank solution in DIW (corresponded to 0.137, 0.069, and 0.027 M oxalate). The standard solutions were then analyzed for P in the FIA and the absorbance peaks were monitored and evaluated. Following evaluation of peaks, a series of 5x, 6x, and 8x dilutions were made and analyzed for peak development to narrow down the dilution factors from 4BD, where interference with peak development was still noticed, and 10BD where peak development was carried out with no interference.

### *Analytical performance*

Analytical performance were assessed on the 8x background dilution (8BD) (corresponding to 0.034 M oxalate).

MDL - twelve runs of 0.048 and two runs of 0.150, 0.100, 0.050, 0.032, and 0.016 mg P L<sup>-1</sup> standard solutions were used to evaluate the method MDL by procedure a. Results for the 0.048 mg P L<sup>-1</sup> 8BD standard solution were used to calculate MDL by procedure b, as described above.

Accuracy (% R) - the soil extracts were split in half. One half was diluted to 8BD with DIW. The other half was spiked with P standard solution (made in DIW background) and brought to 8BD with DIW (1:1:6 ratio of sample: standard: DIW, respectively). Soil 1 was spiked with 1 ml of 2-mg P L<sup>-1</sup> (to end with addition of 0.25 mg P L<sup>-1</sup>). One of the duplicates of Soil 2 was spiked as Soil 1, the other was spiked with 1 ml of 10 mg P L<sup>-1</sup> (to end with 1.25 mg P L<sup>-1</sup>); SRM-2709 extracts were spiked as Soil 2. All samples were analyzed three times. % R was determined based on the recovery of the spiked soil samples and on the recovery of the standards (analyzed as unknown).

Precision (% RSD) was computed from the series of measurements made on the soil extracts and on the standards when run as unknowns.

### *Phosphorus behavior during AAO extraction procedure*

Phosphorus behavior during the two-hour AAO extraction was determined through a kinetic experiment. Duplicates of Soil 1, Soil 2 and SRM-2709 were extracted by AAO at increasing shaking time, from zero to 120 min in 10-min increments. The experiment was conducted in three consecutive batches, extractions of 30-min intervals apart in each, to allow enough time to handle the extract solutions (centrifuge and filtering). Hence, 0, 30, 60, 90, 120-minute shaking times were performed on batch one; 10, 40, 70, and 100-minute shaking times on batch two; 20, 50, 80, and 110-minute shaking times on batch three. Soil 2 was not extracted at time zero. The extract solutions were analyzed for P and Fe. Phosphorus was determined in 8BD by the molybdenum blue ascorbic acid method and iron by flame AA as described above.

To evaluate the possibility of P resorption during the AAO extraction, duplicates of the above soils and SRM were extracted by AAO extraction solution spiked with  $1.2 \text{ mg P L}^{-1}$  and by a non-spiked AAO solution. Resorption was evaluated based on the P recovery of the samples extracted with P-spiked AAO solution.

## Results

Maintaining citrate and oxalate concentration below 51 and 34 mM, respectively, in the analytes resulted in stable development of the colorimetric reaction and in accurate and reproducible determination of AAO- and CD-extractable P analyzed by the molybdenum blue method in an automated continuous FIA system.

### Citrate dithionite extractable P

#### *CD background solution influence on the colorimetric reaction development - peak shape*

The standard solutions at 2BD CD blank as background solution produces disrupted peaks for  $0.320$  (Peaks # 8 and 12), for  $0.800$  (Peaks # 9 and 13), and for  $0.160 \text{ mg P L}^{-1}$  (peak # 11), (Fig. 1A). The colorimetric reaction proceeds as the sample introduced to and from the reaction and the detection medium (front and back tails of the peaks, respectively; Fig. 1A) but collapsed as the bulk of the sample was introduced (the middle section of the peaks; Fig. 1A). The expected peak development (i.e., colorimetric reaction) is illustrated by the dotted line (peak # 8; Fig. 1A). The colorimetric reaction reproduced at the back tailing of the bulk samples, as expressed by the back tail of the expected peaks (Fig. 1A).

Standard solutions at 4BD CD blank as background solution produces distinct smooth bell-shaped peaks for  $0.160$  (Peaks # 8 and 12),  $0.400$  (Peaks # 9 and 13), and  $0.080 \text{ mg P L}^{-1}$  (peak # 11), (Fig. 1B). Peaks for triplicate readings of  $0.040$ ,  $0.160$ , and  $0.080 \text{ mg P L}^{-1}$  in 4BD CD blank are presented in the inset of Fig. 1B (peaks 50-52, 53-



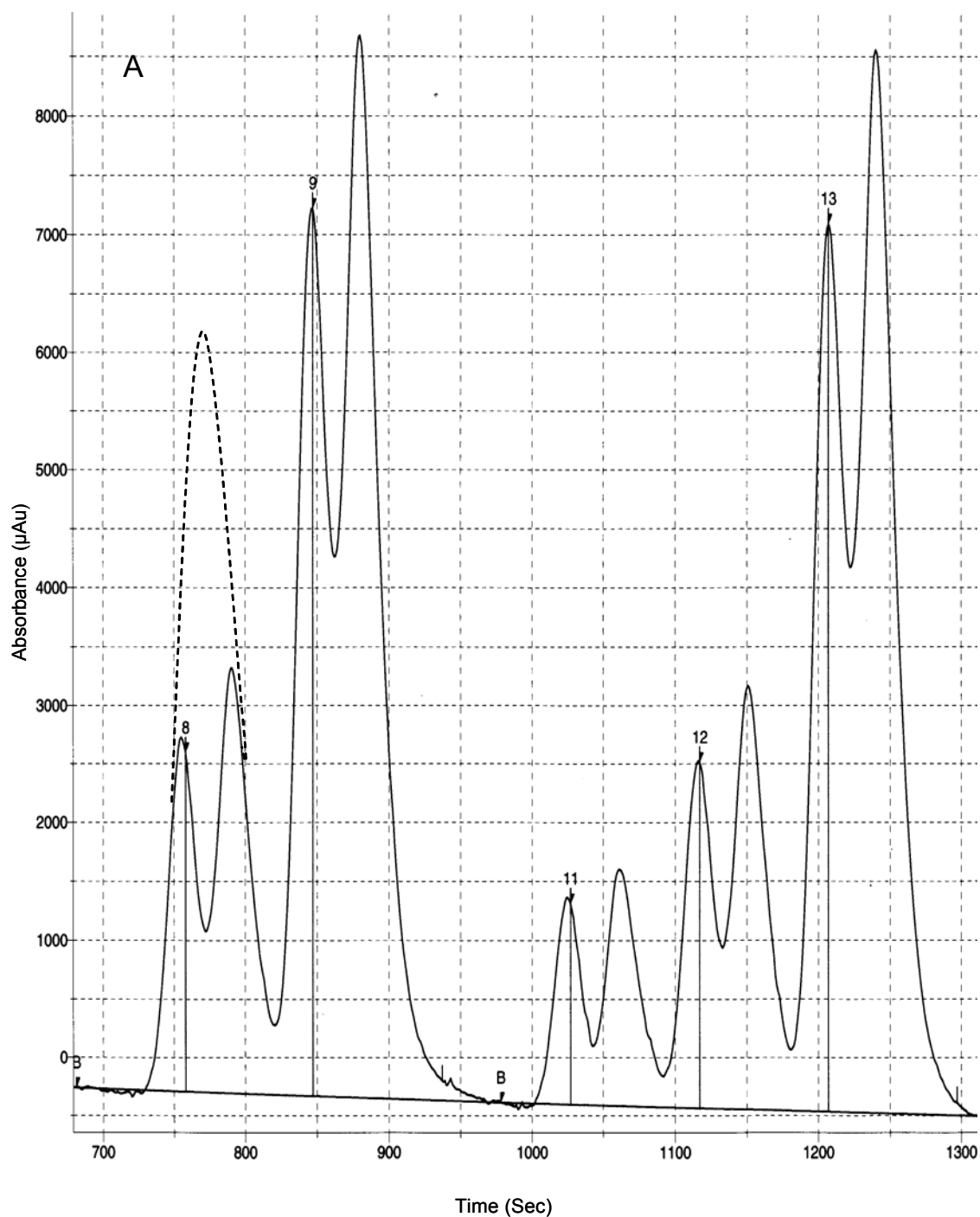


Fig. 1. Phosphorus peaks from standard solutions made in two (A) and four (B) times dilution of citrate-dithionite extraction blanks as background solution, obtained by a continuous flow injection analyzer. An example of expected peaks at the 2x dilution is illustrated by the dotted line (A). In inset: three replicates of 0.080, 0.160, 0.400  $\text{mg P L}^{-1}$  (from left to right) in background of 4x dilution of citrate-dithionite extraction solution.

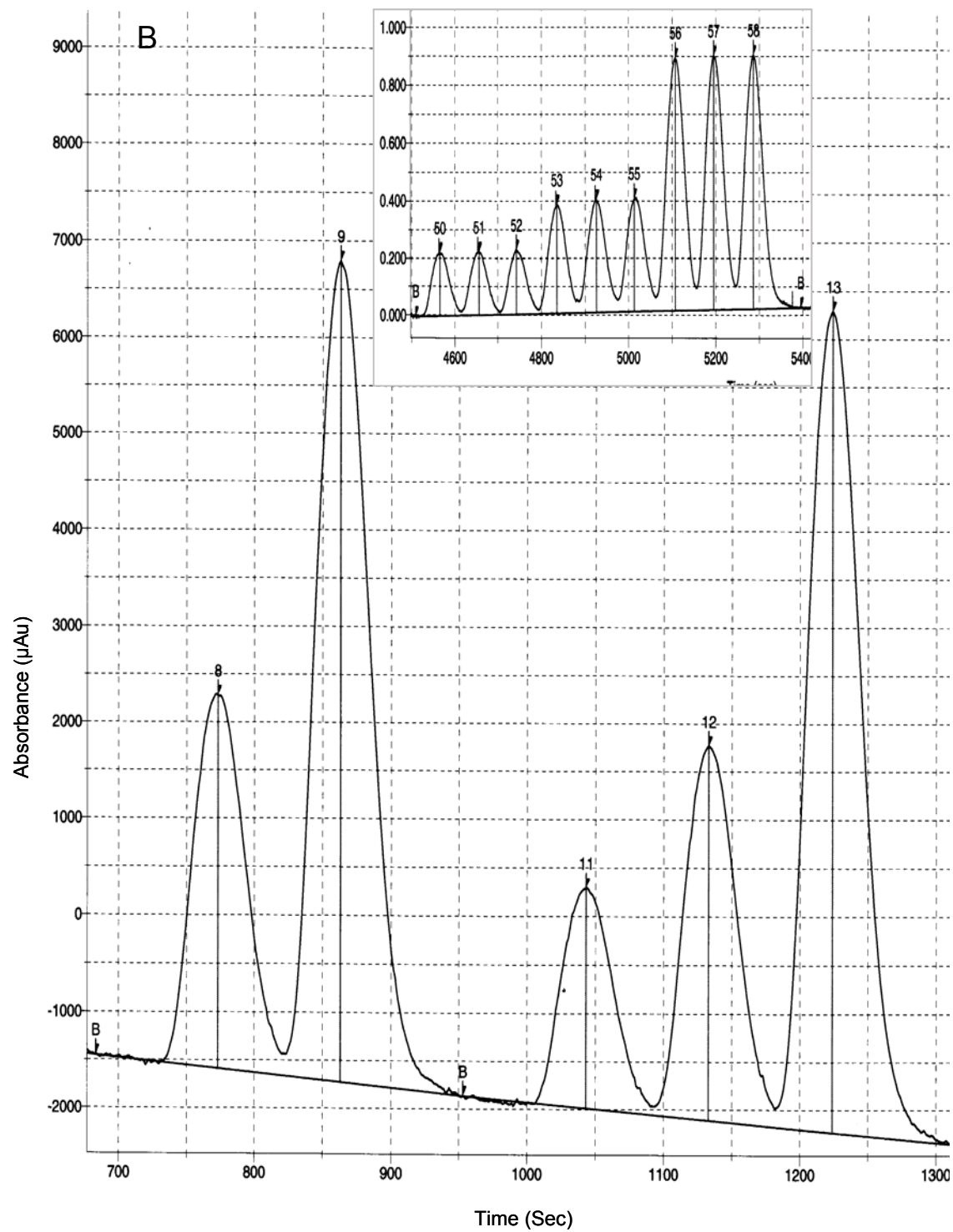


Fig. 1. continued

55, and 56-57, respectively). The smooth bell-shaped peaks obtained at 4x dilution rate indicate smooth and continuous, non-disrupted development of the colorimetric reaction throughout the introduction of the sample in the reaction and detection medium. Citrate concentration in the sample at this dilution rate of the blank CD (4DB) extraction solution corresponded to 0.051 M.

#### *CD analytical performance*

Given the optimal peaks obtained for the P standard solution using the 4BD CD blank the method analytical performance was further investigated using this dilution rate (corresponding to 0.051 M citrate). Analytical performance assessments, % RSD and % R of the standards and spiked SRM-2709, are reported in Table 2.

Table 2. Analytical performance of the continuous flow injection analyzer in the colorimetric determination of citrate-dithionite (CD) extractable P in 4x-diluted aliquots. Results for P standards made in CD blanks background solution (analyzed as unknown) and San-Joaquin SRM-2709 CD spiked extracts (with 1.11 mg P L<sup>-1</sup>) are presented.

Sample	n	P Concentration			% R
		mg L <sup>-1</sup>	% RSD	mg kg <sup>-1</sup>	
		P Standard Solution			
0.080 mg L <sup>-1</sup>	11	0.078	3.97		97.5
0.160 mg L <sup>-1</sup>	11	0.159	3.58		99.7
0.400 mg L <sup>-1</sup>	11	0.403	1.57		100.7
2.000 mg L <sup>-1</sup>	3	2.088	0.30		104.4
SRM-2709					
A	3	0.457	1.04	365.0	
B	3	0.471	0.61	377.1	
C	3	0.474	0.43	379.9	
A spiked	4	1.569	0.64		104.6
B spiked	7	1.595	1.54		105.9
C spiked	7	1.604	1.44		106.5

Average SRM-2709 CD extractable P was  $374.0 \pm 7.3 \text{ mg kg}^{-1}$  with % RSD=1.95 (n= 9). Phosphorus concentration in some of the samples (spiked SRM-2709) exceeded the concentration range used to construct the standard curve, hence  $2.0\text{-mg P L}^{-1}$  standard solution in 4BD was introduced as unknown and read three times to further check the validity of the extrapolation beyond the range of the standards ( $0.08\text{-}0.400 \text{ mg P L}^{-1}$ ). Results for the  $2.0\text{-mg P L}^{-1}$  gave 104.4 % recovery and a % RSD of 0.30 proved to be within the linear dynamic range.

Average % RSD of  $1.65 \pm 1.28 \%$  (0.43 to 1.04 %) and  $3.04 \pm 1.29 \%$  (1.57 to 3.97 %) were found for SRM-2709 and the standards (analyzed as unknowns), respectively. High recoveries (% R) were obtained for the spiked SRM-2709 samples, with an average of  $105.7 \pm 1.0 \%$  (ranging from 105 to 107 %) (Table 2). MDL as determined by the regression line (procedure a) was  $3.3 \text{ } \mu\text{g P L}^{-1}$  ( $Y = 0.0033 + 0.0084X$ ;  $r = 0.81$ ). MDL calculated by the Student's t test (procedure b) was  $8.6 \text{ } \mu\text{g P L}^{-1}$ , using the standard deviation obtained from the eleven runs of  $0.080 \text{ mg-P L}^{-1}$  standard solution (std = 0.0031) and a student's t value of 2.764 (i.e.,  $t_{10, 0.01}$ ). Both calculated MDLs agree with the manufacturer's published value for the above analytical method; i.e.,  $5 \text{ } \mu\text{g P L}^{-1}$  (FS3000 operation manual, Alpkem, OI Analytical). Accounting for the method solution to soil ratio (200), and the pre-analysis dilution factor (4) the resulting detection limit for the method is  $6.88 \text{ mg P kg}^{-1}$ , using the more conservative MDL value ( $8.6 \text{ } \mu\text{g P L}^{-1}$ ).

#### Acid ammonium-oxalate extractable P

##### *AAO background solution influence on colorimetric reaction development - peak shape*

Disrupted peaks were obtained by the continuous FIA for triplicate readings of  $0.100$ ,  $0.200$ , and  $0.300 \text{ mg P L}^{-1}$  standard solutions in 2BD (Fig. 2A) and to a lesser extent at 4BD (data not shown). As with the CD, the colorimetric reaction proceeds as

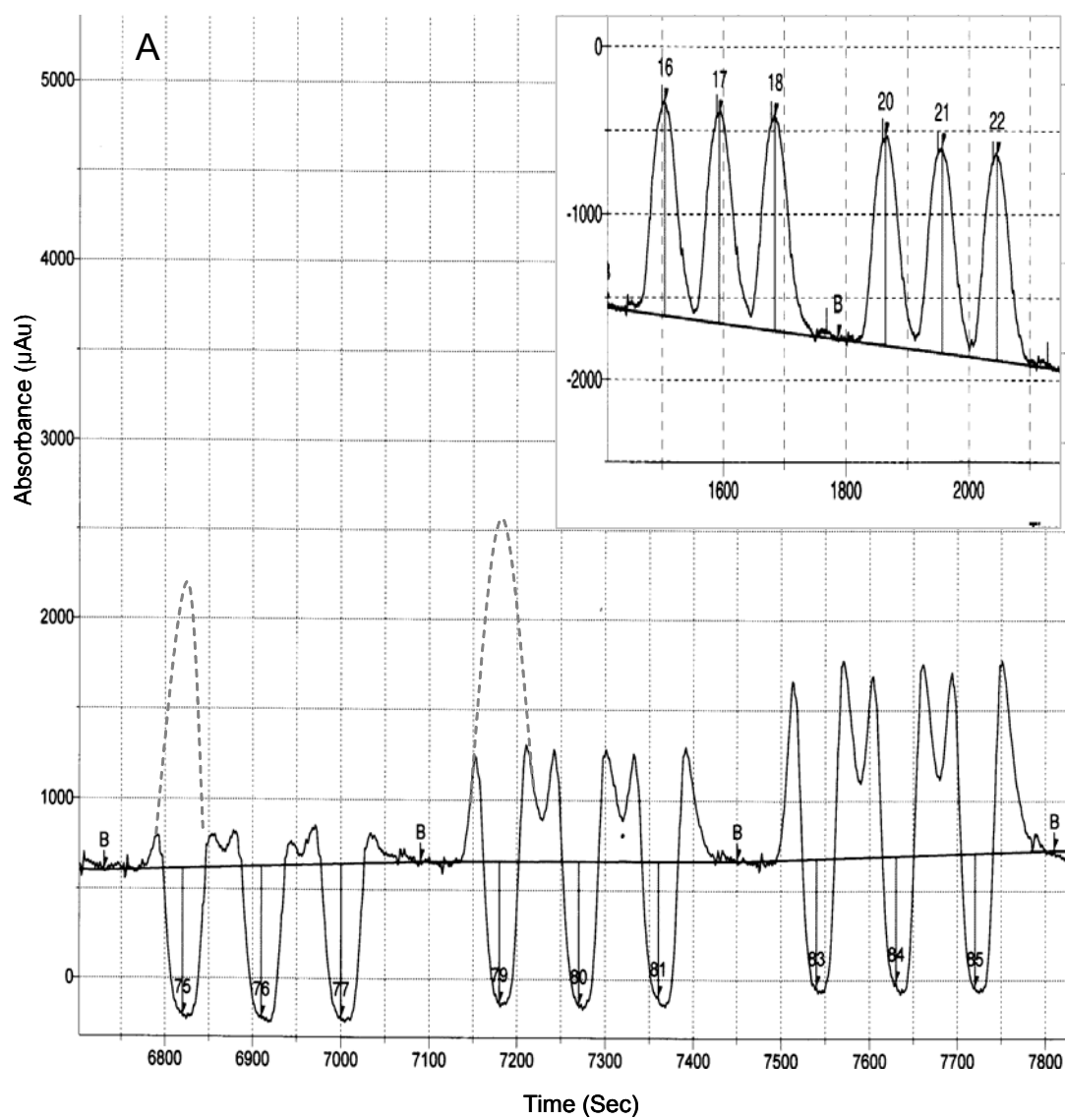


Fig. 2. Three replicate peaks of 0.100, 0.200, and 0.300 mg P L<sup>-1</sup> standard solutions made in background solution of 2x (A) and 10x (B) dilution of acid ammonium-oxalate extraction solution as obtained by the continuous flow injection analyzer. Examples of expected peaks at the 2x dilution are illustrated by the dotted lines (A). In inset are peaks for 0.048 mg P L<sup>-1</sup> at 8x dilution.

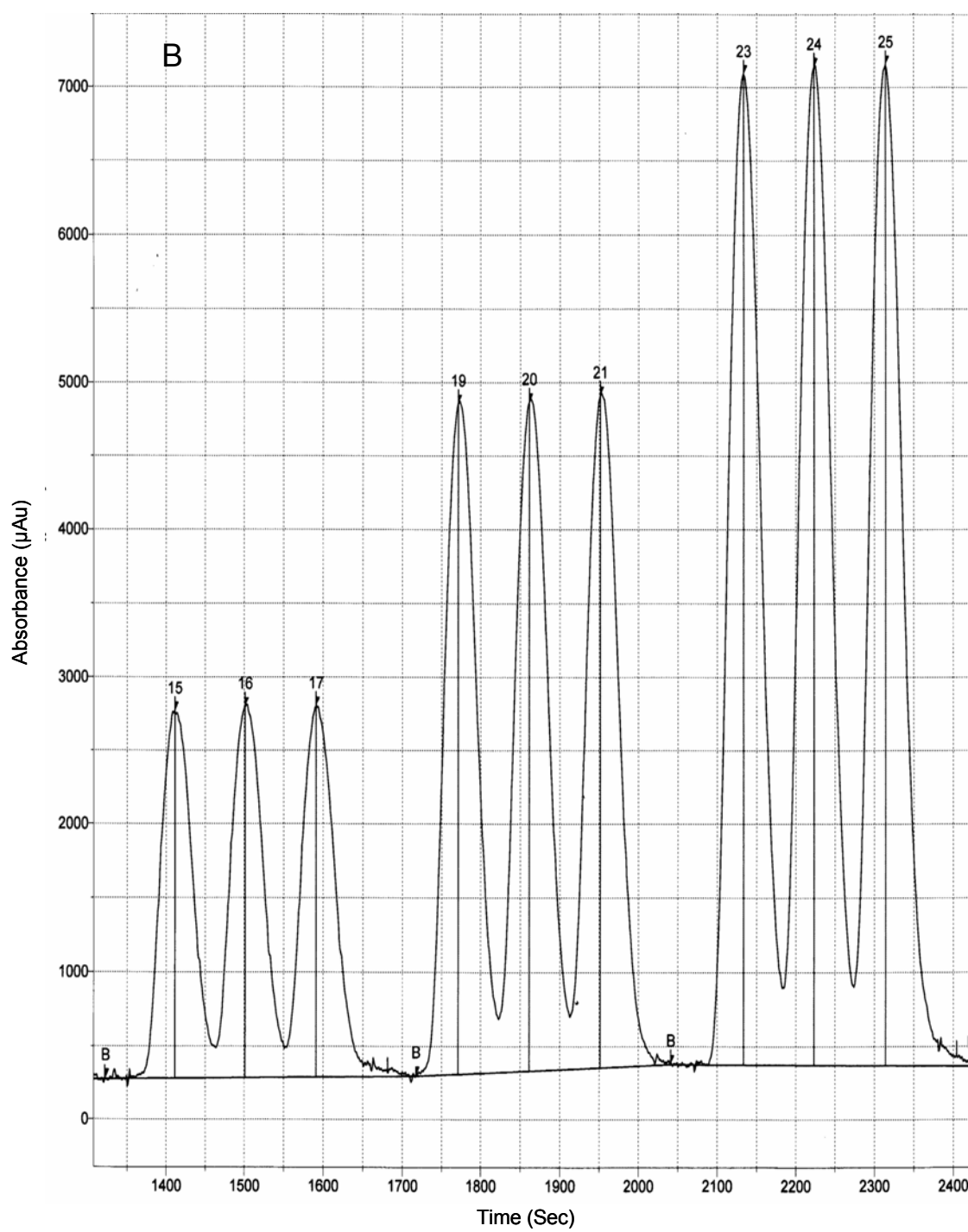


Fig. 2. continued

the sample is introduced to and from the reaction and detection medium, but failed to proceed as the bulk of the sample was introduced (Fig. 2A). The expected peaks are illustrated by the dotted lines (Fig. 2A). At 10BD the colorimetric reaction proceeds with no interference as can be inferred from the smooth bell-shaped peaks obtained at that dilution rate (Fig. 2B). Since 4BD still gave distorted peaks, 5, 6 and 8BD were introduced and analyzed. All three dilution rates produced good peaks. Peaks for  $0.048 \text{ mg P L}^{-1}$  at 8BD are shown in the inset of Fig. 2A.

#### *AAO analytical performance*

The method analytical performance was evaluated on the 8BD of the AAO extracts (corresponding to 0.034 M oxalic acid) (Table 3). Precision (% RSD) ranged from 0.1 to 14.9. The overall % RSD for the soil samples and the standard solutions were  $2.9 \pm 3.7$  (ranged from 0.1 to 10.0) and  $3.4 \pm 5.6$  (ranged from 0.5 to 14.9), respectively. The precision decreased with decreasing P concentration, reaching 14.9 % for  $0.016 \text{ mg P L}^{-1}$  in the standard solution and 10% for the  $0.007 \text{ mg P L}^{-1}$  obtained for soil 2 A (Table 3).

The average accuracy (% R) was  $99.8 \pm 3.8 \%$ , ranging from 95 to 109 % (Table 3). % R for the  $0.048 \text{ mg P L}^{-1}$  standard solution ( $n=12$ ) was  $100.7 \pm 1.7 \%$ , ranging from 98.7 to 103.9 %. Average %R for the spiked soil materials was  $97.4 \pm 1.7 \%$ , ranging from 95 to 99 % (Table 3).

MDL computed according to the linear regression (procedure a), based on all 8BD standards results, was  $0.001 \text{ mg P L}^{-1}$  ( $y = 0.001 + 0.0027X$ ;  $r = 0.14$ ). MDL computed by procedure b, based on the 12 results obtained for the 8BD  $0.048 \text{ mg P L}^{-1}$  standard solution, was  $0.0023 \text{ mg P L}^{-1}$  ( $t_{11, 0.01} = 2.764$ ). The average for the standard was  $0.0483 \pm 0.0008$ , ranging from 0.047 to 0.050. Considering all factors, the solution:soil ratio in the extraction (60) and the dilution factor (8), the resulting detection limit for the method is  $1.09 \text{ mg P kg}^{-1}$ , based on the more conservative MDL ( $0.0023 \text{ mg P L}^{-1}$ ).

Average AAO extractable P from SRM-2709 and Soil 1 and Soil 2 were  $313.3 \pm 4.1$ ,  $22.2 \pm 1.0$ , and  $3.8 \pm 0.5 \text{ mg kg}^{-1}$ , respectively.

Table 3. Analytical performances of the continuous flow injection analyzer in the colorimetric determination of acid ammonium-oxalate (AAO) extractable P in 8x diluted aliquots. Results for P standards made in AAO blank background solution (analyzed as unknown), San-Joaquin's (SRM-2709), and two forest soils' (soil 1 and soil 2) AAO-spiked extracts are presented. Soil 1 was spiked with 0.25 mg P L<sup>-1</sup>; soil 2-A was spiked with 0.25 mg L<sup>-1</sup> P and soil 2-B with 1.20 mg P L<sup>-1</sup>; SRM-2709 was spiked with 1.20 mg P L<sup>-1</sup>.

SRM-2709 was spiked with 1.20 mg P L <sup>-1</sup>					
Sample	n	P Concentration		mg kg <sup>-1</sup>	% R
		Mg L <sup>-1</sup>	% RSD		
P standard solution					
0.150 mg L <sup>-1</sup>	2	0.153	1.4		101.9
0.100 mg L <sup>-1</sup>	2	0.098	0.5		97.8
0.050 mg L <sup>-1</sup>	2	0.051	0.2		102.4
0.048 mg L <sup>-1</sup>	12	0.048	1.7		100.7
0.032 mg L <sup>-1</sup>	2	0.032	1.9		100.8
0.016 mg L <sup>-1</sup>	2	0.018	14.9		109.4
SRM-2709					
A	3	0.660	0.3	316.9	
A spiked	3	1.895	0.1		98.9
B	3	0.649	0.4	309.7	
B spiked	3	1.874	0.1		98.1
Soil 1					
A	3	0.048	0.4	23.1	
A spiked	3	0.290	0.7		96.8
B	3	0.044	3.3	21.4	
B spiked	3	0.284	0.3		95.8
Soil 2					
A	3	0.007	10.0	3.4	
A spiked	3	0.245	0.2		95.1
B	3	0.009	2.9	4.2	
B spiked	3	1.252	0.2		99.4

#### *P behavior during AAO extraction*

During the 120-minute AAO extraction, P release to solution exhibited similar behavior as that of Fe, characterized by initial fast release followed by a decreasing rate of release with increase in extraction time (Fig. 3). AAO extractable Fe after 120 min shaking time was 2543±25, 2024±65, and 467±14 mg Fe kg<sup>-1</sup> for SRM-2709, Soil 1 and Soil 2, respectively. AAO extractable P after 120 min shaking time was 301.6±2.8,



23.8±0.3, and 4.0±0.2 mg kg<sup>-1</sup> for SRM-2709, Soil 1 and Soil 2, respectively. AAO extractable P in Soil 2 was very low (0.007 to 0.009 mg P L<sup>-1</sup>; i.e., 3.4 to 4.3 mg P kg<sup>-1</sup>) leading to unstable results for this soil (Fig. 3). Most of the Fe and P (>80%) were extracted within the first 40 min, and in Soil 2 at earlier stages than in the other two

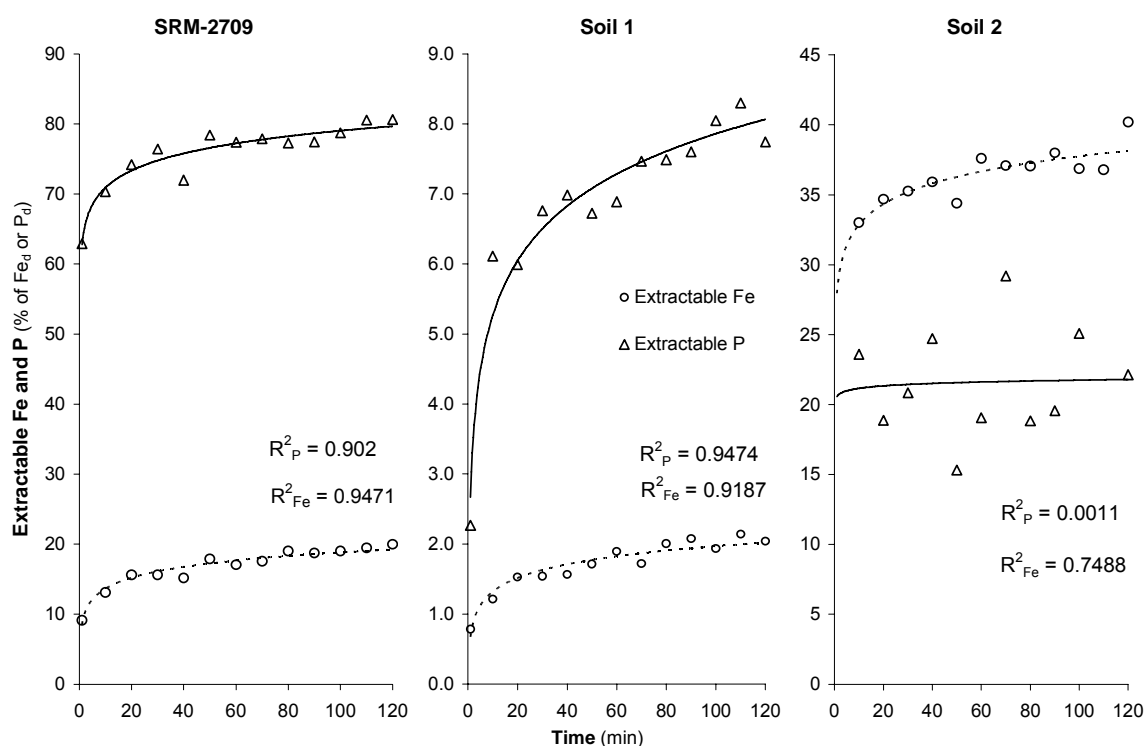


Fig. 3. SRM-2709, soil 1 and soil 2 acid ammonium-oxalate (AAO) extractable Fe and P at different times during the AAO 120-min extraction procedure. Data presented as percent of the citrate-dithionite extractable element.

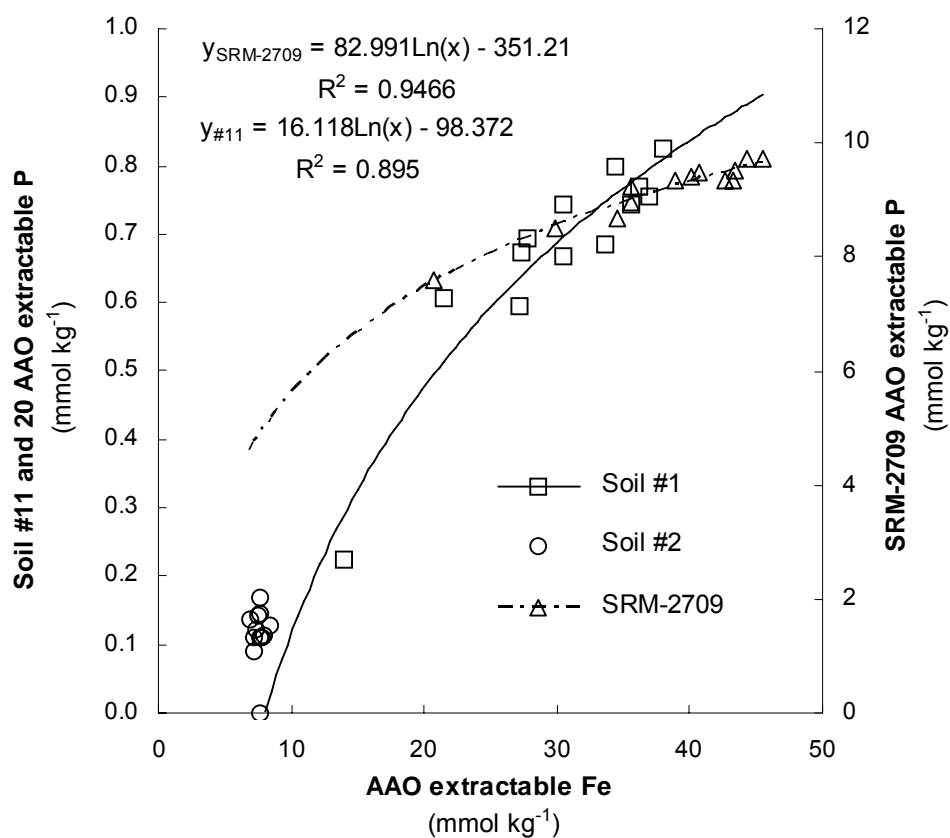


Fig. 4. Relationships between the acid ammonium-oxalate (AAO) extractable Fe and P in SRM-2709 and the two forest soils used in the study. Data from all AAO extraction durations (0 to 120 min) are plotted.

soils. In Soil 1 releases of both elements continued throughout the 120 min of extraction time, without reaching a plateau (Fig. 3). Extractable P was highly correlated with extractable Fe in Soil 1 ( $r = 0.94$ ) and in SRM-2709 ( $r = 0.97$ ) (Fig. 4). In Soil 2 most of the P and Fe were extracted within the first 20 min (96 and 84 %, respectively).

Table 4. Recovery (%) of phosphorus-spiked acid ammonium-oxalate (AAO) extraction solution during the AAO extraction of San-Joaquin SRM-2709 and the two forest soils used in this study. The spiked AAO extract solution contained 1.2 mg P L<sup>-1</sup>.

AAO solution	N	P concentration		% R	
		Avg	% RSD		
SRM-2709					
Non spiked	2	0.041	1.2	99.3	
Spiked	2	1.233	0.5		
Soil 1					
Non spiked	2	0.698	6.9	101.7	
Spiked	2	1.918	2.0		
Soil 2					
Non spiked	2	0.001	15.3	101.1	
Spiked	2	1.216	0.4		

Phosphorus recovery during the AAO extraction procedure as evaluated by the P recovery from the samples extracted by the 1.2-mg P L<sup>-1</sup> spiked AAO solution is presented in Table 4. High recoveries were obtained for all soils, averaging 100.8±1.3 %.

## Discussion

Current methods used to analyze CD- and/or AAO-extractable P detect all forms of the extracted P (i.e., both organic and inorganic). This is whether by predigestion of the sample to destroy the oxalic/citric anions and converting all dissolved P species to inorganic P in the process prior to the colorimetric reaction, or by analyzing for P by ICP, which is inherently incapable of differentiating between the different soluble species. Furthermore, the detection limit of the colorimetric method reaches sub  $\mu\text{g L}^{-1}$  levels, lower than most ICP's, and makes the colorimetric method more desirable (McKelvie et al., 1995). Yuan and Lavkulich (1995) successfully determined citrate-bicarbonate-dithionite extractable P colorimetrically using an analyte dilution approach. Maintaining <2.4 mM citrate in the analyte produced stable results without the need for predigestion. Fiske and Subbarow (1925), using hydroquinone as a reducing agent, showed oxalate at 4.3 mM in blood filtrates to have negligible effects on P determination

by the molybdenum blue method (at 2-8 mg P L<sup>-1</sup>). In the current study, maintaining citrate and oxalate concentration below approximately 51 and 34 mM, respectively, in the analyte resulted in stable development of the colorimetric reaction and in an accurate and reproducible determination of AAO- and CD-extractable P analyzed by the molybdenum blue method in a continuous FIA system. Yet, oxalate is added to overcome P interferences in the determination of dissolved Si by the same procedure (i.e., the ascorbic acid-molybdenum blue procedure). To determine Si 40 mM oxalate in an automated system (method 360.3; Standard Methods 1995b), and 21 mM oxalate in final batch solution (i.e. USEPA method 370.1) are required. The oxalate destroys the phosphomolybdenum complexes, leaving only the Si-molybdenum (Mo) complexes to participate in the color-developing stage (Campbell and Thomas, 1970; Standard Methods, 1995b). Considering the dilution of the sample by the carrier plus reagent in the automated system, the oxalate and citrate concentration of the reaction medium is less than half the corresponding concentration in the analyte. This may further explain the dispersive pattern of the color (peak) development observed in this study. The colorimetric reaction developed in the dispersed plume in the head and tail of the bulk sample, yet failed in the bulk samples of the lower dilution rates of the AAO and CD extraction solutions.

Changing the colorimetric reactant stoichiometry, i.e. increasing Mo and antimony (Sb), is used to overcome oxalate interferences in determining AAO extractable P (Owens et al., 1977; Wolf and Baker, 1990; Drouillon and Merckx, 2003). Yet the chemical reactions, and hence the analytical performance of the colorimetric method are highly sensitive to the reactant stoichiometry and concentration. Different Mo:P ratios in solution, under fixed temperature and reaction time, resulted in different product preferences, ranging from a single P-Mo complex (the “molybdenum blue”) at high ratios, to polymerization of P-Mo complexes (the “heteropoly P-Mo”) in low ratios, which further resulted in different degrees of linearity between P concentration and the developed color intensity (Towns, 1986). Fiske and Subbarow (1925) discussed that changing the ratio between color developers by 2.5 (molybdenum and hydroquinone)

increased blank readings by more than 10 %. The hypsochromic effect (i.e., shift in absorption to shorter wavelength) due to alteration in conjugation (due mainly to protonation) affects the reading too, shifting the absorbance intensity, especially at the 700-900 nm wavelength range (Towns, 1986). Balanced proportions of acid and Mo (4:1, in Murphy and Riley, 1962) were important in avoiding Si interferences. Increases in acidity decreased the rate of P-Mo complex and color formation, yet Si complexes develop slower than those of P, and hence increases in acidity (and Mo at the same rate) result in diminished Si interference (zero at acidity of 0.8 N) (Broberg and Petterson, 1988). At low acidity the color develops from the reaction of the molybdate itself (in absence of P); at high acidity the color development falls rapidly, leaving a range of “acid-stability plateau” (i.e., the range in acidity where color development is independent of pH) in between (Jackson, 1958; Rodriguez et al., 1994). The range of the acid-stability plateau in turn decreases with increases in P concentration (Jackson, 1958; Rodriguez et al., 1994). Increases in Sb concentration to somewhat higher concentrations from the one prescribed by Murphy and Riley (1962) (0.4 mg Sb 50 ml<sup>-1</sup>) increased solution turbidity and formed precipitates at high P concentrations (assumed to be of Sb-P-Mo, P concentrations not mentioned) (Olsen, 1967).

Given the empirical nature of the colorimetric analysis, any manipulation of the chemical conditions in the reaction subjects the analytical procedure to possible biases. Hence, the analyte dilution procedure used in this study seems to be the preferred approach. The nil P resorption, and behavior during the AAO extraction, as demonstrated in the kinetic experiment support and reinforce the quantitative reliability of applying the AAO extraction procedure for soil P. The high correlation between extractable Fe and P obtained in the acid ammonium-oxalate extraction implies that the extracted inorganic P is associated with the extracted amorphous phases of iron oxide. This is within agreement with the expected relationships between soil P and iron oxides. Still, speciation between organic and inorganic forms of the AAO extractable-P should be evaluate with respect to the reported overestimation of inorganic P (Dick and Tabatabai, 1977), resulting from hydrolysis of organic P moieties in the acidic medium

of the molybdenum blue method ( $\approx 0.4$  N). In addition, further investigation of the potential of “spontaneous” conversion of organic P during the AAO (pH 3.0) extraction is needed for sound inferences on the different species.

## Conclusions

The visual evidence of the peak development and the computed analytical performances presented in this study demonstrate the ability to determine CD and AAO extractable P colorimetrically by simple dilution, without predigestion of the sample or manipulating the colorimetric reaction conditions. Hence, this method enables the determination and differentiation between the inorganic and the organic CD- or AAO-extractable P. The sufficient dilution rates for stable and reproducible readings of the CD and AAO extracts were 4x and 8x of the extracts, respectively. This results in detection limits of  $8.6 \mu\text{g P L}^{-1}$  ( $6.9 \text{ mg kg}^{-1}$ ) and  $2.3 \mu\text{g P L}^{-1}$  ( $1.1 \text{ mg kg}^{-1}$ ), respectively. No P resorption occurred during AAO extraction of the three representative soils used in this study and the extractable P pattern during the extraction followed that of the extractable Fe.

The ability to analyze the AAO and CD extracts without predigestion enables the differentiation between the organic and inorganic P in these selective extracts for soil iron oxides. This further enables a more detailed insight into the complex relationships of soil P within the Al and Fe organo-mineral complex in soil environments.

## PHOSPHORUS DISTRIBUTION IN THE PROFILE OF TWO EAST TEXAS FOREST SOILS OF DIFFERENT SITE DRAINAGE CHARACTERISTICS

### Overview

Phosphorus retention in weathered soils is controlled by organic matter and iron and aluminum oxides phases. Soil phosphorus behavior (e.g., plant availability and solubility) is further influenced by its distribution among the different phases and the stability of these phases under soil environmental conditions. Changes in the soil microenvironment and in particular soil redox, can result in marked changes in the availability and solubility of soil P. Relationships between iron and Al oxides, P distribution among organic and inorganic, amorphous and crystalline phases, and P retention in weathered soils were examined by characterizing the distribution of Al, Fe, Mn, and P between amorphous and crystalline phases and within the profile of two East Texas Ultisols. The two soils differed markedly in their drainage characteristics. Total soil P content was much higher in the well-drained soil than in the poorly drained one ( $469 \pm 140$  and  $44.2 \pm 12.8$  mg kg<sup>-1</sup>, respectively). Although base saturation and clay distribution in the profile were similar, iron oxide content and distribution within the profile differed markedly between the two soils. Soil P was highly correlated with the iron oxide content in both soils ( $r = 0.88$  and  $0.81$ , in the well and poorly drained soils, respectively). Soil P followed the same distribution as that of the iron oxides. Iron oxide role as a sink for soil P, determined by the  $P_d/Fe_d$  mole ratio was higher in the well-drained compared to the poorly drained soil. Amorphous phases of iron oxides, determined by  $Fe_{ox}/Fe_d$  were higher in the poorly drained soil and further coincided with the  $P_d/Fe_d$  pattern in that soil profile. This suggested that the amorphous phase dominated the role of iron oxides as a P sink under the poor drainage conditions. Al-

containing phases were significantly correlated ( $p < 0.001$ ) with soil P in the poorly drained soil but not in the well-drained one.

## **Introduction**

Soil phosphorus (P) chemistry is closely related to soil organic matter (OM) and iron (Fe) and aluminum (Al) oxy/hydroxides (henceforth referred to as Fe and Al oxides). These phases are more dominant in highly weathered soils than in less-developed ones. Phosphorus behavior (e.g., solubility, availability) in the soil is therefore markedly influenced by the properties and stability of these solid phases. Wood et al. (1984), using sorption experiments, postulated that P retention in northern USA Spodosols under hardwood forests is controlled by biological and geochemical processes vertically stratified in the soil profile. Phosphorus is controlled by biological processes in the topsoil (e.g., OM decomposition, plant and microbial uptake) and by geochemical processes (mainly sorption on Fe and Al oxides) below the top 20 cm of profile (Wood et al., 1984). Walbridge et al. (1991), applying the same approach used by Wood et al. (1984), found the proposed stratification processes to be much less profound in two southern Appalachian forest soils (Inceptisol and Ultisol). Amorphous Al and Fe oxides markedly contributed to P retention in the surface horizons (Walbridge et al., 1991). Beck and Elsenbeer (1999) characterized P distribution between operationally defined forms (using the Hedley procedure) within the profile of alpine Spodosols under different vegetation. They found no distinct vertical stratification. Furthermore, chemical processes, rather than biological ones, were found to dominate P retention in these soils. Mesquita and Torrent (1993) further showed Al and Fe oxides dominated control over P retention in the surface horizons of highly weathered Brazilian soils.

Al and Fe oxides interchangeably contribute to P retention in soils (Burt et al., 2002; Agbenin, 2003; Senwo et al., 2003). Aluminum oxides usually control P retention in highly weathered soils (Brennan et al., 1994), but the influence of both Fe and Al oxides increase with soil development. A decrease in total P, redistribution of P from apatite minerals into (and onto) Fe and Al oxides, and an increase in the proportion of



organic P increase with soil weathering (Walker and Syers, 1976; Sharpley et al., 1987). Aluminum and Fe form amorphous phases in the presence of OM. Given the abundance of OM in the surface soil, the formation of amorphous, and hence more reactive, oxide phases in topsoil is expected (Schwertmann, 1988). Yet, Fe oxides, being subjected to reductive dissolution under anaerobic conditions and precipitation under aerobic conditions, are sensitive to changes in soil redox potential (Sah et al., 1989). Changes in Fe oxide mineralogy and stability further influence P solubility (Patrick and Khalid, 1974; Willett, 1989; Sanyal and De Datta, 1991). Under alternating soil redox conditions, amorphous Fe oxides are expected to control both Fe (Brennan and Lindsay, 1998) and P (Sah et al., 1989) solubility.

Accordingly, Fe and P forms and their abundance in weathered soils will be influenced by the soil moisture regime and the intensity of reductive weathering processes. Since Al oxides are less susceptible to these weathering processes than Fe oxides, their contribution to soil P retention is expected to increase under these conditions. In this study, we explore the relationships between Fe and Al oxides and P retention in weathered soils under different intensities of reductive weathering pedogenic processes. We examine the distribution of Al, Fe, manganese (Mn), and P between amorphous and crystalline phases and within the profiles of two East Texas Ultisols, differing markedly in drainage conditions.

## **Materials and Methods**

### Study sites

The two East Texas Ultisols used in this study are under loblolly pine stands and have B<sub>t</sub> horizons below 50-cm, but differ in their drainage classes (Table 5). The soil profiles were sampled within the control plots of fertilization experiments conducted in this area (Ngono and Fisher, 2001). The study sites are located between longitudes N30° and 31° and latitudes W93° and 94°. The regional climate is humid warm temperate with a mean annual temperature of 20°C and mean annual precipitation from 1100 to 1400 mm along a northwest-southeast gradient, respectively. Site 11 is located in Nacogdoches County,

Table 5. Selected chemical and physical properties of the soils included in the study.

Depth <sup>#</sup> cm	Texture			pH	CEC cmol <sub>c</sub> kg <sup>-1</sup>	Total C* g kg <sup>-1</sup>
	Sand	Silt	Clay			
Site 11- Well-drained; Typic Hapludult						
0-10	58	24	18	6.2	10.3	27.7
10-20	68	16	17	6.3	5.8	14.7
20-30	60	20	20	6.4	4.0	8.8
30-40	66	14	20	6.3	3.9	6.4
40-50	40	14	46	5.7	8.0	
50-70	38	8	54	5.4	9.4	
70-85	41	11	48	5.2	8.7	
85-100	48	4	49	5.0	9.0	
Site 33 – Poorly drained; Arenic Plinthic Paleudult						
0-10	67	22	11	5.3	5.6	11.3
10-20	63	27	11	5.8	3.0	6.9
20-30	67	20	13	5.8	2.6	3.0
30-40	56	18	26	5.4	6.1	2.3
40-50	48	18	35	5.2	10.0	
50-70	36	17	47	5.1	13.5	
70-85	31	16	52	5.1	16.0	
85-100	26	21	53	5.1	19.6	

<sup>#</sup> - Depth is recorded from the surface mineral soil.

<sup>\*</sup> - No total C measurements were taken below the soil upper 40 cm.

northwest of site 33, located in Jasper County, both in East Texas, USA (Fig. 5). Site 11 is underlain by a well-drained Typic Hapludult on a 15-25 percent slope, formed in weakly consolidated loamy, sandy, and shale materials, mainly of the Claiborne geological group of Tertiary age (NRCS, Nacogdoches County survey). The soil under site 33 is a poorly drained Arenic Plinthic Paleudult on a 2-4 percent slope, formed in sandy and loamy sediments of Pleistocene age, mainly of the Willis formation (NRCS, Jasper County survey).

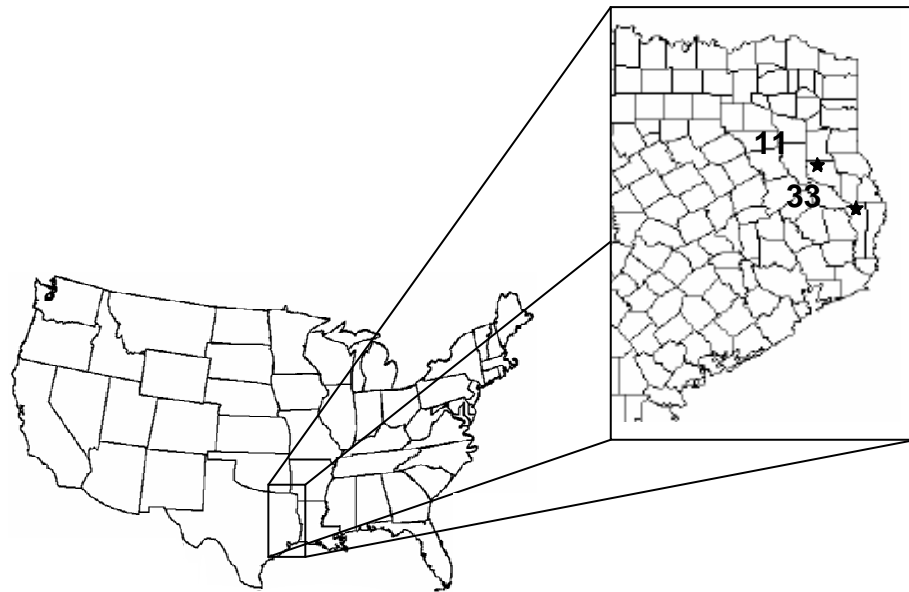


Fig. 5. A USA map with the location of study sites 11 and 33 in East Texas (enlarged).

#### Soil sampling and handling

The soils were sampled during January and February of 2004. On each site, the control plot of a previously installed fertilization experiment (Ngono and Fisher, 2001) was sampled. The sample plots were divided into five 2-m strips along the site elevation contour lines. Each strip was further divided by three to supply fifteen rectangles of 6.6 m<sup>2</sup> each. Soil core samples were taken from each rectangle. Samples from each strip and depth interval were combined into one composite sample, to end up with five composite samples per plot per depth. After removing the organic layer, soil core samples were taken down to 100 cm using an 8-cm diameter auger. The soil cores were laid on plastic sheets on the surface where a typical genetic profile was characterized and used for further verification of soil classification, as adapted from the county and the owner (Temple-Inland Forest Products Corporation) soil surveys. The cores were sampled at eight depth intervals (0-10, 10-20, 20-30, 30-40, 40-50, 50-70, 70-85, and 85-

100 cm). Each composite sample was mixed and subsamples of about 1.5 kg were air dried and ground to pass a 2-mm sieve. About 15 g of each sample were further ground to pass a 150- $\mu\text{m}$  sieve. The <150  $\mu\text{m}$  samples were stored in plastic bags at 4° C and the rest of the samples were stored at room temperature, before further analysis.

#### Chemical and physical analysis

Soil characteristics (i.e., pH, CEC, texture, exchangeable acidity and bases) were determined on the middle strip composite sample of each soil. All soil samples were analyzed for total P ( $P_T$ ); citrate dithionite (CD) extractable Al ( $Al_d$ ), Fe ( $Fe_d$ ), Mn ( $Mn_d$ ) and P ( $P_d$ ), and acid ammonium-oxalate (AAO) extractable Al ( $Al_{ox}$ ), Fe ( $Fe_{ox}$ ) and P ( $P_{ox}$ ). The top 40-cm samples were analyzed for total nitrogen (N) and carbon (C) as well.

Iron in crystalline Fe oxides ( $Fe_{d-ox}$ ) was calculated by the difference between the CD and the AAO extractable Fe following Parfitt and Childs (1988). Soil pH was determined in distilled water at a 1:2 soil-solution ratio using a combination glass electrode; exchangeable bases (potassium (K), calcium (Ca), magnesium (Mg), sodium (Na)) and exchangeable acidity were determined by the  $NH_4OAc$  (at pH 5.5) and the  $BaCl_2$ -TEA methods, respectively, following Thomas (1982). Texture was determined by the hydrometer method (Day, 1965). CEC was calculated as the sum of the exchangeable acidity and bases. Nitrogen and C were determined by NC analyzer (Thermo Finnigan, Flash EA 1112 series, Milano, Italy) on 50-mg soil samples. Total P was determined by  $HClO_4$  digestion following Kuo (1996). The AAO (2 h, pH 3.00, in the dark) and CD (at room temp for 16 h) extraction procedures followed Loeppert and Inskeep (1996) protocols. Extractable Fe, Mn, and Al were determined by flame AA (Varian SpectrAA 220FS, Mulgrave, Victoria, Australia), P was determined colorimetrically by the ascorbic acid method using a continuous flow injection analyzer (OI Analytical, APKEM FS 3000, College Station, TX). The  $P_d$  and  $P_{ox}$  were determined without pre-digestion of the extracts. Alternatively, sample aliquots were diluted prior to the analysis, at a rate where no interferences from oxalate or citrate were observed during the colorimetric reaction. This was achieved by monitoring the peak

development of a series of AAO and CD blank dilutions spiked with a known amount of P. Eight and 4x dilution of the AAO and CD extracts, respectively, were found to be adequate for the colorimetric reaction to proceed without extract medium interference. At these dilution rates, spiked soil extracts were further used to verify the accuracy and precision performance of the analytical procedure, as described in details in the first section. Pre-dilution at the above rates was used in determining the AAO and CD extractable P colorimetrically.

Based on  $P_T$ , distribution of  $P_d$  and  $P_{ox}$  P between the following operationally defined forms was calculated accordingly:  $P_{d-ox}$ , P associated with crystalline Fe oxides, calculated by the difference between  $P_d - P_{ox}$ ;  $P_{ox}$ , adsorbed P and P associated with amorphous minerals; and  $P_{T-d}$ , total P not extracted by citrate dithionite, calculated by the difference between  $P_T - P_d$ . Under the analytical procedures used in this study,  $P_T$  includes all soil P (i.e., organic and inorganic P). In the CD and AAO extractions, only P arriving at the colorimetric reaction medium as orthophosphate ( $PO_4^{-3}$ ) is detected. Thus, AAO- and CD-extractable organic P is analytically excluded from being detected, and hence from being accounted for in  $P_d$  and  $P_{ox}$ . Given the soil weathering stage and acidic nature, a minor contribution of P from apatite is expected. Therefore,  $P_{T-d}$  is assumed to be associated mostly with organic P.

#### Statistical analysis

Statistical analysis was carried out using JMP 5.0.1.a (JMP, 2002) and SigmaStat 2.03 (SigmaStat, 1997) software packages. Correlation analysis was done by Pearson correlation (at  $p < 0.05$ ). Multiple comparison was done by Tukey HSD (at  $p < 0.05$ ).

## Results

The profile characteristics reflected soil drainage classes. Although soil redox was not measured, the poorly drained site, given its inundation conditions in the presence of a continuous supply of decomposable OM from the forest floor and the regionally high temperature, was expected to exhibit much more intense reducing conditions than the well-drained site. As expected, the soil of site 11, the well-drained site, consisted of an oxidized profile as indicated by its dominant reddish hue and high value and chroma. The soil of poorly drained site 33 is under much wetter and more intense reducing conditions as reflected by the grayish and yellowish hue. This is even more apparent as seen in the redoximorphic features in the lower part of the profile (Fig. 6). The soil base saturation averaged  $21 \pm 11$  % and  $32 \pm 15$  % throughout the upper 100 cm soil profiles of sites 11 and 33, respectively.

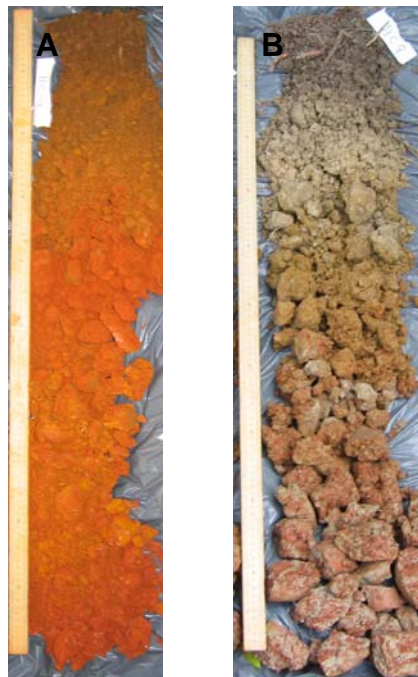


Fig. 6. Representative core soil profile (0-100 cm) from site 11 (A) and site 33 (B).

Table 6. Total P ( $P_T$ ) and citrate-dithionite (subscript d) and acid ammonium-oxalate (subscript ox) extractable Al, Fe, Mn, and P in the soil profile of site 11 and site 33. Values within a column followed by the same letter are not significantly different (at  $p < 0.05$ ).

Depth <sup>#</sup>	P <sub>T</sub>	P <sub>d</sub>	P <sub>ox</sub>	Mn <sub>d</sub>	Fe <sub>d</sub>	Fe <sub>ox</sub>	Al <sub>d</sub>	Al <sub>ox</sub>
cm	mg kg <sup>-1</sup>			g kg <sup>-1</sup>		mg kg <sup>-1</sup>		
Site 11								
0-10	514.6a	307.9a	22.3a	269a	99.2a	2003abc	6099de	1493abcde
10-20	558.3a	353.9a	18.5ab	275a	113.9a	2073ab	6666bcd	1314cde
20-30	545.8a	362.5a	15.5ab	256ab	120.7a	1870abcd	6661bcd	1018def
30-40	486.5a	357.2a	23.6a	239ab	121.8a	2476a	7460bcd	2160ab
40-50	444.1a	347.4a	16.3ab	147bcd	112.9a	1745abcd	9812ab	2108ab
50-70	397.8a	337.1a	10.9bc	150bc	106.7a	1182cde	12949a	1401bcde
70-85	446.3a	346.2a	16.5ab	152bc	110.0a	1247bcde	9917abc	2223a
85-100	362.6a	284.6a	12.5b	111cde	85.7a	1048de	7229bcd	1816abc
Site 33								
0-10	40.1b	7.7b	3.2cd	46cde	1.6b	545e	636f	462f
10-20	31.0b	6.1b	1.9d	54cde	1.5b	513e	599f	482f
20-30	23.8b	6.8b	1.5d	34de	1.9b	391e	478f	352f
30-40	37.7b	28.3b	0.4d	19e	5.7b	564e	2555ef	845ef
40-50	55.3b	39.6b	0.3d	13e	13.0b	625e	5883de	1307cde
50-70	56.4b	35.3b	0.2d	9e	17.3b	622e	6539cd	1676abcd
70-85	56.8b	33.0b	0.3d	4e	16.1b	841e	7873bcd	2193ab
85-100	52.0b	19.0b	0.4d	2e	11.3b	787e	4857de	2008abc

<sup>#</sup>Depth is reported from the surface of the mineral soil.

All forms of all elements (except for  $Al_{ox}$ ), were higher on site 11 than on site 33. The  $Al_{ox}$  concentration in the lower half of the profile of site 33 ( $2.0 \pm 0.6$  g kg<sup>-1</sup>) was somewhat higher than that on site 11 ( $1.8 \pm 0.6$  g kg<sup>-1</sup>). Average content of  $P_T$ ,  $P_d$ , and  $P_{ox}$  throughout the profile on site 11 was  $469 \pm 140$ ,  $337 \pm 94$ , and  $17.0 \pm 6.5$  mg kg<sup>-1</sup>, respectively. This was an order of magnitude higher than on site 33 ( $44.2 \pm 12.8$ ,  $2.0 \pm 14.6$ , and  $1.0 \pm 1.1$  mg kg<sup>-1</sup>, respectively). The  $Fe_d$  and  $Fe_{ox}$  were much higher on site 11 throughout the profile (Table 6).

The two soils had similar clay distribution patterns in the profile (Fig. 7), but their  $P_T$  and  $Fe_d$  distribution patterns differed markedly (Fig. 7). Yet, the patterns of  $P_T$  and  $Fe_d$  in each profile were similar (Fig. 7). On site 33 the  $Fe_d$  and  $P_T$  distribution within the profile followed that of the clay. However, on site 11 the increase in clay content with depth did not follow an increase in  $Fe_d$  or  $P_T$  (Fig. 7). The similarity between  $Fe_d$  and  $P_T$  distribution patterns in the soil profile suggests that P distribution in

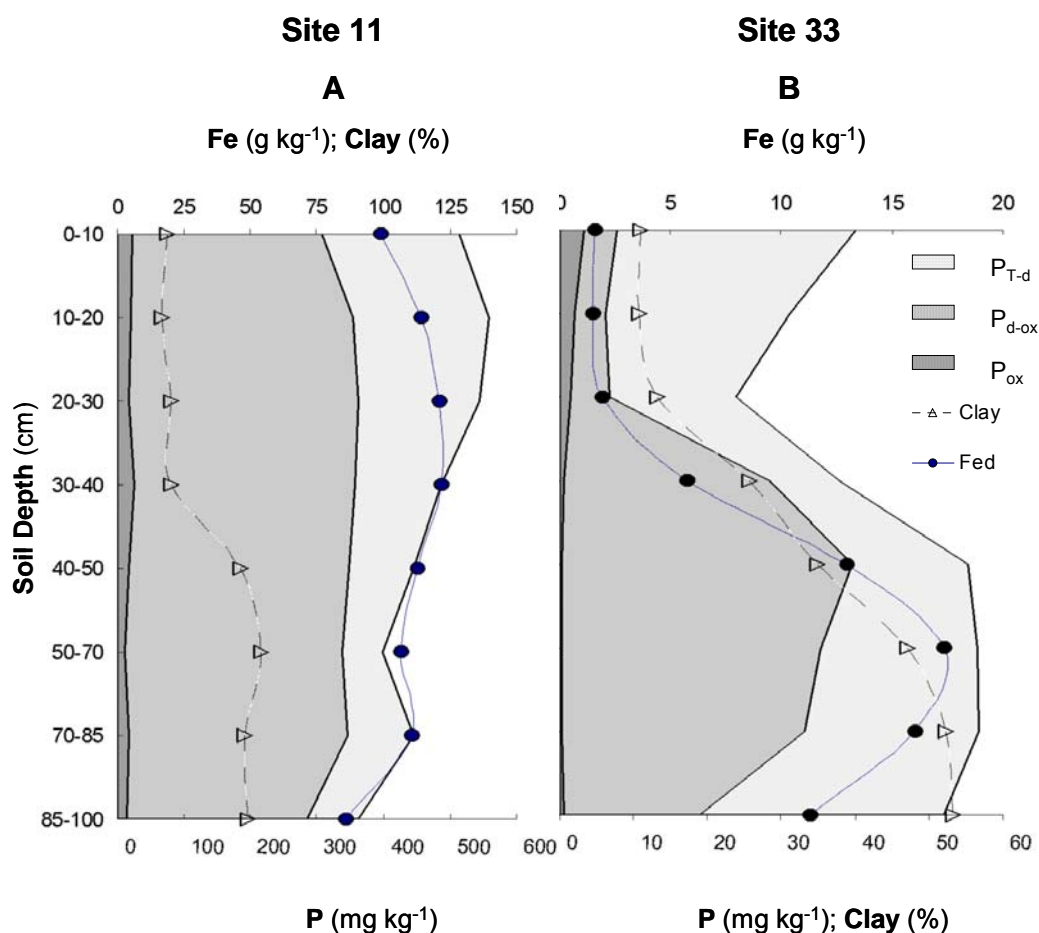


Fig. 7. Distribution of citrate-dithionite (CD) extractable iron ( $Fe_d$ ), acid ammonium-oxalate (AAO) extractable phosphorus ( $P_{ox}$ ), P associated with crystalline iron oxides ( $P_{d-ox}$ ), organic P ( $P_{T-d}$ ), and clay content in the soil profile of site 11 (A) and site 33 (B).  $P_{d-ox}$  is calculated by difference between CD-extractable P ( $P_d$ ) and  $P_{ox}$ ;  $P_{T-d}$  is calculated by the difference between total P (as determined by the perchloric acid digestion) and  $P_d$ .



the profile is coupled with that of Fe oxides. The deviation of  $P_T$  pattern from that of the  $Fe_d$  at the upper part of the profile of site 33 (Fig. 7) likely resulted from higher organic P content in the surface horizon. Since the CD-extractable organic P is not detectable by the analytical method used in the study (i.e., colorimetric determination on a non-digested sample) soil organic P is included in  $P_T$  but is not accounted for in the CD extraction. The  $P_d$  accounted for  $73 \pm 9$  and  $46 \pm 23$  % of  $P_T$  throughout the profiles, resulting in about twice as much organic P ( $P_{T-d}$ ) on site 33 than on site 11 (54 and 27 % throughout the profile, respectively).

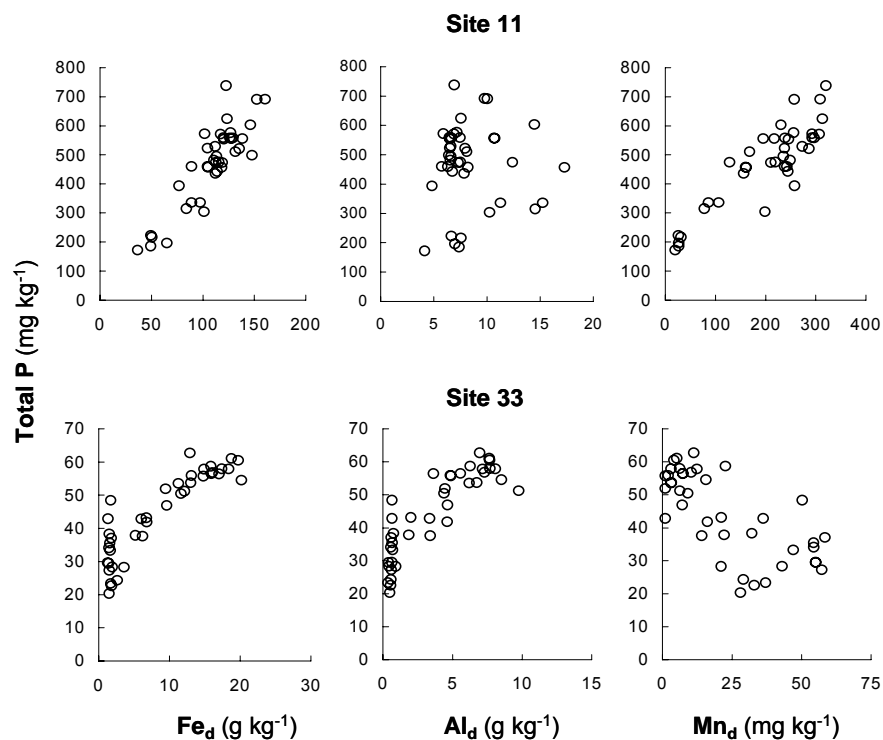


Fig. 8. Relationships between total phosphorus and citrate-dithionite extractable iron ( $Fe_d$ ), aluminum ( $Al_d$ ), and manganese ( $Mn_d$ ) on sites 11 and 33. Data from all depth intervals and from all five composite samples are included.

Table 7. Relationships between total phosphorus and selected soil properties at sites 11 and 33. Pearson correlation coefficients with \* are significant at  $p < 0.05$ ; \*\* significant at  $p < 0.001$ .

Site	Depth	% Clay	Mn <sub>d</sub>	Fe <sub>d</sub>	Al <sub>d</sub>	Fe <sub>ox</sub>	Al <sub>ox</sub>
11	-0.413*	-0.422*	0.880**	0.881**	0.011	0.507**	0.009
33	0.515**	0.652**	-0.682**	0.807**	0.861**	0.193	0.571**

Soil P<sub>ox</sub> distribution and its relatively rapid decrease in depth at site 33 (from  $3.2 \pm 0.3$  at 0-10 to  $0.4 \pm 0.2$  mg kg<sup>-1</sup> at 30-40 cm) coincide with the decrease in P<sub>T-d</sub> and Fe<sub>ox</sub> at these intervals (Fig. 7 and Table 6, respectively).

Soil P<sub>T</sub> was positively correlated ( $p < 0.001$ ) with Fe<sub>d</sub> in both sites, yet significantly correlated ( $p < 0.001$ ) with Al<sub>d</sub> and Al<sub>ox</sub> only at site 33 (Fig. 8; Fig. 9; Table 7), and with Fe<sub>ox</sub> only at site 11 (Table 7, Fig. 9). P<sub>T</sub> was also highly correlated with Mn<sub>d</sub>, soil depth, and percent clay in both sites, though contrasting relationships were found (Table 7). Total P was positively correlated with Mn<sub>d</sub> and negatively correlated with both soil depth and percent clay at site 11. Opposite relationships were found at site 33 (Fig. 8; Table 7).

Given the higher susceptibility of Mn oxides than of Fe oxides to reducing conditions, the negative correlation between Mn<sub>d</sub> and Fe<sub>d</sub> in the poorly drained site ( $r = -0.79$ ,  $p < 0.0001$ , at site 33) suggests a deviation from the co-migration of these elements. A positive correlation between Mn<sub>d</sub> and Fe<sub>d</sub> was found on well-drained site 11 ( $0.76$ ,  $p < 0.0001$ ). Both Fe<sub>d</sub> and Al<sub>d</sub>, and Fe<sub>ox</sub> and Al<sub>ox</sub> were highly correlated ( $p < 0.001$ ) on site 33 ( $r = 0.92$  and  $0.55$ , respectively) but not significantly correlated on site 11.

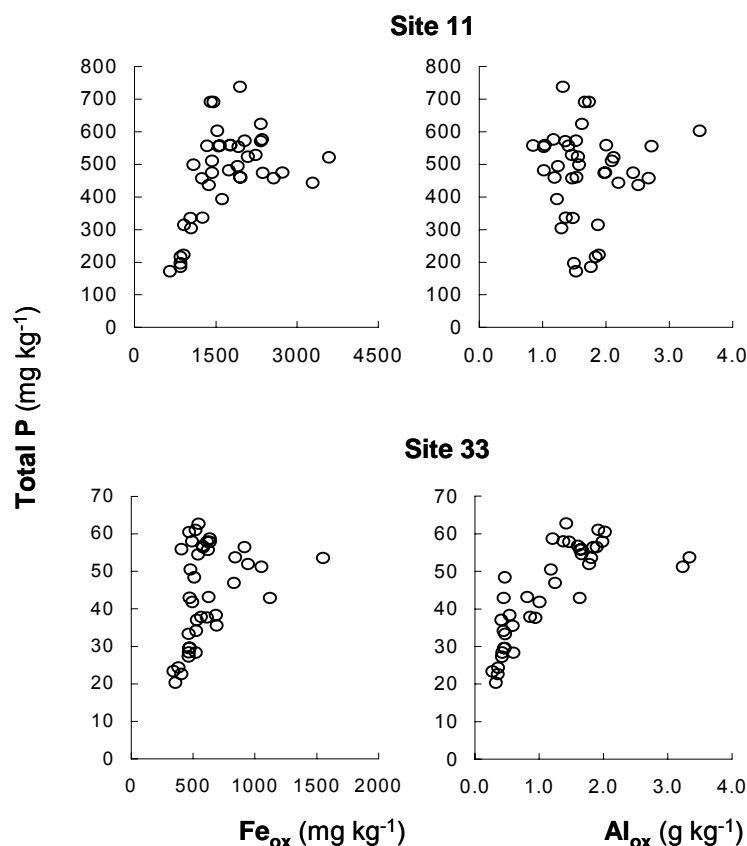


Fig. 9. Relationships between total phosphorus and acid ammonium-oxalate extractable iron ( $\text{Fe}_{\text{ox}}$ ) and aluminum ( $\text{Al}_{\text{ox}}$ ) on site 11 and site 33. Data from all depth intervals and from all five composite samples are included.

$\text{P}_d$  was highly correlated ( $p < 0.0001$ ) with  $\text{Fe}_d$  at both sites, with regression coefficients (the slope of the linear regression line, Fig. 10) of 0.0056 and 0.0032 for sites 11 and 33, respectively (Fig. 10). Expressing P associated with free Fe oxides by the  $\text{P}_d/\text{Fe}_d$  mole ratio led to a fairly unified value throughout the profile of site 11 (Fig. 11). This is implied by the high linear correlation between the two fractions ( $R^2 = 0.92$ ; Fig. 10). The  $\text{P}_d/\text{Fe}_d$  mole ratio in the profile of site 33 decreases from 0.009 at the surface soil to 0.003 at 85-100 cm (Fig. 11).

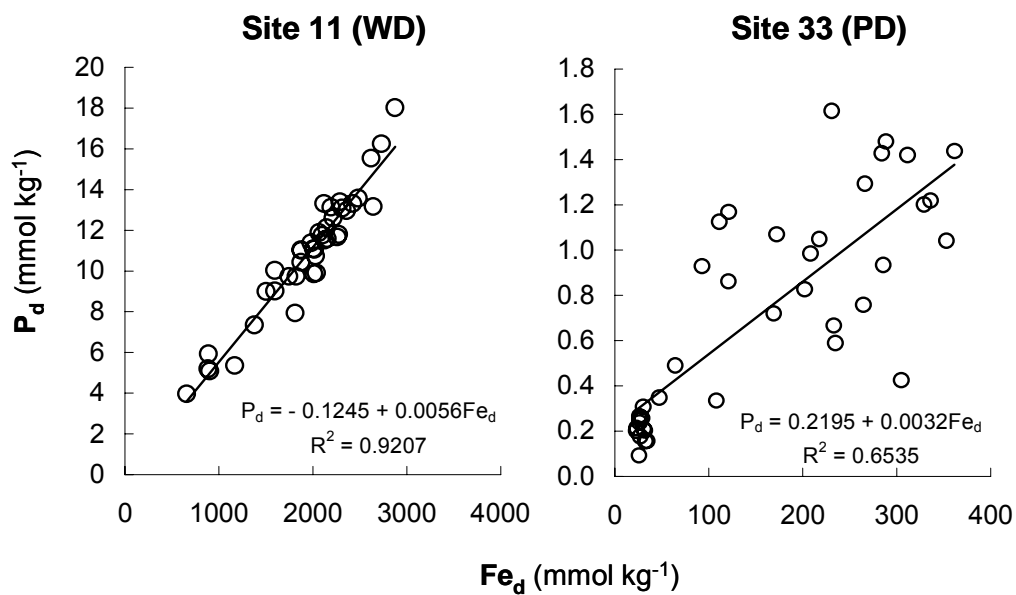


Fig. 10. Relationships between citrate-dithionite extractable phosphorus ( $P_d$ ) and iron ( $Fe_d$ ) in the soils of sites 11 and 33. Data from all depth intervals are included.

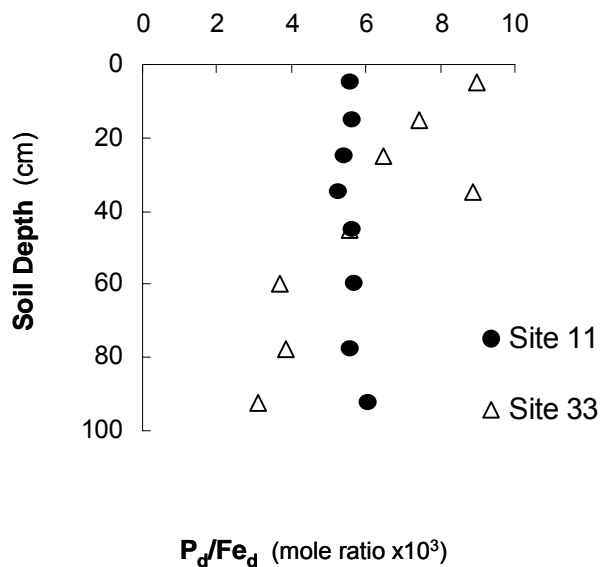


Fig. 11. Distributions of the mole ratio ( $P_d/Fe_d$ ) between citrate-dithionite extractable phosphorus ( $P_d$ ) and iron ( $Fe_d$ ) in the soil profile of sites 11 and 33.

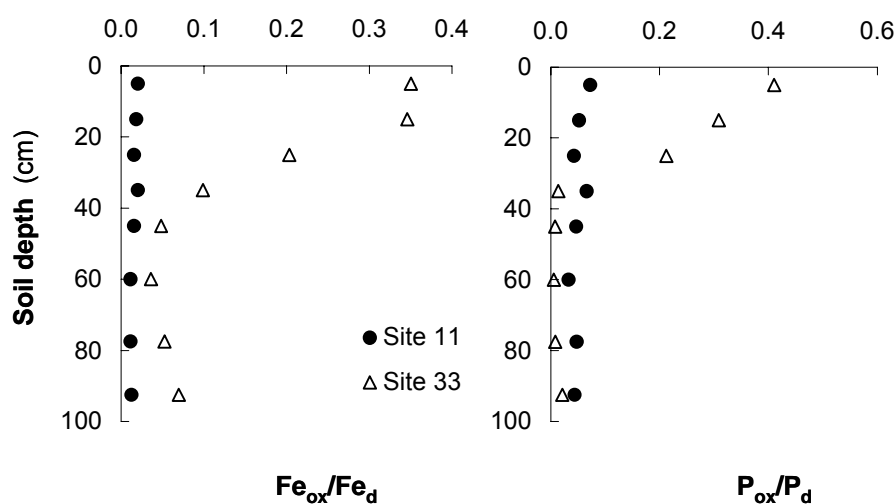


Fig. 12. Distributions of the  $Fe_{ox}/Fe_d$  and of  $P_{ox}/P_d$  ratios in the soils profiles.  $Fe_{ox}$  and  $P_{ox}$  are acid ammonium-oxalate extractable iron and phosphorus, respectively;  $Fe_d$  and  $P_d$  citrate-dithionite extractable iron and phosphorus, respectively.

Amorphous Fe oxide, as a fraction of free Fe oxides (i.e.,  $Fe_{ox}/Fe_d$  ratio) was low ( $0.016 \pm 0.005$ ) with moderate changes (ranging from 0.007 to 0.029) in the profile of site

11 (Fig. 12). In site 33 a much higher  $\text{Fe}_{\text{ox}}/\text{Fe}_{\text{d}}$  ratio was found in the surface soil (0.354), decreasing rapidly between 0-40 cm and averaging 0.052 thereafter (Fig. 12). The same pattern was found for the  $\text{P}_{\text{ox}}/\text{P}_{\text{d}}$  ratio in the soil profile, with relatively more P associated with amorphous Fe oxides on the poorly drained (site 33) than on the well-drained soil (site 11). There were higher  $\text{P}_{\text{ox}}/\text{P}_{\text{d}}$  values in the topsoil (Fig. 12).

## Discussion

Although no direct mineralogical identification was made, based on the soil color it is clear that the Fe oxides on site 11 are hematite dominated compared to the goethite dominance on site 33. The differentiation between hematite and goethite domination is known to be a characteristic of soil wetness, with a higher proportion of goethite (yellowish color) in wetter soils (Schwertmann, 1988). The distinct redoximorphic features and the overall yellowish, goethite-derived hue of the soil profile on site 33, compared to the reddish, hematite-derived hue on site 11, indicate that soil from site 33 is under a much wetter and reducing regime than the soil at site 11. Along a climosequence of Hawaiian forest soils, Miller et al. (2001) reported similar patterns of lower soil P, lower soil Fe oxide content, lower P associated with Fe oxides, coupled with an increase in P in organic form on wetter sites. They found depletion in the soil Al and Fe oxides and P along a gradient in annual rainfall, which was coupled with increased intensity of the soil reducing conditions. An increase of organic P from about 20 to 60%, and a decrease in recalcitrant P (the residual fraction in the Hedley fractionation procedure) was noted (Miller et al., 2001). A similar pattern of increase in  $\text{P}_{\text{T}}$  with depth in an Ultisol and Inceptisol was reported by Walbridge et al. (1991). The difference in total P between the two soils in the current study followed the expected decrease in total P with increase in soil wetness and reducing conditions, yet other factors, like the differences in site geological formation and parent materials are likely to influence the soils' inherent P content.

The similar distribution patterns between  $\text{P}_{\text{T}}$  and  $\text{Fe}_{\text{d}}$  throughout the profiles in this study suggest that soil P is highly associated with the Fe oxides in both profiles. Schwertmann and Fanning (1976) used the  $\text{P}_{\text{d}}/\text{Fe}_{\text{d}}$  mole ratio to evaluate the efficiency of

Fe oxides as a sink for P in soils of different moisture regimes. In their study,  $P_d/Fe_d$  ratio ranged from 0.003 in the wetter soils to 0.073 in the drier soils. In our study, similar patterns were found (0.003 and 0.006 in wetter and drier soils, respectively), yet both values were within the lower end of the range reported by Schwertmann and Fanning (1976). The results in this study are still low even when accounting for the fact that Schwertmann and Fanning worked on soil Fe-Mn concretions (with P concentration factor of up to five times compared to the bulk P concentration, in the drier soil members). This may result from the nature of the soils in this study, being at a more advanced weathering stage (Ultisols) compared to the soils in the Schwertmann and Fanning study (Inceptisol, Mollisol and Alfisol).

Different weathering stage can result in significant differences in the ratio, pointing to the behavior of soil P and Fe under soil weathering processes. The acidic and oxidizing nature of early stages of soil weathering result in a release of P from dissolving apatite minerals (Walker and Syers, 1976; Sharpley et al., 1987), coupled with an increase in “free” Fe oxides, as a result of release of Fe from primary and secondary dissolving minerals and its precipitation as Fe oxides (Miller, 1983; Schwertmann and Taylor, 1989). The  $P_d/Fe_d$  ratio is then expected to increase, given that Fe oxide becomes the more dominant solid phase controlling P retention. Further down the pedologic sequence, P is both depleted and redistributed to organic forms, which may lead to a lower  $P_d/Fe_d$  ratio, as is the case in this study.

Furthermore, in the current study the CD-extractable organic P is not accounted for in  $P_d$ , which results in “underestimation” of traditionally obtained  $P_d$ . Since a pre-dilution, rather than pre-digestion step, of the CD and AAO extracts prior to the colorimetric determination of extractable P was used in this study, only the inorganic extractable P was detected. This analytical approach makes it possible to clear the “mask” of organic P extracted during the CD and AAO procedures. This in turn is expected to result in a lower  $P_d/Fe_d$  ratio. This does not mean that organic P is not associated with Fe oxide, but only that the extractable organic P under these extraction conditions (i.e., CD and AAO extractions) is not necessarily associated with the Fe

oxides specifically. A more complex relationship between OM and oxides exists. Yet the exchange of OM-associated polyvalent cations by monovalent ones is expected to promote OM solubilization. The polyvalent cations contribute to OM-mineral and OM-OM interactions and stabilization (Stevenson, 1994). Exchanging the polyvalent cations associated with soil OM (e.g.  $\text{Fe}^{3+}$ ,  $\text{Al}^{3+}$ ) by monovalent cations in the CD and AAO extraction procedures (i.e.,  $\text{Na}^+$ ,  $\text{H}^+$  and  $\text{NH}_4^+$ , respectively), and by complexation of the polyvalent cations with citrate or oxalate, respectively, is expected to promote solubilization of OM and the organic P within. The soluble organic P may later be included in  $\text{P}_d$  if determined colorimetrically using pre-digestion. This will result in overestimation of the amount of P associated directly with Fe oxides. This effect will occur to a greater extent in highly weathered systems where soil P content in the organic fraction is high. Therefore, the pre-dilution approach used in this study is believed to target more specifically the P associated with Fe oxides.

The  $\text{P}_d/\text{Fe}_d$  ratio in this study was also found to follow its relationship with soil wetness within the profile of the wetter soil (site 33), being higher at the surface horizon (0.009) and decreasing with increasing depth down to 0.003 in the 85-100 cm. This suggests that Fe oxides are more efficient as a sink for P in the upper horizon than farther down the profile. Since this pattern coincided with the distribution of  $\text{Fe}_{\text{ox}}/\text{Fe}_d$  in the profile of this soil, it further suggests that the amorphous Fe oxides ( $\text{Fe}_{\text{ox}}$ ) maintained the higher sink for P in the upper part of the profile.

The higher proportion of amorphous Fe oxides ( $\text{Fe}_{\text{ox}}/\text{Fe}_d$ ) on the poorly drained site can be explained by the stability and redistribution of the different Fe oxides under reducing conditions. Under alternately reducing/oxidizing conditions, dissolution of Fe oxides and their re-precipitation in an amorphous phase is expected (Breemen, 1988a, 1988b; Brennan and Lindsay, 1998), resulting in a higher proportion of amorphous Fe oxides. The current study for the poorly drained site found that these conditions resulted in a higher proportion of amorphous Fe oxides (i.e., higher  $\text{Fe}_{\text{ox}}/\text{Fe}_d$  ratio). This situation applied more to the topsoil, where the presence of OM is believed to stimulate the formation of amorphous phases.



The correlation of  $P_T$  and  $Al_d$  and  $Al_{ox}$  in the poorly drained soil suggests that Al oxides become more dominant in P retention in intensely reducing environments. This is expected, given the fact that Al oxides are less susceptible to reductive dissolution than Fe oxides. The reductive weathering processes further result in depletion of Fe oxides coupled with the relative increase in Al oxides, as in the extremes of the weathering sequence; i.e., the lateritic soils, which are composed mostly of gibbsite and kaolinite. Yet even in the extreme case of lateritic soils, the same tendency to increase in amorphous phases (in that case amorphous Al oxides) under hydromorphic conditions was observed (Drummond et al., 2002).

The high correlations of  $P_T$  with  $Al_d$  and  $Al_{ox}$ , and that of  $Al_d$  and  $Al_{ox}$  with corresponding  $Fe_d$  and  $Fe_{ox}$  in the poorly drained site may reflect a higher association between Al and Fe. This may include co-precipitation in organo-mineral complexes and amorphous phases, as well as in Al substitution for Fe in the precipitated Fe oxides under the poorly drained conditions. Al-substituted Fe oxides in turn resulted in more reductive dissolution resistance Fe oxide (Gonzalez et al, 2002). Yet Al substitution was found to hinder Fe oxide P sorption (Ainsworth and Summer, 1985).

Soil Mn oxides are more sensitive to the intensity (i.e., extent and duration) of the reducing conditions than Fe oxides (Schwertmann and Fanning, 1976; Stumm and Morgan, 1996). Spatial relationships in the soil  $Mn_d/Fe_d$  mole ratio were found to reflect Eh-pH-potential gradients in the North Carolina Piedmont Ultisol-based landscape (McDaniel and Buol, 1991). This ratio was used as a pedochemical indicator of field-scale water movement (McDaniel et al., 1992), and also as an alternative indicator to the colorimetric tests for  $Fe^{2+}$  in identifying aquic and nonaquic Mollisols in a catena in central Iowa (Khan and Fenton, 1996). The highly correlated, yet contrasting relationships, between  $P_T$  and  $Mn_d$  in the soils of the current study ( $r=0.88$  and  $-0.65$  in the well- and the poorly drained soil, respectively) point toward a potential use of this relationship (i.e.  $P_T/Mn_d$ ) as an indicator of the shift from Fe oxides to Al phases as the main solid phase in retaining soil P.

Identifying whether P retention is controlled by Al or Fe oxides is valuable given the fact that P retained in Fe oxide is much more susceptible to increases in solubility under natural, or anthropogenic-induced changes in the soil moisture regime. Examples for such systems may include clearcutting of forest stands or construction/restoration of wetlands. The indicative nature of the above relationships between  $M_d$  and  $P_d$  needs further investigation. Its validation as such an indicator was beyond the scope of this study.

## Conclusions

The distribution and association of soil P content with the different solid phases of the two Ultisols included in this study was highly influenced by soil drainage. Soil P relative distribution between organic and inorganic forms followed previously reported patterns of increases in organic P with increases in wetting and reducing conditions. Total soil P distribution in the profile and between organic and inorganic forms differed between the two soils. This characteristic was highly correlated with the soil Fe oxide and followed its distribution in each soil profile, suggesting Fe oxides to dominate in P retention under both drainage conditions. Iron oxides' role as a sink for soil P, as determined by the  $P_d/Fe_d$  mole ratio, was higher in the well-drained soil than in the poorly drained one. The poorer drainage conditions favored the formation of amorphous Fe oxides, as shown by the higher  $Fe_{ox}/Fe_d$  ratio in the poorly drained site. Furthermore, the pattern of  $Fe_{ox}/Fe_d$  ratio in the profile of the poorly drained soil coincides with that of the  $P_d/Fe_d$  mole ratio. This suggests that amorphous Fe oxides dominate Fe oxide P retention capacity under poorly drained conditions. The interactions between the different forms of P, Al, and Fe in the poorly drained site suggest an increase in Al-containing phases to increase in their contribution to P retention under wet and reduced environments.

## PHOSPHORUS RETENTION IN FERTILIZED FOREST SOILS OF DIFFERENT DRAINAGE CLASSES: THE ROLE OF IRON OXIDES AND THE POTENTIAL INFLUENCE ON PHOSPHORUS AVAILABILITY IN SUBSEQUENT ROTATIONS

### Overview

Soil phosphorus (P) distribution within the soil profile and among selective operationally defined solid phases in seven East Texas forest soils of different drainage classes was evaluated near the end of a 30-year loblolly pine (*Pinus taeda* L.) rotation, eight years after mid-rotation P fertilization (100 kg P ha<sup>-1</sup>). Forest floor mass and P content, as well as citrate dithionite (CD) and acid ammonium-oxalate (AAO) extractable P, Al and Fe within the mineral soil upper 100 cm were determined. Phosphorus in the soil extracts was determined colorimetrically without pre-digestion of the samples. This enabled us to restrict the detected P from the CD and AAO extractions ( $P_d$  and  $P_{ox}$ , respectively) to the inorganic P (the “molybdenum reactive P”), excluding most of the CD and AAO extractable organic P. Soil total P ( $P_T$ ) and CD-extractable P ( $P_d$ ) were highly correlated with CD-extractable Fe across sites, drainage classes, treatments, and depth intervals ( $r = 0.92$  and  $0.98$ , respectively;  $p < 0.0001$ ). The  $P_d/P_T$  ratio, representing the fraction of  $P_T$  associated with iron oxides, was 0.53, 0.54, and 0.44 in the well-drained (WD), the excessively well-drained (ExWD) and in the poorly drained (PD) sites, respectively, suggesting that lower proportions of  $P_T$  are associated with iron oxides in the PD sites. Soil  $P_T$  and  $P_d$  content in the mineral soils was in the order: WD > ExWD > PD.  $P_T$  and  $P_d$  distribution from the surface horizons to lower parts of the profile were in the order: PD > WD > ExWD. The P fertilization treatment generally resulted in significantly higher P content in the forest floor and in  $P_T$  and  $P_d$  in the soil upper 10 cm. The exception was the site with the poorest drainage (site 20), where a decrease in  $P_d$  in the soil upper 10 cm was found. Average treatment effects on  $P_T$ ,  $P_d$ , and that of  $P_d$  after subtracting the AAO extractable P ( $P_{d-ox}$ ) in the soil upper 10

cm were  $18.6 \pm 10.4$ ,  $10.8 \pm 8.4$ , and  $5.7 \pm 8.8$  kg P ha<sup>-1</sup>, respectively, across sites. Treatment effect on P<sub>T</sub> in the forest floor, across sites, was  $5.8 \pm 3.5$  kg P ha<sup>-1</sup>. The treatment effect on P in the forest floor, overall organic P in the forest floor and within the mineral soil upper 10 cm, and P<sub>T</sub>, P<sub>d</sub> and P<sub>d-ox</sub> in the upper 10 cm of the mineral soil was equivalent to 6, 14, 19, 11 and 6%, respectively, of the applied P (i.e. 100 kg P ha<sup>-1</sup>). Treatment effect on P accumulation in the forest floor and in the potentially reducible iron oxide phases in the soil upper 10 cm and the potential contribution of these pools to P availability in subsequent rotations, following clearcutting, are discussed.

## Introduction

Phosphorus (P) fertilization normally increases stand production on highly weathered soils (Albaugh et al., 2004; Jokela et al., 2004; Sayer et al., 2004), and has become a common practice in commercial pine plantations in the southeastern USA (Wells and Allen, 1985; Jokela et al., 1988). Phosphorus fertilization also increases forest floor litter mass (Wienand and Stock, 1995; Comerford et al., 2002; Butnor et al., 2003; Franklin et al., 2003), and has positive residual effect on subsequent rotations (Gentle et al., 1986; Gresham, 2002; Turner et al., 2002). Turner et al. (2002) found that P fertilization positively influenced stand growth in the next two consecutive rotations, including higher growth response to fertilization 50 years after application. The accumulated P in the forest floor of fertilized stands is suspected to account for the residual effect of P fertilization in subsequent rotations (Polglase et al., 1992; Comerford et al., 2002).

Yet, some physicochemical characteristics of weathered soils and common silvicultural practices may both promote redistribution of inorganically combined P into a more available form. Organic matter (OM), and iron (Fe) and aluminum (Al) oxy/hydroxides (henceforth referred to as Fe and Al oxides) are the major soil components contributing to the physicochemical characteristics of weathered soils (Fox, 1980; Juo, 1980; Parfitt, 1980) and hence to the soil P chemical behavior and retention capacity (Burt et al., 2002; Agbenin, 2003; Senwo et al., 2003). Much of the applied P, in highly weathered soils, resides in phases of inorganic Fe oxides phases (e.g. NaOH-Pi,

in the Hedley procedure) (Beck and Sanchez, 1996; Bowman et al., 1998; Dobermann et al., 2002; Senwo et al., 2003). This is more evident when P is applied in inorganic form and as superphosphate more than as rock phosphate (Gentle et al., 1986; Zheng et al., 2002). The former is the principal P fertilizer source in forestry (when only P is required) (Jokela and Long, 2000).

Iron oxides are subjected to reductive dissolution under anaerobic conditions and hence are sensitive to changes in soil redox potential (Sah et al., 1989). Changes in Fe oxide mineralogy and mineral stability further influence P solubility (Ponnamperuma, 1972; Patrick and Khalid, 1974; Willett, 1989; Sanyal and De Datta, 1991). Under alternating soil redox conditions, amorphous Fe oxides are expected to control the solubility of both Fe (Brennan and Lindsay, 1998) and P (Sah et al., 1989). The P associated with amorphous phases in general, and with amorphous Fe oxides in particular, is further considered to be plant available (Guo and Yost, 1999; Dobermann et al., 2002).

Clearcutting, probably the most common harvesting technique in the region, has been shown to alter the site hydrological conditions, resulting in seasonally elevated watertables and soil moisture for several years following cutting (Riekerk, 1989; Sun et al., 2001; Bliss and Comerford, 2002; Xu et al., 2002). Pothier et al. (2003), working in a lowland conifer stand in eastern Canada, showed that the rise in the watertable was linearly correlated to the percentage of stand cut.

High temperatures and soil moisture content, high content of decomposable organic matter and low pH all favor reducing conditions (Liu et al., 1997), and are all characteristic of the region's highly weathered forest soils. Hence, reducing conditions in a clearcut are likely to occur to the extent that they will influence Fe oxides and P solubility. Under these conditions Fe oxides are expected to shift from a sink for the applied and native P during the rotation to a source for soluble and more available P following harvesting and regeneration. In this study, through the use of single selective chemical extractions and correlation analysis, we evaluate the relationships between native and applied P and Al and Fe oxides in some East Texas forest soils differing in

their drainage characteristics, eight years after mid-rotation P fertilization. Fertilization effects on total P accumulation in the forest floor and on total and potentially reducible P in the mineral soil upper 10 cm were evaluated.

## **Materials and Methods**

### Study sites

A fertilization experiment was installed on the property of Temple-Inland Forest Products Corporation during the spring of 1996 in mid-rotation commercial loblolly pine stands at 20 different locations in East Texas (Ngono and Fisher, 2001). Seven of these sites, located in five counties (Angelina, Houston, Jasper, Nacogdoches, Trinity) between longitudes N30°-31° and latitudes W93°-94° were used in the current study. The regional climate is humid warm temperate with a mean annual temperature of 20° C and mean annual precipitation from 1100 to 1400 mm along a northwest-southeast gradient.

The experimental plots were established on pre-selected sites that responded positively to nitrogen (N) and P fertilization. Each treatment was applied on a 0.04-ha plot (20x20 m) with a central 10x10-m sampling plot and 10-m buffer zones between treatment plots. The P treatments included hand-broadcasting triple superphosphate at a rate of 100 kg P ha<sup>-1</sup>. The sites were grouped into three drainage classes: 1) Excessively Well-Drained (ExWD), 2) Well-Drained or Moderately Well-Drained (WD), and 3) Poorly Drained or Somewhat Poorly Drained (PD) (Table 8). Soil classification was based on the county surveys and those of the landowner (Table 8). The sampled soil cores (1 m) were further used to verify soil classification as obtained by the above survey.

### Forest floor and mineral soil sampling and preparation

The P-fertilized treatment and the non-fertilized control plots from seven of the original 20 study sites were sampled from January to March 2004. Each sample plot was divided into five 2-m strips along the site elevation contour lines. Each strip was

Table 8. Soils taxonomic class, drainage class, and A horizon characteristics in the study sites.

Site	Soil Taxonomic Class	A horizon						Drainage Class <sup>##</sup>
		Sand	Clay	pH	CEC <sup>*</sup>	Carbon	Fe <sub>d</sub> <sup>#</sup>	
		— % —		1:2	cmol kg <sup>-1</sup>	— g kg <sup>-1</sup> —		
9	Loamy, siliceous, Arenic Paleudults	75	11	4.6	7.97	13.4	1.4	ExWD
11	Clay, mixed, Typic Hapludults	58	18	6.2	10.34	27.7	99.2	WD
20	Fine-loamy, siliceous, Aquic Glossudalfs	63	11	5.8	7.17	13.0	1.2	PD
22	Fine, smectitic, Vertic Hapludalfs	14	46	5.4	18.83	23.3	36.1	WD
25	Coarse-loamy, siliceous, Typic Glossudalfs	54	14	5.9	5.82	12.1	1.3	WD
33	Loamy, siliceous, semiactive, Arenic Plinthic Paleudults	67	11	5.3	5.63	11.3	1.6	PD
49	Coarse-loamy, siliceous, Glossic Paleudalfs	50	13	6.0	6.81	14.5	2.7	WD

<sup>\*</sup> Cation exchange capacity

<sup>#</sup> Citrate dithionite extractable Fe.

<sup>##</sup> ExWD- excessively well-drained; WD- well-drained; PD- poorly drained.

further divided into three rectangles to make 15 3.3x2-m rectangles per plot. Each rectangle was sampled, and the three samples from each strip were composited into one sample, giving five composite samples per plot. Before sampling the mineral soil, we placed a 20x20-cm wooden frame on the forest floor within each rectangle to allow the organic material within to be carefully cut at the frame edge, collected and combined with its other sub-samples to a composite sample, according to the layout described above. After removing the organic matter, hereafter referred to as “forest floor”, soil core samples were taken to 100 cm using an 8-cm diameter auger. The soil cores were

laid on plastic sheets on the surface where a typical genetic profile was characterized and used for verification of the soil classification as adapted from the soil surveys. The cores were sampled at eight depth intervals (0-10, 10-20, 20-30, 30-40, 40-50, 50-70, 70-85, and 85-100 cm). No distinction was made between depth intervals 70-85 and 85-100 cm in site 22, but rather a 70-100 cm depth interval was sampled. The soil at each depth increment was composited according to the same layout described above. Each composited soil sample was mixed and a 1.5-kg subsample was air dried and ground to pass a 2-mm screen. Fifteen grams of soil from each sample were further ground to pass a 150- $\mu$ m sieve. The <150- $\mu$ m samples were stored in plastic bags at 4°C and the rest of the sample was stored at room temperature for further analysis. The forest floor samples were dried at 65° C to constant weight in an air-circulating drying oven, weighed, and subsampled. The forest floor total dry weight was used to calculate the forest floor mass. The sub-samples were ground to pass a 250- $\mu$ m sieve and stored in sealed plastic containers at room temperature.

#### Soil and forest floor analysis

Soil characteristics (i.e., pH, cation exchange capacity (CEC), texture, exchangeable acid and bases) were determined on the middle strip composited samples of the control plot from each site. Soil pH was determined in distilled water at a 1:2 soil-solution ratio using a combination glass electrode; exchangeable bases (potassium (K), calcium (Ca), magnesium (Mg), and sodium (Na)) and exchangeable acidity were determined by the  $\text{NH}_4\text{OAc}$  (at pH 5.5) and the  $\text{BaCl}_2$ -TEA methods, respectively, following Thomas (1982). CEC was calculated as the sum of the exchangeable acidity and bases. Texture was determined by the hydrometer method (Day, 1965). Soil water holding capacity and bulk density were estimated from the soil texture according to Saxton et al. (1986). The composited samples of the forest floor and the upper 40 cm of the mineral soil were analyzed for total nitrogen (N), carbon (C), and P. Nitrogen and C were determined by an NC analyzer (Thermo Finnigan, Flash EA 1112 series, Milano, Italy) on 10- and 50-mg samples from the forest floor and the mineral soil, respectively. Available P was determined by the double dilute acid extraction procedure (i.e.,



Mehlich-1) according to Olsen and Sommers (1982). Total P ( $P_T$ ) was determined on 0.1- and 0.2-g forest floor and soil samples, respectively, by  $HClO_4$  digestion following Kuo (1996). Separate soil samples were also extracted by acid ammonium-oxalate (AAO) (2 h, pH 3.00, in the dark), and citrate dithionite (CD) (at room temp for 16 h) following the procedures outlined by Loeppert and Inskeep (1996). Citrate-dithionite extractable Al ( $Al_d$ ) and Fe ( $Fe_d$ ), and AAO-extractable Al ( $Al_{ox}$ ) and Fe ( $Fe_{ox}$ ) were determined by flame atomic absorption (Varian SpectrAA 220FS, Mulgrave, Victoria, Australia). Iron in crystalline Fe oxides ( $Fe_{d-ox}$ ) was calculated by the difference between the CD and the AAO-extractable Fe following Parfitt and Childs (1988).

Total P, CD and AAO-extractable P ( $P_d$ , and  $P_{ox}$ , respectively) were determined colorimetrically by the molybdenum-ascorbic acid method using a continuous flow injection analyzer (OI Analytical, APKEM FS 3000, College Station, TX). The  $P_d$  and  $P_{ox}$  were determined without pre-digestion of the extracts. Alternatively, sample aliquots were diluted prior to the analysis, at a rate where no interferences from oxalate or citrate were observed during the colorimetric reaction. This was achieved by monitoring the peak development of a series of AAO and CD blank dilutions spiked with a known amount of P. Eight and 4x dilution of the AAO and CD extracts, respectively, were found to be adequate for the colorimetric reaction to proceed without the extract medium interference. At these dilution rates, spiked soil extracts were further used to verify the accuracy and precision performance of the analytical procedure, as described in details in the colorimetric determination of soil P in AAO and CD extracts in section two. Pre-dilution at the above rates was further used to colorimetrically determine the AAO- and CD-extractable P from the soil samples.

Based on  $P_T$ ,  $P_d$  and  $P_{ox}$ , P distribution between the following operationally defined forms was calculated accordingly:  $P_{d-ox}$ , or P associated with crystalline Fe oxides, was calculated by the difference between  $P_d - P_{ox}$ ;  $P_{ox}$ , was adsorbed P and P associated with amorphous minerals. Under the analytical procedures used in this study, i.e., CD and AAO pre-dilution rather than pre-digestion prior to the colorimetric reaction, AAO- and CD-extractable organic P were analytically excluded from being

detected, and hence from being accounted for in  $P_d$  and  $P_{ox}$  and hence from the derived subsequent P forms.

The amount of P in the forest floor or the mineral soil's upper 10 cm was further calculated for each composite sample based on its P concentration and its forest floor mass (or its estimated bulk density for mineral soil).

#### Statistical analysis

The average value from the five composited samples of each treatment plot was used for statistical analysis using SAS PROC GLM (SAS Institute, 2002). Linear contrasts were used to compare drainage classes. The drainage groups are summarized above (Table 8). SigmaStat 2.03 (SigmaStat, 1997) was used for regression and paired t-test analyses. Multiple comparisons were determined by Tukey HSD (at  $p < 0.05$ , unless otherwise specified) using JMP 5.0.1.a (JMP, 2002).

### **Results**

#### Phosphorus in the mineral soil

Eight years after mid-rotation P fertilization, near the end of a 30-yr rotation, a marked treatment effect was found in the forest floor and the mineral soil P content and P distribution within the soil profile and between the different operationally defined P forms. Total P ( $P_T$ ), Mehlich 1 (M-1),  $P_{ox}$ , and  $P_d$  in the mineral soil profile of the experimental plots in the different sites are presented in Table 9. Mehlich-1 P in the upper 20 cm was significantly higher in the fertilized plots

Table 9. Mehlich 1 (M-1) P, total phosphorus ( $P_T$ ) and acid ammonium-oxalate ( $P_{ox}$ ) and citrate-dithionite ( $P_d$ ) extractable P (as % of  $P_T$ ) in the soil profile of the experimental plots. Values are averages of five composite samples.

Depth (cm)	Control Plot				Fertilized Plot			
	P <sub>T</sub>	M-1	P <sub>ox</sub>	P <sub>d</sub>	P <sub>T</sub>	M-1	P <sub>ox</sub>	P <sub>d</sub>
	— mg kg <sup>-1</sup> —		% of P <sub>T</sub>		— mg/kg —		% of P <sub>T</sub>	
site 9								
0-10	48.5	0.54	16	32	66.1	3.99	14	44
10-20	48.2	0.54	8	24	63.9	4.55	16	42
20-30	41.9	0.40	14	54	55.9	1.67	8	33
30-40	42.7	0.36	8	57	49.0	0.57	8	38
40-50	43.7	0.41	12	61	45.6	0.57	10	39
50-70	41.9	0.42	11	74	44.7	0.54	12	55
70-85	43.9	0.43	11	69	41.7	0.48	12	56
85-100	46.2	0.42	8	90	46.1	0.34	9	63
site 11								
0-10	514	1.29	4	60	262	3.45	10	68
10-20	558	1.02	3	63	216	0.83	9	71
20-30	545	0.77	3	66	222	0.60	7	67
30-40	486	0.54	5	73	215	0.55	5	71
40-50	444	0.44	4	78	211	0.46	10	76
50-70	397	0.51	3	85	193	0.39	9	67
70-85	446	0.63	4	78	165	0.39	11	70
85-100	362	0.55	3	78	157	0.42	6	69
site 20								
0-10	64.0	0.75	7	28	67.8	1.52	10	23
10-20	55.9	0.42	8	25	50.1	0.68	8	25
20-30	37.4	0.29	8	32	38.7	0.35	7	24
30-40	31.5	0.18	10	41	33.0	0.28	8	36
40-50	30.3	0.16	12	2	32.5	0.24	6	31
50-70	30.2	0.20	9	5	33.3	0.17	5	26
70-85	34.1	0.26	11	33	43.5	0.16	6	62
85-100	41.8	0.29	10	31	57.0	0.19	6	10
site 22								
0-10	385	0.95	6	45	406	1.69	5	44
10-20	321	0.62	5	42	270	0.83	4	38
20-30	264	0.43	4	28	241	0.72	5	26
30-40	233	0.39	5	29	210	0.65	5	25
40-50	207	0.34	3	22	190	0.52	7	25
50-70	197	0.30	3	19	182	0.38	3	25
70-100	207	0.31	3	30	178	0.37	3	32

Table 9. continued.

Depth (cm)	Control Plot				Fertilized Plot			
	P <sub>T</sub>	M-1	P <sub>ox</sub>	P <sub>d</sub>	P <sub>T</sub>	M-1	P <sub>ox</sub>	P <sub>d</sub>
	— mg kg <sup>-1</sup> —		% of P <sub>T</sub>		— mg kg <sup>-1</sup> —		% of P <sub>T</sub>	
site 25								
0-10	65.7	0.91	5	10	85.4	5.42	16	20
10-20	45.3	0.73	6	20	65.5	3.23	11	18
20-30	38.4	0.51	7	12	39.8	0.70	3	25
30-40	26.9	0.36	5	22	35.5	0.43	2	26
40-50	25.9	0.25	6	23	34.9	0.34	4	36
50-70	31.7	0.20	4	16	41.2	0.29	7	58
70-85	45.3	0.27	4	49	50.9	0.25	6	41
85-100	50.0	0.28	2	63	54.1	0.24	4	47
site 33								
0-10	40.1	0.65	8	19	49.8	1.70	5	29
10-20	31.0	0.39	6	20	36.3	0.92	2	29
20-30	23.8	0.27	6	29	29.8	0.58	6	44
30-40	37.7	0.22	1	75	32.6	0.34	3	64
40-50	55.3	0.24	1	72	38.9	0.30	1	67
50-70	56.4	0.35	0	63	55.5	0.31	1	82
70-85	56.8	0.27	0	58	60.7	0.35	1	99
85-100	52.0	0.24	1	37	53.7	0.38	0	100
site 49								
0-10	51.5	0.92	5	20	56.7	4.10	17	34
10-20	47.8	0.50	4	19	36.7	1.07	9	30
20-30	44.3	0.28	4	30	37.8	0.36	3	43
30-40	51.6	0.21	3	33	41.5	0.22	4	53
40-50	71.0	0.25	4	36	45.6	0.23	3	59
50-70	51.9	0.22	5	66	49.8	0.20	3	59
70-85	62.5	0.22	3	54	53.2	0.19	5	82
85-100	47.9	0.25	6	77	49.5	0.19	5	84

than in the control plots, with no significant differences between treatments or depth thereafter (Fig. 13). Average M-1 in the 0-10 and 10-20 cm layers were 0.86 and 0.60 mg P kg<sup>-1</sup> in the control plots, and 3.12 and 1.73 mg P kg<sup>-1</sup> in the fertilized plots, respectively. Total P, P<sub>d</sub>, and P<sub>ox</sub> were not significantly different among treatments or depth across sites (Fig. 13).

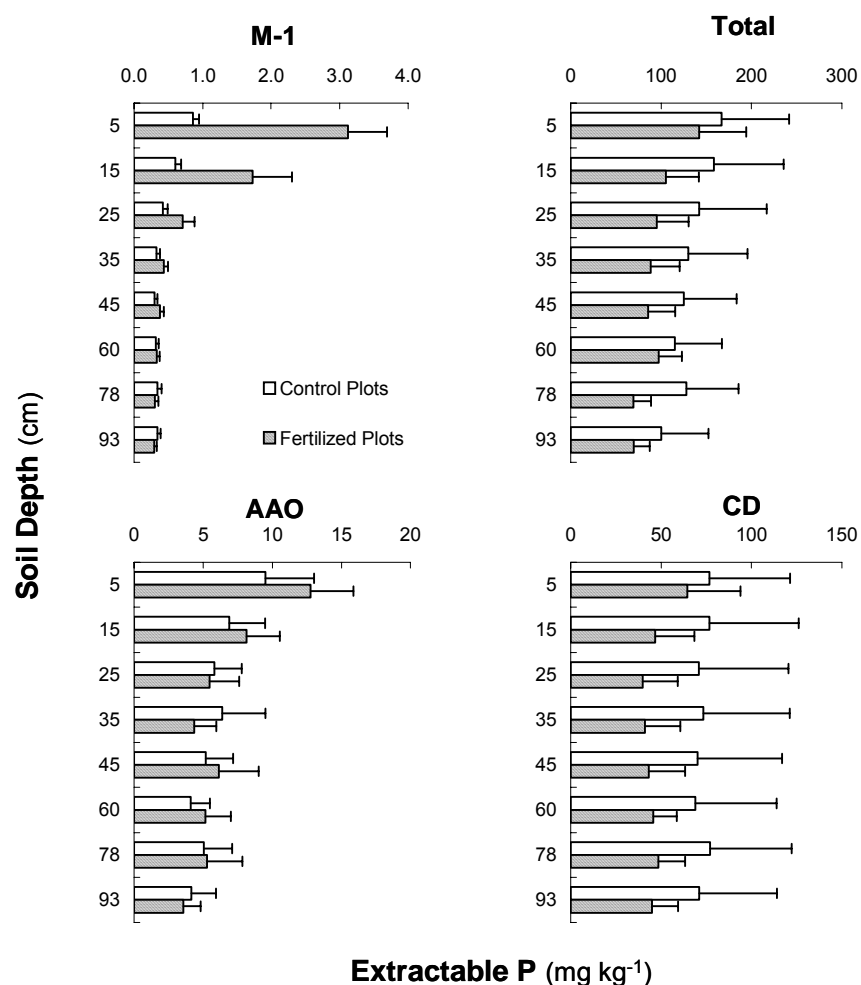


Fig. 13. Phosphorus (P) distribution in the profiles of the different experimental plots. Average values of total, citrate-dithionite (CD), acid ammonium-oxalate (AAO) and Mehlich 1 (M-1) extractable P across sites experimental plots are presented (n=7). Soil depth is specified as the middle of the soil-sampling interval. Error bars are one standard error.

The  $P_T$  and  $P_d$  values in the control plot of site 11 were much higher than in the fertilized plot. Yet, omitting site 11  $P_T$  and  $P_d$  from the statistical analysis did not change the above pattern and statistical significance. Treatment effect by site and depth, evaluated by a paired t-test, was significant only for  $P_T$  ( $p < 0.01$ ) and  $P_d$  ( $p < 0.02$ ) in the soil upper 0-10 cm (when excluding site 11 data).

All P forms were significantly different among drainage classes. Both  $P_T$  and  $P_d$  in the WD sites (169 and 89 mg P kg<sup>-1</sup>, respectively) were significantly higher than in the ExWD and PD sites (48 and 26 mg P kg<sup>-1</sup>, and 43 and 19 mg P kg<sup>-1</sup>, respectively) across depths and treatments. The  $P_d/P_T$  ratios, representing the fraction of  $P_T$  associated with Fe oxides, were 0.53, 0.54, and 0.44 in the WD, ExWD and the PD sites, respectively. This suggests that the PD sites have a lower proportion of their  $P_T$  associated with Fe oxides. The value  $P_d - P_{ox}$  ( $P_{d-ox}$ ), which reflects the P associated with crystalline Fe oxide was calculated as well.  $P_{d-ox}$  had the same pattern and significance as was found for  $P_d$ , with  $P_{d-ox}$  values of 81, 19, and 17 mg P kg<sup>-1</sup>, in the WD, ExWD and PD sites, respectively.  $P_{ox}$  was significantly different among drainage classes across depths and treatments, with WD > ExWD > PD (8.3, 5.4, and 2.2 mg P kg<sup>-1</sup>, respectively), suggesting more P is associated with amorphous phases under WD conditions. Yet, although not significantly different, the  $P_d$  fraction associated with amorphous phases, as indicated by the  $P_{ox}/P_d$  ratio, was higher on the poorly drained sites (0.46, 0.24, and 0.16 in the PD, ExWD, and WD, respectively). This implies that although higher amounts of P reside in the amorphous phases under well-drained conditions, its relative distribution in the  $P_{ox}$  (as a fraction of  $P_d$ ) is yet not significantly different among drainage classes. Moreover, in the control plot on site 20, a poorly drained site,  $P_{ox}$  exceeds  $P_d$  within the 40-70 cm depth intervals (Table 9), where soil moisture was found to be highest (181 % of its moisture content at field capacity) and  $P_T$  to be the lowest (Fig. 14) at this site. The higher pH at this depth interval (average of 6.5 at 40-70 cm compared to an average of 5.8 below and above) and the higher base saturation (75 %; Fig. 15) suggests that Ca-P minerals may precipitate at this depth and were further dissolved under the acidic condition of the AAO extraction procedure (pH=

3.00), but not under that of the CD ( $\text{pH} \approx 6.2$ ). Furthermore, since bicarbonate is not included in the CD extraction, the promotion of Ca-P solubility by the common ion effect

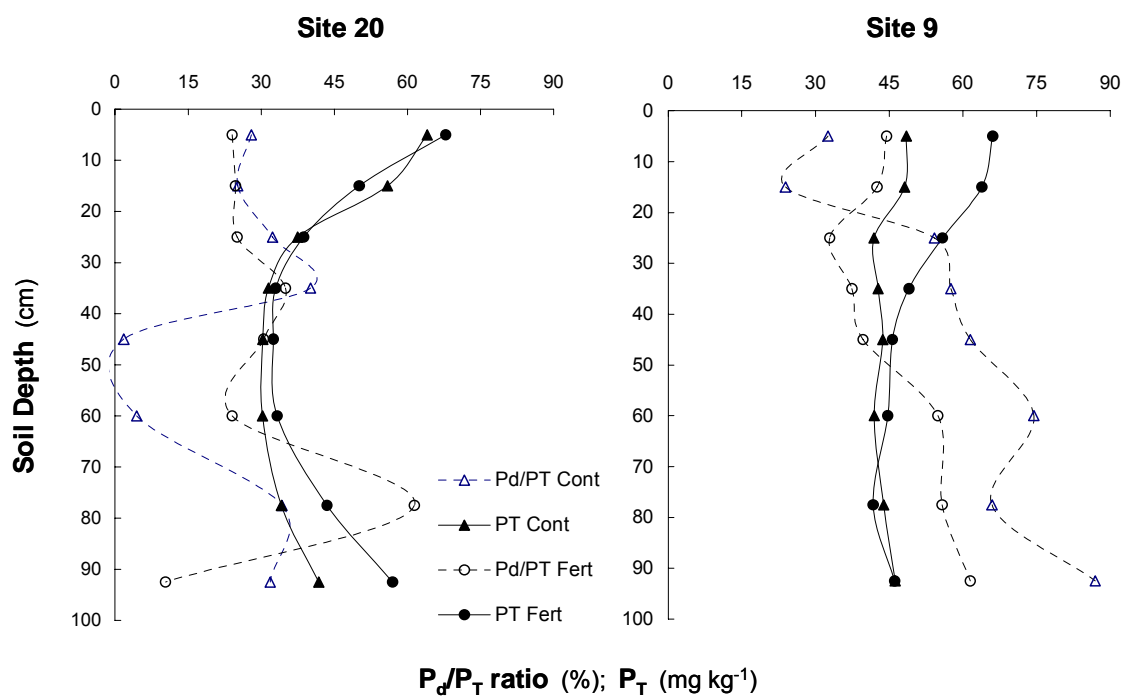


Fig. 14. Distribution of total phosphorus ( $P_T$ ) and  $P_d/P_T$  ratio in the control plots (Cont) and P-fertilized plots (Fert) in the soil profile in site 20 and site 9. The  $P_T$  and  $P_d/P_T$  values are averages of five composite samples.

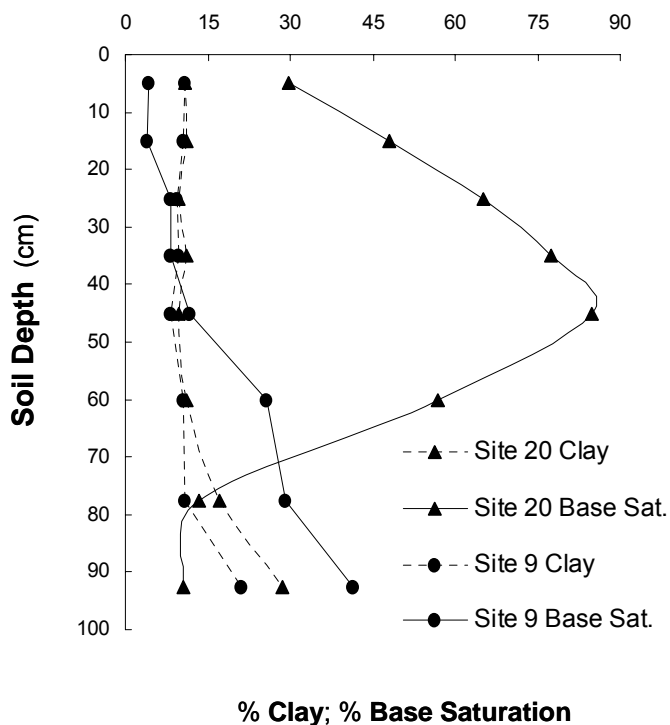


Fig. 15. Distribution of % clay and % base saturation (base sat.) in the soil profile in site 20 and site 9.

(i.e., carbonate; Olsen et al., 1954) is omitted. The acidic conditions of the AAO may further promote hydrolysis of organic P and result in inclusion of some hydrolysable organic P (under the AAO extraction conditions) as  $P_{ox}$ . Yet, excluding site 20 40-70 cm  $P_{ox}/P_d$  ratio data from the statistical comparison did not influence the negligible significance differences found between drainage classes or treatments, across depths. Moreover,  $P_T$  content in the soil profiles of site 20 were the lowest at this depth (40-70 cm) in both the control and the fertilized plots (Table 9, Fig. 14) ; suggesting low P retention in this section, regardless of the controlling (contributing) solid phase. The increase in  $P_T$  in the fertilized plot coincides with an increase in  $P_d/P_T$  (open symbols, Fig. 14) in both sites, suggesting an increase in Fe oxide-associated P in the zone of treatment  $P_T$  accumulation. The overall  $P_{ox}/P_d$  in this study was still well below 0.5 with



an average of  $0.26 \pm 0.70$  and a median at 0.137 (mean of  $0.18 \pm 0.15$  and median of 0.136 when excluding data from site 20 control 40-70 cm).

Total P distribution in the profile of site 9, the excessively drained soil, and in site 20, a poorly drained soil, was markedly different although both soils had similar clay content and clay distribution in their profiles (Fig. 14). Fertilization resulted in an increase in  $P_T$  in the upper 30 cm in the ExWD site, followed by a diminishing treatment effect further down the profile. Both native and applied P seemed to accumulate in the topsoil at the ExWD site. Fertilization in the PD site resulted in an apparent increase in  $P_T$  below 60 cm, where  $P_T$  in the upper soil profile seemed to be less affected by the treatment (Fig. 14). As in the ExWD,  $P_T$  decreased with depth in the upper part of the profile, yet both native and applied  $P_T$  seemed to accumulate below 60 cm in the PD site.

The distribution pattern of applied P in the soil profile under the soil drainage characteristics in this study is shown for site 9 (excessively well-drained), sites 25 and 49 (well-drained), and site 33 (poorly drained) (Fig. 16).  $P_d$  and  $P_T$  distribute from the surface horizons to lower parts of the profile in the order: PD > WD > ExWD. This suggests that P movement in the soil profile is more limited in the ExWD than in the WD, and in both less than in the PD soil. The more level terrain and yellowish hue in the profile in site 49 suggests this soil is subjected to higher wetness conditions than the other WD members, where much more red hues prevailed, and hence may represent drainage characteristics between WD and PD.

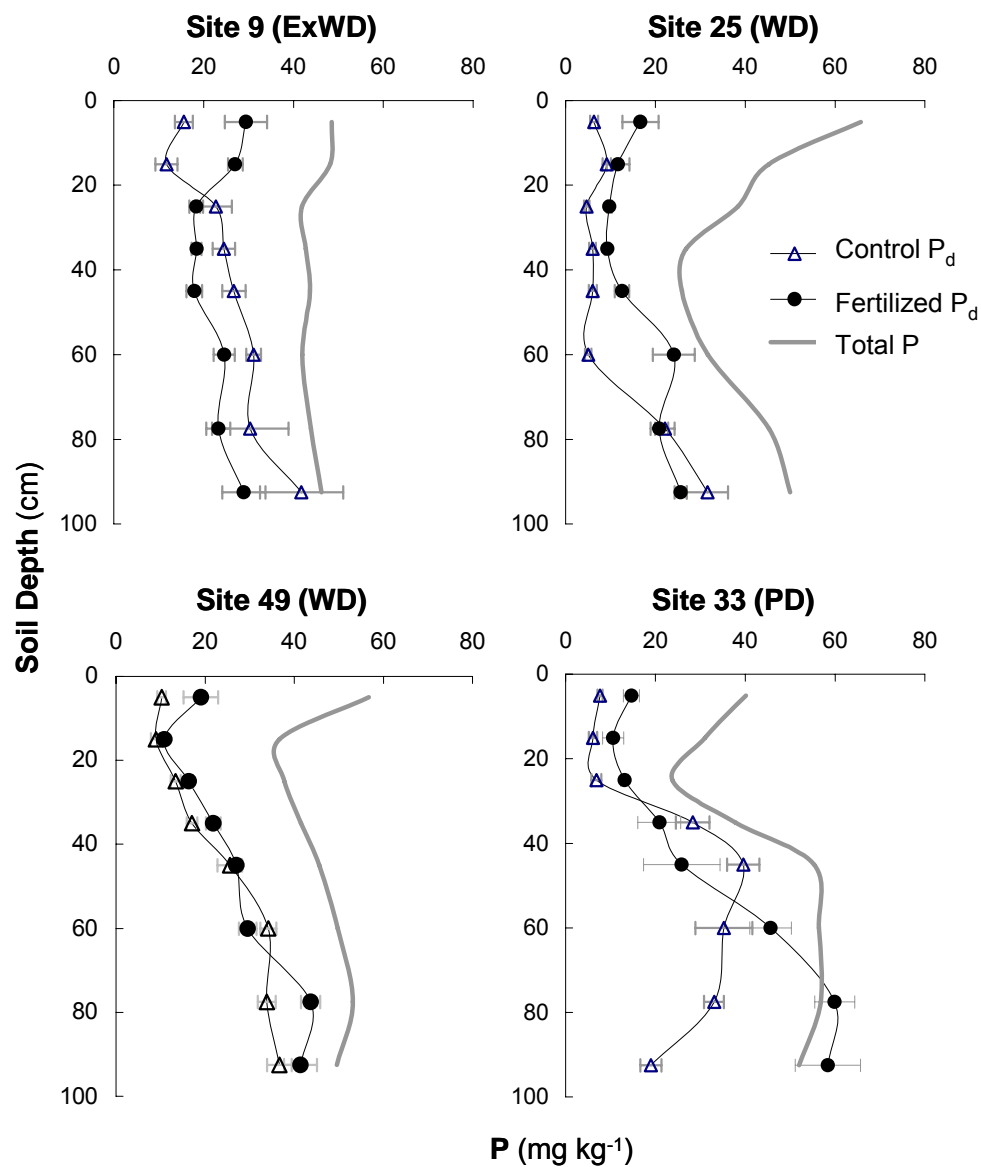


Fig. 16. Citrate-dithionite extractable P ( $P_d$ ) distribution in the profile of soil from different drainage classes.  $P_d$  in the treatment plot (closed symbols), control plot (open symbols), and total P in the treatment plots (solid line, no symbols) in the profile of excessively drained (site 9), well-drained (site 25, 49) and in poorly drained sites (site 33) are presented. For clarification selected profiles are included. Results are averages of five composite samples from each plot; error bars are of one SE.

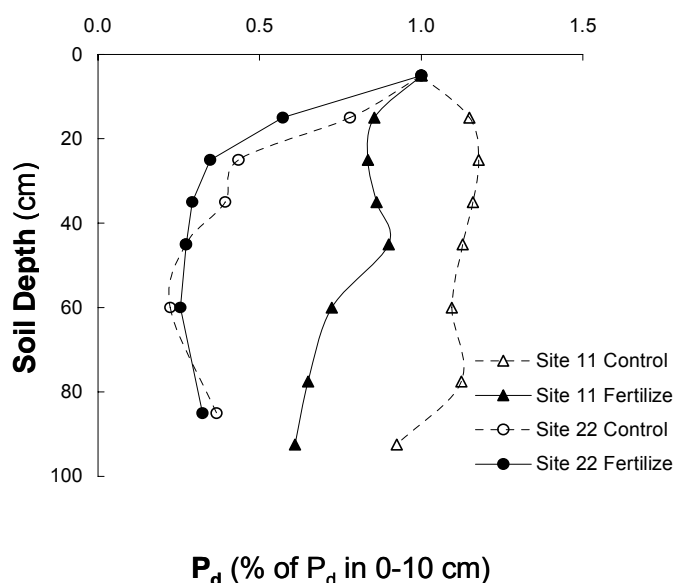


Fig. 17. Distribution of citrate-dithionite extractable phosphorus ( $P_d$ ) in site 22 and site 11, well-drained site with high clay and iron oxide contents. Values are averaged of five composite samples at each plot presented as a fraction of the soil 0-10 cm  $P_d$  content. Error bars are one SE.

Furthermore, on well-drained soils with high Fe oxides and/or clay contents, the redistribution of native and applied  $P_d$  down the soil profile was much more limited (Fig. 17). The soil on site 22 is composed of much finer texture than all other soils, with average clay content throughout the profile of  $74 \pm 17\%$  on Site 22 and  $22 \pm 14\%$  on the other sites. This site also contains high Fe oxides (Table 8). A similar, yet less pronounced accumulation of  $P_d$  in the soil upper 10 cm and limited distribution down the profile thereafter was found in site 11 (Fig. 17). This site contained less clay (18%) but higher Fe oxides ( $99 \text{ g kg}^{-1}$ ) than site 22 (46 % clay and  $36 \text{ g kg}^{-1}$  Fe oxides). On both sites, similar  $P_d$  concentration was found in the upper 10 cm of the fertilized plots ( $179$  on site 11 and  $178 \text{ mg P kg}^{-1}$  on site 22), about ten times higher than in all other soils ( $19.1 \pm 6.0$ ). The differences in clay and Fe oxide content, and moreover the soil pH differences (6.2 and 5.4 in site 11 and 22, respectively) (Table 9) between sites 11 and 22 may further imply higher contributions of Al oxides to P retention in site 22.

Total P,  $P_d$  and  $P_{ox}$  from all sites, depths and treatments were further examined by correlation analysis with respect to soil  $Fe_d$ ,  $Fe_{ox}$ ,  $Al_d$ , and  $Al_{ox}$ . All correlations were highly significant ( $p < 0.0001$ ).  $P_T$  and  $P_d$  were highly correlated with  $Fe_d$  ( $r = 0.92$  and

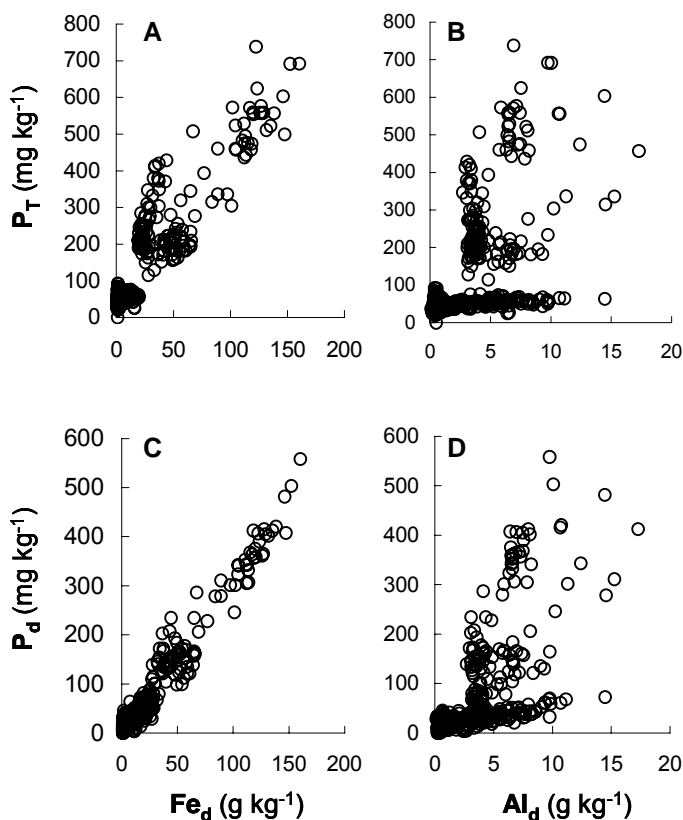


Fig. 18. Relationships of total phosphorus ( $P_T$ ) and citrate-dithionite (CD) extractable P ( $P_d$ ) with CD extractable iron ( $Fe_d$ ), (A and C, respectively) and with aluminum ( $Al_d$ ), (B, and D, respectively). Results from all sites, treatments, and depth are presented.

0.98, respectively; Fig. 18A and C) and to a much lesser extent with  $Al_d$  ( $r = 0.58$  and 0.67, respectively; Fig. 18B and D).

$P_T$  and  $P_{ox}$  correlation with  $Fe_{ox}$  and  $Al_{ox}$  were lower than their CD-extractable counterparts. Yet,  $Fe_{ox}$  correlation with  $P_T$  and  $P_{ox}$  ( $r = 0.65$  and 0.58, respectively; Fig.

19A and C) was higher than that of  $Al_{ox}$  ( $r = 0.53$  and  $0.49$ , respectively; Fig. 19B and D). The high correlation between  $P_T$  and  $P_d$  with  $Fe_d$  across sites, drainage

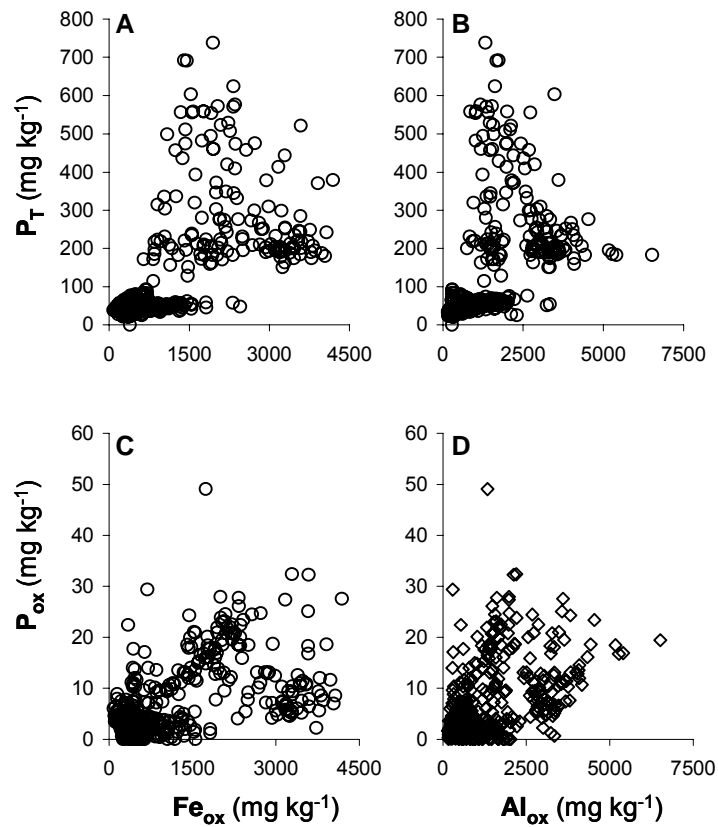


Fig. 19. Relationships of total phosphorus ( $P_T$ ) and acid ammonium-oxalate (AAO) extractable P ( $P_{ox}$ ), with AAO extractable iron ( $Fe_{ox}$ ), (A and C, respectively) and with AAO extractable aluminum ( $Al_{ox}$ ), (B and D). Results from all sites, treatments and depths are presented.

classes, depths and treatments strengthen the apparent relationship between soil P and soil Fe oxides.

Table 10. Correlation coefficients of analysis between acid ammonium-oxalate extractable P and Mehlich-1 extractable-P in the soil 0-20 cm layers (n=10).

Treatment	Site						
	9	11	20	22	25	33	49
Control	-0.056	0.477	0.037	0.539	0.402	0.788**	0.666*
Fertilized	0.968***	0.958***	0.796**	0.805**	0.986***	0.983***	0.985***

\* Significant at  $p<0.05$ ; \*\* Significant at  $p<0.01$ ; \*\*\* Significant at  $p<0.001$

Available P, as indicated by M-1 extraction, was significantly and highly correlated with  $P_{ox}$  in the 0-20 cm of all fertilized plots (Table 10).

#### Phosphorus in the forest floor

Phosphorus fertilization resulted in an increase in both P concentration and in total mass of the forest floor (Table 11). Phosphorus concentration in the fertilized plots ( $449\pm 82$  mg P  $kg^{-1}$ ) was significantly higher than that in the control plots ( $321\pm 62$  mg P  $kg^{-1}$ ) (Fig. 20), ranging from 353 to 620 mg P  $kg^{-1}$  and from 269 to 390 mg P  $kg^{-1}$ , respectively (Table 11).

Table 11. Forest floor mass and phosphorus concentration and content in the forest floor in the experimental plots. Values are averages of five composite samples.

Site	Control plot			Fertilized plot		
	Forest Floor	Phosphorus		Forest Floor	Phosphorus	
	Mg ha <sup>-1</sup>	mg kg <sup>-1</sup>	kg ha <sup>-1</sup>	Mg ha <sup>-1</sup>	mg kg <sup>-1</sup>	kg ha <sup>-1</sup>
9	42	269	11	50	448	22
11	21	366	8	35	353	13
20	17	246	4	29	423	13
22	25	377	12	26	620	16
25	25	390	10	24	427	10
33	15	254	4	26	437	11
49	14	343	5	20	432	9

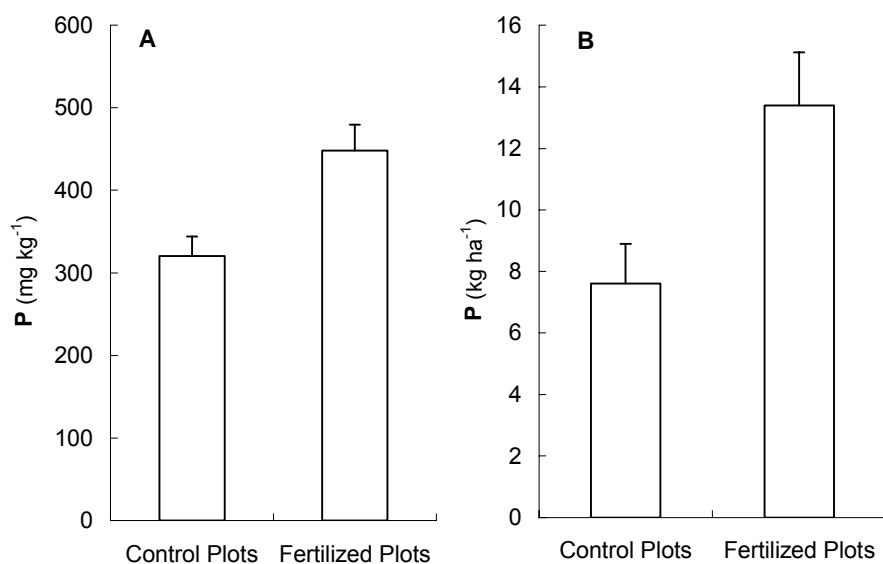


Fig. 20. Average phosphorus (P) concentration (A) and content (B) in the forest floor of the control and the fertilized plots (n=7). Vertical bars are one standard error.

The generally higher accumulation in forest floor mass in the fertilized plots than in the control plots (average  $30.1 \pm 9.8$  and  $22.1 \pm 9.6$  Mg ha<sup>-1</sup>, respectively) resulted in

significantly ( $p < 0.005$ ) higher P content in the fertilized than in the control plots ( $13.4 \pm 4.6$  and  $7.6 \pm 3.4$  kg P ha<sup>-1</sup>, respectively) (Fig. 20).

#### Treatment effect on forest floor and on upper 10-cm mineral soil P contents

The amount of  $P_T$  and  $P_d$  in the soil upper 10 cm in each plot was estimated and the treatment effect was evaluated by the difference between the treatment and the control plot at each site. Phosphorus content in the upper 10 cm was calculated based on the concentration of the relevant P form and the estimated bulk density for the soil upper 10 cm (based on its texture; Saxton et al., 1986). Treatment effects on P content in the forest floor and on the different P forms in the upper 10 cm of the mineral soils are reported (Table 12).

Fertilization resulted in an average increase of  $8.0 \pm 5.1$  Mg ha<sup>-1</sup> and  $5.8 \pm 3.5$  kg ha<sup>-1</sup> in the forest floor mass and P content, respectively (Table 12). The treatment effect on  $P_T$  and  $P_d$  in the soil upper 10 cm was the highest on site 9, the ExWD and the lowest on site 20, a poorly drained site, where a negative treatment effect on  $P_d$  was found ( $21.5$  and  $-3.3$  kg  $P_d$  ha<sup>-1</sup>, respectively) (Table 12). Across sites (excluding site 11), fertilization resulted in an average increase of  $18.6 \pm 10.4$  and  $10.8 \pm 8.4$  kg P ha<sup>-1</sup> in  $P_T$  and  $P_d$ , respectively. Given the much higher  $P_T$  and  $P_d$  concentrations in the mineral soil of the control plot on site 11 (Table 9), this site results for the differences between treatments were excluded from the comparison and from the overall calculated average difference between treatments.



Table 12. Fertilization treatment effect on forest floor mass and total phosphorus ( $P_T$ ) content in the forest floor, and on  $P_T$  and  $P_d$  content in the soil upper 10-cm eight years after application. Reported values are the difference between the forest floor mass and P contents in the fertilized and the control plots. P content per ha was calculated based on the forest floor mass for the forest floor, and on an estimated bulk density (see text for details) for the soil upper 10 cm.

Site	Forest Floor		Mineral Soil (0-10 cm)	
	Mass	$P_T$	$P_T$	$P_d$
	Mg ha <sup>-1</sup>	kg ha <sup>-1</sup>	kg ha <sup>-1</sup>	
9	7.6	11.2	27.4	21.5
11	14.1	4.7	— <sup>#</sup>	—
20	12.8	8.5	5.8	-3.3
22	5.9	4.3	26.2	7.6
25	-0.9	0.4	29.4	15.4
33	10.8	7.5	15.0	10.8
49	5.9	3.9	7.8	13.1
Average	8.0±5.1	5.8±3.5	18.6±10.4	10.8±8.4

<sup>#</sup> Site 11 results were omitted from the comparison (see text for details)

The average treatment effect on  $P_{d-ox}$  in the soil upper 10 cm was  $5.7±8.8$  kg P ha<sup>-1</sup> across sites. This value is comparable to the increase in P content in the forest floor ( $5.8±3.5$  kg P ha<sup>-1</sup>). Considering that CD organic P is excluded by the analytical approach used in this study (i.e., pre-dilution instead of pre-digestion before the colorimetric determination) the difference  $P_T - P_d$  can be used to estimate the organic P. The overall treatment effect on organic P in the forest floor and within the mineral soil upper 10 cm is  $13.5±11.9$  kg P ha<sup>-1</sup>, across sites. The treatment effect on P in the forest floor, organic P in the forest floor and the mineral soil upper 10 cm, and  $P_T$ ,  $P_d$  and  $P_{d-ox}$  in the upper 10 cm of the mineral soil is equivalent to 6, 14, 19, 11 and 6 % of the applied P (i.e., 100 kg P ha<sup>-1</sup>), respectively, equivalent to a total of 24 % of the applied P. Other pools where the applied P may reside include above- and below-ground vegetation, as well as in the mineral soil below the top 10 cm. As shown in Fig. 16, the treatment effect is shifting down the mineral soil profile with increase in the site moisture regime. This further suggests that treatment effect on accumulated P in the mineral soil will be higher for PD sites if lower parts of the profile are included.

## Discussion

Similar trends of decrease in total P and in P associated with Fe oxides with increase in site wetness and reducing regime were reported by Miller et al. (2001) along a climosequence in Hawaiian forest soils. A similar pattern of increase in total P with depth was reported by Walbridge et al. (1991) in an Ultisol and Inceptisol. Kuo and Mikkelsen (1979), comparing soil cultivated 56 years for rice to an adjacent pasture soil, showed a similar shift in P distribution in the soil profile as was found in this study among sites of different drainage classes. Iron oxide-associated P (defined as the NaOH extractable P in the modified Chang and Jackson sequential extraction; Williams et al., 1967) increased in the rice cultivated soil below the upper 40 cm compared to the pasture soil, as was found in the poorly drained sites in this study when compared to the other drainage classes. Yet, one needs to account for the different geologic formation, and hence the different parent materials and the initial P content when evaluating the differences in P content obtained between the soils of the different drainage classes.

Accumulation of P in the forest floor of fertilized forest stands was suspected to account for the residual effect of fertilization on subsequent rotations (Comerford et al., 2002). Phosphorus in intensively P-fertilized agricultural soils increased in the potentially reducible Fe oxides phases (Ruiz et al., 1997). The two pools were evaluated in this study. The overall treatment effect on soil P resulted in significant increases in total P in the soil upper 10 cm, most of which was associated with Fe oxides. The comparable, or higher, treatment effect on Fe oxide-associated P in the mineral soil upper 10 cm, compared to the P content in forest floor exemplifies the role of Fe oxides as a sink for P during the stand rotation. Subtracting the AAO-extractable P from the CD extractable P in the upper 10 cm of the mineral soil resulted in equal amounts of P accumulation in that layer and in the forest floor in response to the treatment. The former extraction (i.e. AAO) is considered to represent amorphous Fe oxide-associated elements, yet a broader suite of solid phases contributes to the overall extractable P by this method. Hence, subtracting the AAO-extractable P from the CD extractable P should be considered a more conservative estimation of Fe oxide-associated P. The

analytical procedure used in this study (i.e., pre-dilution instead of pre-digestion prior to the colorimetric determination) is thought to restrict the detectable P, in either extraction, mostly to P in inorganic form (or the “molybdenum reactive” P). Hence, considering the above and the characteristics of the soils used in this study (e.g. weathering stage, pH) contribution from phases other than Fe oxides is much less likely. Aluminum oxides and Ca-P, as was suggested in site 22 and at distinct locations of higher pH in the profile in site 20, respectively, are likely to be the main other contributors to the AAO-extractable P. Still, estimating the Fe oxide-associated P by the above subtraction approach combined with the analytical exclusion of organic P gives a sound basis for the estimation of crystalline Fe oxide-associated P, yet underestimates the overall Fe oxide associated-P by excluding the amorphous Fe oxide-associated P (i.e. AAO-extractable P). Furthermore, since Fe oxide-associated P was shown to redistribute from crystalline Fe oxides phases to amorphous ones, under alternating inundation conditions (Kuo and Mikkelsen, 1979) the above subtraction approach will be biased towards well-drained sites over poorly drained sites. Yet, under any approach used in operationally defining the phase association of the extractable P in this study, a substantial portion of the native and applied P was found to be associated with Fe oxide by the end of the 30-yr rotation, and in higher proportions in the surface soils of the well and extensively well-drained sites than in the poorly drained ones. As such, this P pool (i.e., Fe oxide-associated P) is potentially subjected to changes induced by forest harvesting on soil Fe oxide stability.

The removal of the site evapotranspirational pump by clearcutting<sub>7</sub> has been shown to increase site soil moisture content, to elevate the watertable, and in level terrain to increase the frequency and duration of flooding events for several consecutive years following the disturbance (Riekerk, 1989; Bliss and Comerford, 2002; Pothier et al., 2003). Considering the regional environmental conditions (e.g., high temperatures) these changes in site hydrology are likely to enhance reducing conditions. Under alternating redox conditions ferrihydrite is expected to control Fe (Breemen 1988a; Brennan and Lindsay, 1998) and P (Sah et al., 1989) solubility. Hence, the reducing environment, induced by clearcutting likely promotes the redistribution of Fe oxide-

associated P from less available forms (e.g., occluded within the Fe oxide crystalline phase) to more available forms (e.g., adsorbed on amorphous Fe oxides). Moreover, since forest soil upper 0 to 20 cm exhibit higher reducible organic matter and a lower redox potential than further down the profile (Ding et al., 1984) it is the P in these depth intervals that is suggested to be more susceptible to the above proposed redistribution upon enhancement in soil moisture. Hence, a larger effect may be expected on the well-drained site, where accumulation of P in the soil upper 10 cm was found to be more pronounced than on the poorly drained ones in this study (Table 12). Since amorphous phases have a higher sorption capacity than their crystalline counterparts (Parfitt et al., 1975; Breemen, 1988b; Parfitt, 1989) most of the released P (from reductive dissolution of Fe oxides as well as from organic matter mineralization) is expected to readsorb on the newly precipitated amorphous phases (Patrick and Khalid, 1974; Willett, 1989; Phillips, 1998; Zhang et al., 2003). Hence, if the site hydraulic system is of low enough energy (i.e., limited lateral or vertical flows), minimal off-site discharge may be expected.

The similarity between the AAO extraction conditions (i.e., low molecular organic acid and low pH) and plant and soil biota mechanisms for acquiring P in P-limited soils (excretion of low molecular organic acid and induced pH changes), (Miyasaka and Habte, 2001; Ryan et al., 2001) suggest the AAO-extractable P represents the available P in weathered and flooded soils, as indicated by the high correlation between the available P indices (i.e., M-1 extractable P) and  $P_{ox}$  on the fertilized plots in this study. This is further supported by previous work where AAO-extractable P was shown to correlate with plant uptake and plant available P indices in weathered and flooded soils (Shahandeh et al., 1994; Guo and Yost, 1999; Dobermann et al., 2002).

Lockaby et al. (1997) in summarizing previous research on silvicultural effects on ecological processes reported that organic P mineralization following harvesting decreased or increased in uplands and floodplains, respectively. The trend was attributed to less favorable conditions (e.g., moisture and temperature) for microbial activity on the upland sites. Phosphorus mineralization following harvesting in

floodplains was influenced by the disturbance induced by the harvesting equipment, with up to 20% P mineralization up to 56 weeks following harvest (Lockaby et al., 1997). Yet, substantial amounts of the surface soil's  $\text{Fe}^{3+}$  oxides (1 to 20 %, and sometimes up to 90 %) can be reduced under waterlogging conditions within one to three months (Breemen, 1988a). The extent to which the Fe oxides are redistributed to more reactive amorphous phases and the associated P is redistributed to a more available form will depend on the intensity of the reducing conditions and the initial Fe oxide mineralogical and physical characteristics (e.g., surface area). However, considering that most of the solid phase associated P is associated with mineral surfaces (Pierzynski et al., 1990), considerable amounts of the P adsorbed during the rotation is expected to be subject to the proposed P solid phase redistribution upon clearcutting-induced soil moisture changes. Moreover, this model may be used to explain the well-documented high growth response to P fertilization of pine forest stands on poorly drained sites compared to well-drained sites (Kushla and Fisher, 1980; Pritchett and Comerford, 1982; Jokela et al., 1988; Jokela, 2000; Borders and Bailey, 2001); that is, the continuous inundation conditions maintain high proportions of applied P in AAO extractable (available) form.

## Conclusions

By the end of a 30-yr rotation, seven mid-rotation P-fertilized forest soils in East Texas showed a marked increase in forest floor mass, P content in the forest floor and in P associated with Fe oxide-reducible phases in the upper 10 cm of the mineral soil. Soil P was highly correlated with Fe oxides in the soils included in the study. Phosphorus distribution to lower parts of the soil profile increased with site wetness. The proportion of P associated with amorphous phases was higher on the poorly drained sites than on the well-drained ones. Treatment effects on the amount of P associated with Fe oxides in the soil upper 10 cm was equal to or greater than that accumulated in the forest floor. The accumulation of P associated with Fe oxides in the soil upper 10 cm was higher on the well and excessively drained sites than on the poorly drained ones. This suggests that the Fe oxide-associated P accumulated in the mineral soil during the rotation can be

expected to become more available with increases in soil moisture regime upon clearcutting.

## SUMMARY

Mid-rotation P fertilization in seven loblolly pine (*Pinus taeda*) stands in East Texas resulted in marked influences on forest floor mass and P content in the forest floor and the mineral soils' upper 10 cm near the end of a 30-yr rotation, eight years after P application. Different trends in forest floor mass, and in Fe oxides and P distributions within the soil profiles and between operationally defined solid phases were found in sites of different drainage classes.

Soil  $P_T$  and  $P_d$  were highly correlated with  $Fe_d$  across sites, drainage classes, treatments, and depth intervals. Soil  $P_T$  and  $P_d$  content in the mineral soils were in the order: WD > ExWD > PD and their distribution from the surface horizons to lower parts of the profile were in the order: PD > WD > ExWD. Soil P distribution patterns in the soil profile differed among the different drainage classes, yet followed iron oxide distribution in all classes. Iron oxide's role as a sink for soil P was higher in the well-drained compared to the poorly drained sites. The amorphous phases of iron oxides (i.e.,  $Fe_{ox}/Fe_d$ ) were higher in the poorly drained soil and followed the  $P_d/Fe_d$  pattern in the soil profile, suggesting that the amorphous phase dominated the role of iron oxides as a P sink under the poor drainage conditions. Aluminum-containing phases were significantly correlated with soil P in the poorly drained soil but not in the well-drained one.

Fertilization resulted in significantly higher P content in the forest floor and in  $P_T$  and  $P_d$  in the soil upper 10 cm. The treatment effect on P in the forest floor, overall organic P in the forest floor and within the mineral soil upper 10 cm, and  $P_T$ ,  $P_d$  and  $P_{d-ox}$  in the upper 10 cm of the mineral soil were equivalent to 6, 14, 19, 11 and 6 % of the applied P (i.e. 100 kg P ha<sup>-1</sup>), respectively.  $P_{ox}$  was highly correlated with M-1 in the fertilized plot, supporting previous research in suggesting AAO-extractable P as an indicator for its availability in highly weathered soils.

The analytical performance of the molybdenum-blue colorimetric method for P determination in a continuous flow injection analyzer was assessed for water extracts containing oxalate and citrate (i.e. AAO and CD extraction solutions) using non-digested blanks and soil extracts at a wide range of dilution rates. Four and eight time dilutions of the citrate-dithionite and the acid ammonium-oxalate extracts, respectively, were needed to produce undisturbed peaks during the colorimetric reaction. High precision and recoveries were found for both extractions. The resulting P minimum detection limits were 6.9 and 1.1 mg P kg<sup>-1</sup> soil in the citrate-dithionite and the acid ammonium-oxalate extraction procedure, respectively.



## REFERENCES

- Agbenin, J.O. 2003. Extractable iron and aluminum effects on phosphate sorption in a savanna alfisol. *Soil Sci. Soc. Am. J.* 67:589-595.
- Ainsworth, C.C., and M.E. Summer. 1985. Effect of aluminum substitution in goethite on phosphorus adsorption: II. Rate of adsorption. *Soil Sci. Am. J.* 49:1149-1153.
- Albaugh, T.J., H.L. Allen, P.M. Dougherty, and K.H. Johnsen. 2004. Long term growth responses of loblolly pine to optimal nutrient and water resource availability. *Forest Ecol. Manag.* 192:3-19.
- Ballard, R. 1980. Phosphorus nutrition and fertilization of forest trees. p. 763-804. *In* F.E. Khasawneh et al. (ed.) *The role of phosphorus in agriculture*. ASA, CSSA SSSA, Madison, WI, USA.
- Barberis, E., F.A. Marsan, R. Scalenghe, A. Lammers, U. Schwertmann, A.C. Edwards, R. Maguire, M.J. Wilson, A. Delgado, and J. Torrent. 1996. European soils overfertilized with phosphorus: part 1 basic properties. *Fert. Res.* 45: 199-207.
- Barnes, B.V., D.R. Zak, S.R. Denton, and S.H. Spurr. 1998. *Forest ecology*. John Wiley and Sons Inc., New York, NY, USA.
- Beck, M.A., and P.A. Sanchez. 1996. Soil phosphorus movement and budget after 13 years of fertilized cultivation in the Amazon basin. *Plant Soil* 184:23-31.
- Beck, M.A., and H. Elsenbeer. 1999. Biogeochemical cycles of soil phosphorus in southern Alpine spodosols. *Geoderma* 91:249-260.
- Binkley, D. 1986. *Forest nutrition management*. John Wiley and Sons Inc., New York, NY, USA.
- Bliss, C.M., and N.B. Comerford. 2002. Forest harvesting influence on water table dynamics in a Florida flatwoods landscape. *Soil Sci. Soc. Am. J.* 66:1344-1349.
- Borders, B.E., and R.L. Bailey. 2001. Loblolly pine-pushing the limits of growth. *Southern J. Appl. For.* 25:69-74.
- Bowman, R. A., J. B. Rodriguez, and J.R. Self. 1998. Comparison of methods to estimate occluded and resistant soil phosphorus. *Soil Sci. Soc. Am. J.* 62:338-342.
- Breemen, N. Van. 1988a. Effects of seasonal redox processes involving iron on the chemistry of periodically reduced soils. p. 797-809. *In* J.W. Stucki et al. (ed.) *Iron in Soils and Clay Minerals*. NATO ASI Series, D. Reidel Pub. Comp. Dordrecht, The Netherlands.

- Breemen, N. Van. 1988b. Long-term chemical, mineralogical, and morphological effects of iron-redox processes in periodically flooded soils. p. 811-823. *In* J.W. Stucki et al. (ed.) *Iron in Soils and Clay Minerals*. NATO ASI Series, D. Reidel Pub. Comp. Dordrecht, The Netherlands.
- Brennan, E.W., and W.L. Lindsay. 1998. Reduction and oxidation effect on the solubility and transformation of iron oxides. *Soil Sci. Soc. Am. J.* 62:930-937.
- Brennan, R.F., M.D.A. Bolland, R.C. Jeffery, and D.G. Allen. 1994. Phosphorus adsorption by a range of Western Australian soils related to soil properties. *Commun. Soil Sci. Plan.* 25:2785-2795.
- Broberg, O., and K. Pettersson. 1988. Analytical determination of orthophosphate in water. *Hydrobiologia* 170:45-59.
- Burt, R., M.D. Mays, E.C. Benham, and M.A. Wilson. 2002. Phosphorus characterization and correlation with properties of selected benchmark soils of the United States. *Commun. Soil Sci. Plan.* 33:117-141.
- Butnor, J.R., K.H. Johnsen, R. Oren, and G.G. Katul. 2003. Reduction of forest floor respiration by fertilization on both carbon dioxide-enriched and reference 17-year-old loblolly pine stands. *Glob. Change Biol.* 9:849-861.
- Campbell, F.R., and R.L. Thomas. 1970. Automated method for determining and removing silica interference in determination of soluble phosphorus in lake and stream waters. *Environ. Sci. Technol.* 16:602-604.
- Carmean, W.H. 1975. Forest site quality evaluation in the United State. *Adv. Agron.* 27:175-269.
- Chang, S. C., and M. L. Jackson. 1957. Fractionation of soil phosphorus. *Soil Sci.* 84:133-144.
- Coile, T.S. 1952. Soil and the growth of forest. *Adv. Agron.* 6:330-399.
- Comerford, N. B., R. F. Fisher, and W. L. Pritchett. 1983. Advances in forest fertilization on the southeastern coastal plain. General Technical Report, Pacific Northwest Forest and Range Experiment Station, USDA Forest Service. 163: 370-378.
- Comerford, N.B., M. McLeod, and M. Skinner. 2002. Phosphorus form and availability in the pine rotation following fertilization. P fertilization influences P form and potential bioavailability to pine in the subsequent rotation. *Forest Ecol. Manag.* 169:203-211.
- Condon, L.M. 2004. Phosphorus-surplus and deficiency. p. 69-84. *In* P. Schjonning et al. (ed.) *Managing soil quality: challenges in modern agriculture*. CAB International Pub. Wallingford, UK
- Covell, R.R., and D.C. McClurkin. 1967. Site index of loblolly pine on Ruston soils in the southern coastal plain. *J. Forest.* 65:263-264.

- D'Angelo, E.M., M.V. Vandiviere, W.O. Thom, and F. Sikora. 2003. Estimating soil phosphorus requirements and limits from oxalate extract data. *J. Environ. Qual.* 32:1082-1088.
- Day, P.R. 1965. Particle fractionation and particle-size analysis. p. 545-577. *In* C.A. Blacket et al. (ed.) *Methods of soil analysis. Part 1 physical and mineralogical properties*. ASA Madison, WI, USA.
- Dick, W.A., and M.A. Tabatabai. 1977. Determination of orthophosphate in aqueous solutions containing liable organic and inorganic phosphorus components. *J. Environ. Qual.* 6:82-85.
- Ding, C.P., Z.G. Liu, and T.R. Yu. 1984. Oxidation-reduction regimes in some oxisols of tropical China. *Geoderma* 32:287-295.
- Dobermann, A., T. George, and N. Thevs. 2002. Phosphorus fertilizer effects on soil phosphorus pools in acid upland soils. *Soil Sci. Soc. Am. J.* 66:652-660.
- Drouillon, M., and R. Merckx. 2003. The role of citric acid as a phosphorus mobilization mechanism in highly P-fixing soils. *Gayana Bot.* 60:55-62.
- Drummond, A.F., C.V. Gilkes, and R.D. Hart. 2002. Amorphous alumino-silicate materials in a Brazilian hydromorphic lateritic soil. *Aust. J. Soil Res.* 40:465-481.
- Fisher, R.F., and D. Binkley. 2000. *Ecology and management of forest soils*. John Wiley and Sons Inc., New York, NY, USA.
- Fiske, C.H., and Y. Subbarow. 1925. The colorimetric determination of phosphorus. *J. Biol. Chem.* 66:375-400.
- Fox, R.L. 1980. Soil with variable charge: agronomic and fertility aspects. p. 195-224. *In* B.K.G. Theng (ed.) *Soils with variable charge*. New Zealand Society of Soil Science, Lower Hutt, NZ.
- Franklin, O., P. Hogberg, A. Ekblad, and G.I. Agren. 2003. Pine forest floor carbon accumulation in response to N and P K additions: bomb  $^{14}\text{C}$  modeling and respiration studies. *Ecosystems* 6:644-658.
- Furrer, G., and W. Stumm. 1986. The coordination chemistry of weathering: I. dissolution kinetics of  $\delta\text{-Al}_2\text{O}_3$  and BeO. *Geochim. Cosmochim. Acta* 50: 1847-1860.
- Geelhoed, J.S., W.H. Van Riemsdijk, and G.R. Findenegg. 1999. Simulation of the effect of citrate exudation from roots on the plant availability of phosphate adsorbed on goethite. *Eur. J. Soil Sci.* 50:379-390.
- Gentle, S.W., F.R. Humphreys, and M.J. Lambert. 1986. Continuing response of *Pinus radiata* to phosphatic fertilizers over two rotations. *Forest Sci.* 32:822-829.
- Gonzalez, E., M.C. Ballesteros, and E.H. Rueda. 2002. Reductive dissolution kinetics of Al-substituted goethites. *Clay Clay Miner.* 50:470-477.

- Graustein, W.C., K. Cromack Jr., and P. Sollins. 1977. Calcium oxalate: occurrence in soils and effect on nutrient and geochemical cycle. *Science* 198:1252-1254
- Gresham, C.A. 2002. Sustainability of intensive loblolly pine plantation management in the South Carolina coastal plain, USA. *Forest Ecol. Manag.* 155:69-80.
- Grierson, P.F., P. Smithson, G. Nziguheba, S. Radersma, and N.B. Commerford. 2004. Phosphorus dynamics and mobilization by plant. p. 127-142. *In* M. Van Noordwijk et al. (ed.) *Below-ground interactions in tropical agroecosystems: concepts and models with multiple plant components*. CAB International Pub. Wallingford, UK.
- Guo, F., and R.S. Yost. 1999. Quantifying the available soil phosphorus pool with the acid ammonium oxalate method. *Soil Sci. Soc. Am. J.* 63:651-656.
- Gurlevik, N., D.L. Kelting, and H.L. Allen. 2003. The effect of vegetation control and fertilization on net nutrient release from decomposing loblolly pine needles. *Can. J. Forest Res.* 33:2491-2502.
- Hinsinger, P. 2001. Bioavailability of soil inorganic P in the rhizosphere as affected by root-induced chemical changes: a review. *Plant Soil* 237:173-195.
- Jackson, M.L., 1958. *Soil chemical analysis*. Prentice-Hall Inc., Englewood Cliffs, NJ, USA.
- JMP, 2002. JMP statistical software, version 5.0.1.a., SAS Inst., Cary, NC, USA.
- Jokela, E.J., B. Harding, and J.L. Troth. 1988. Decision-making criteria for forest fertilization in the Southeast: an industrial perspective. *South. J. Appl. For.* 12:153-160.
- Jokela, E. J., and A.J. Long. 2000. Using soils to guide fertilizer recommendations for southern pines. Cir. 1230, School of Forest Resources and Conservation, University of Florida, Gainesville, FL, USA.
- Jokela, E.J., P.M. Dougherty, and T.A. Martin. 2004. Production dynamics of intensively managed loblolly pine stands in the southern United States: a synthesis of seven long-term experiments. *Forest Ecol. Manag.* 192:117-130.
- Juo, A.S.R. 1980. Mineralogical characteristics of Alfisols and Ultisols. p. 69-86. *In* B.K.G. Theng (ed.) *Soils with variable charge*. New Zealand Society of Soil Science, Lower Hutt, NZ.
- Khan, F.A., and T.E. Fenton. 1996. Secondary iron and manganese distributions and aqueous conditions in a mollisol catena of central Iowa. *Soil Sci. Soc. Am. J.* 60:546-551.
- Koopmans, G.F., W.J. Chardon, P.A.I. Ehlert, J. Dolfing, R.A.A. Suurs, O. Oenema, and W.H. Van Riemsdijk. 2004. Phosphorus availability for plant uptake in a phosphorus-enriched noncalcareous sandy soil. *J. Environ. Qual.* 33:965-975.

- Kuo, S. 1996. Phosphorus. p. 869-919. *In* D.L. Sparks et al. (ed.) *Methods in soil analysis. Part 3 chemical methods*. SSSA, Madison, WI, USA.
- Kushla, J.D., and R.F. Fisher. 1980. Predicting slash pine response to nitrogen and phosphorus fertilization. *Soil Sci. Soc. Am. J.* 44:1303-1306.
- Lindsay, W.L., P.L.G. Vlek, and S.H. Chien. 1989. Phosphate minerals. p. 1089-1130. *In* J.B. Dixon, and S.B. Weed (ed.) *Minerals in soil environments*. SSSA, Madison, WI, USA.
- Liu, Z.G., C.P. Ding, Y.X. Wu, S.Z. Pan, and K. Xu. 1997. Oxidation-reduction reactions. p. 442-472. *In* T.R. Yu (ed.) *Chemistry of variable charge soils*. Oxford Univ. Press, New York, NY, USA.
- Lockaby, B.G., J.A. Stanturf, and M.G. Messina. 1997. Effects of silvicultural activity on ecological processes in floodplain forests of the southern United States: a review of existing reports. *Forest Ecol. Manag.* 90:93-100.
- Loeppert, H. R., and W.P. Inskeep. 1996. Iron. p. 639-664. *In* D.L. Sparks et al. (ed.) *Methods in soil analysis. Part 3 chemical methods*. SSSA, Madison, WI, USA.
- Louw, J.H., and M. Scholes. 2002. Forest site classification and evaluation: a South African perspective. *Forest Ecol. Manag.* 171:153-168.
- Martin, J.P., and K. Haider. 1986. Influence of mineral colloids on turnover rates of soil organic carbon. p. 284-304. *In* P.M. Huang, and M. Schnitzer (ed.) *Interaction of soil minerals with natural organics and microbes*. SSSA, Special Pub. No. 17, SSSA, Madison WI, USA.
- McDaniel, P.A., and S.W. Buol. 1991. Manganese distributions in acid soils of the North Carolina Piedmont. *Soil Sci. Soc. Am. J.* 55:152-158.
- McDaniel, P.A., G.R. Bathke, S.W. Buol, D.K. Cassel, and A.L. Falen. 1992. Secondary manganese/iron ratios as pedochemical indicators of field-scale throughflow water movement. *Soil Sci. Soc. Am. J.* 56:1211-1217.
- McKee, W.H. Jr. 1970. Chemical properties of a forest soil affected by fertilization and submergence. *Soil Sci. Soc. Am. Proc.* 34:690-693.
- McKelvie, I.D., D.M.W. Peat, and P.J. Worsfold. 1995. Techniques for the quantification and speciation of phosphorus in natural waters. *Anal. Proc. Anal. Commun.* 32:437-445.
- Mehra, O.P., and M.L. Jackson. 1960. Iron oxide removal from soils and clays by a dithionite-citrate system buffered with sodium bicarbonate. *Clays Clay Miner.* 7:317-327.
- Mesquita, M.V.F., and J. Torrent. 1993. Phosphate sorption as related to mineralogy of a hydrosequence of soils from the Cerrado region (Brazil). *Geoderma* 58:107-123.
- Miller, A.J., E.A.G. Schuur, and O.A. Chadwick. 2001. Redox control of phosphorus pools in Hawaiian montane forest soils. *Geoderma* 102: 219-237.

- Miller, B.J. 1983. Ultisols. p.283-323. *In* L.P. Wilding et al. (ed.) Pedocenes and soil taxonomy, the soil order. Elsevier, Amsterdam, The Netherlands.
- Miller, W.P. L.W. Zelazny, and D.C. Martens. 1986. Dissolution of synthetic crystalline and noncrystalline iron oxides by organic acids. *Geoderma* 37:1-13.
- Miyasaka, S.C., and M. Habte. 2001. Plant mechanisms and mycorrhizal symbioses to increase phosphorus uptake efficiency. *Commun. Soil Sci. Plan.* 32:1101-1147.
- Murphy, J., and J.P. Riley. 1962. A modified single solution method for the determination of phosphorus in natural waters. *Anal. Chem. Acta* 27:31-36.
- Ngono, G., and R.F. Fisher. 2001. Predicting response of southeast Texas loblolly pine to fertilization. *South. J. Appl. For.* 25: 84-87.
- Nyland, R. D. 1996. *Silviculture, concepts and applications*. McGraw-Hill Inc., New York, NY, USA.
- Oades, J.M. 1989. An introduction to organic matter in mineral soils. p.89-160. *In* J.B. Dixon, and S.B. Weed (ed.) *Minerals in soil environments*. SSSA, Madison, WI, USA.
- Olsen, S. 1967. Recent trends in the determination of orthophosphate in water. p. 63-105. *In* H.L. Golterman, and R.S.N.V. Clymo (ed.) *Chemical environment in the aquatic habitat*. Noord-Hollandsche, Amsterdam, The Netherlands.
- Olsen, S.R., C.V. Cole, F.S. Watanabe, and L.A. Dean. 1954. Estimation of available phosphorus in soils by extraction with sodium bicarbonate. USDA Circular 939 Washington DC, USA.
- Olsen, S.R., and L.E. Sommers. 1982. Phosphorus. p. 403-430. *In* A.L. Page et al. (ed.) *Methods of soil analysis part 2 chemical and microbiological properties*. 2<sup>nd</sup> ed. ASA SSSA, Madison, WI, USA.
- Owens, L.B., D.W. Nelson, and L.E. Sommers. 1977. Determination of inorganic phosphorus in oxalate extracts of soils. *Soil Sci. Soc. Am. J.* 41:148-149.
- Parfitt, R.L., R.J. Atkinson, and R.C. Smart. 1975. The mechanism of phosphate fixation by iron oxides. *Soil Sci. Am. Proc.* 39:837-841.
- Parfitt, R.L. 1980. Chemical properties of variable charge soils. p. 167-194. *In* B.K.G. Theng (ed.) *Soils with variable charge*. New Zealand Society of Soil Science, Lower Hutt, NZ.
- Parfitt, R.L., and Childs, C.W. 1988. Estimation of forms of Fe and Al: a review, and analysis of contrasting soils by dissolution and moessbauer methods. *Aust. J. Soil Res.* 26:121-144.
- Parfitt, R.L. 1989. Phosphate reactions with natural allophone, ferrihydrite and goethite. *J. Soil Sci.* 40:359-369.

- Patrick, Jr. W.H., and R.A. Khalid. 1974. Phosphate release and sorption by soils and sediments: effect of aerobic and anaerobic conditions. *Science* 186:53-55.
- Pautler, M.C., and J.T. Sims. 2000. Relationships between soil test phosphorus, soluble phosphorus, and phosphorus saturation in Delaware soils. *Soil Sci. Soc. Am. J.* 64:765-773.
- Phillips, I.R. 1998. Phosphorus availability and sorption under alternating waterlogged and drying conditions. *Commun. Soil Sci. Plan.* 29:3045-3059.
- Pierzynski, G.M., T.J. Logan, S.J. Traina, and J.M. Bigham. 1990. Phosphorus chemistry and mineralogy in excessively fertilized soils: descriptions of phosphorus-rich particles. *Soil Sci. Soc. Am. J.* 54:1583-1589.
- Polglase, P.J., N.B. Comerford, and E.J. Jokela. 1992. Mineralization of nitrogen and phosphorus from soil organic matter in southern pine plantations. *Soil Sci. Soc. Am. J.* 56:921-927.
- Ponnamperuma, F.N. 1972. The chemistry of submerged soils. *Adv. Agron.* 24:29-96.
- Pothier, D., M. Prevost, and I. Auger. 2003. Using the shelterwood method to mitigate water table rise after forest harvesting. *Forest Ecol. Manag.* 179:573-583.
- Pritchett, W.L. 1979. Properties and management of forest soils. John Wiley and Sons Inc., New York, NY, USA.
- Pritchett, W.L., and N.B. Comerford. 1982. Long term response to phosphorus fertilization on selected southeastern coastal plain soils. *Soil Sci. Soc. Am. J.* 46:640-644.
- Ralston, C.W. 1964. Evaluation of forest site productivity. *Int. Rev. For. Res.* 1:172-201
- Riekerk, H. 1989. Influence of silvicultural practices on the hydrology of pine flatwoods in Florida. *Water Resour. Res.* 25:713-719.
- Rodriguez, J.B., J.R. Self, and P.N. Soltanpour. 1994. Optimal conditions for phosphorus analysis by the ascorbic acid-molybdenum blue method. *Soil Sci. Soc. Am. J.* 58:866-870.
- Ruiz, J.M., A. Delgado, and J. Torrent. 1997. Iron-related phosphorus in overfertilized European soils. *J. Environ. Qual.* 26:1548-1554.
- Ryan, P.R., E. Delhaize, and D.L. Jones. 2001. Function and mechanisms of organic anion exudation from plant roots. *Annu. Rev. Plant Phys.* 52:527-60.
- Sah, R.N., D.S. Mikkelsen, and A.A. Hafez. 1989. Phosphorus behavior in flooded-drained soils. II iron transformation and phosphorus sorption. *Soil Sci. Soc. Am. J.* 53:1723-1729.
- Sanchez-Rodriguez, F., R. Rodriguez-Soalleiro, R., E. Espanol, C.A. Lopez, and A. Merino. 2002. Influence of edaphic factors and tree nutritive status on the

- productivity of *Pinus radiata* D. Don plantations in northwestern Spain. *Forest Ecol. Manag.* 171:181-189.
- Sanyal, S.K., and S.K. De Datta. 1991. Chemistry of phosphorus transformations in soil. *Adv. Soil Sci.* 16:1-120.
- SAS Institute. 2002. Statistical analysis systems, version 9.0. SAS Inst., Cary, NC, USA.
- Saxton, K.E., W.J. Rawls, J.S. Romberger, and R.I. Papendick. 1986. Estimating generalized soil-water characteristics from texture. *Soil Sci. Soc. Am. J.* 50:1031-1036.
- Sayer, M.A.S., J.C.G. Goelz, J.L. Chambers, Z. Tang, T.J. Dean, J.D. Haywood, and D.J. Leduc. 2004. Long-term trends in loblolly pine productivity and stand characteristics in response to thinning and fertilization in the West Gulf region. *Forest Ecol. Manag.* 192:71-96.
- Schonau, A.P.G. 1988. Problems in using vegetation or soil classification in determining forest site quality. p. 3-11. In D.W. Cole and S. P. Gessel (ed.) *Forest site evaluation and long-term productivity*. University of Washington Press, Seattle, WA, USA.
- Schultz, R.P. 1997. Loblolly pine: the ecology and culture of loblolly pine (*Pinus taeda* L.) USDA Forest Service, Washington DC, USA.
- Schwertmann, U. 1973. Use of oxalate for Fe extraction from soils. *Can. J. Soil Sci.* 53:244-246.
- Schwertmann, U., and D.S. Fanning. 1976. Iron-manganese concertion in hydrosequences of soils in loess in Bavaria. *Soil Sci. Soc. Am. J.* 40:731-738.
- Schwertmann, U. 1988. Occurrence and formation of iron oxides in various pedoenvironments. p. 267-308. In J.W. Stucki et al. (ed.) *Iron in soils and clay minerals*. NATO ASI Series, D. Reidel Pub. Comp. Dordrecht, The Netherlands.
- Schwertmann, U., and R.M. Taylor. 1989. Iron oxides. p. 379-438. In J.B. Dixon, and S.B. Weed (ed.) *Minerals in soil environments*. SSSA, Madison WI, USA.
- Senwo, Z.N., R.W. Taylor, and K.R. Sistani. 2003. Phosphorus distribution in five highly weathered Alabama soils. *Commun. Soil Sci. Plan.* 34:97-109.
- Shahandeh, H., L.R. Hossner, and F.T. Turner. 1994. Phosphorus relationships in flooded rice soils with low extractable phosphorus. *Soil Sci. Soc. Am. J.* 58:1184-1189.
- Sharpley, A.N., H. Tiessen, and C.V. Cole. 1987. Soil phosphorus forms extracted by soil tests as a function of pedogenesis. *Soil Sci. Soc. Am. J.* 51: 362-365.
- Sharpley, A.N., J.L. Weld, D.B. Beegle, P.J.A. Kleinman, W.J. Gburek, P.A. Moore Jr., and G. Mullins. 2003. Development of phosphorus indices for nutrient management planning strategies in the United States. *J. Soil Water Conserv.* 58:137-152.



- SigmaStat, 1997. SigmaStat statistical software, version 2.03. SPSS Inc. Chicago, IL USA.
- Simonson, R.W. 1970. Loss of nutrient elements during soil formation. p. 21-46. *In* O.P. Engelstad (ed.) Nutrient Mobility in Soil: accumulation and losses. SSSA, Special Pub. No. 4, Madison, WI, USA.
- Sims, J.T., R.O. Maguire, A.B. Leytem, K.L. Gartley, and M.C. Pautler. 2002. Evaluation of Mehlich 3 as an agri-environmental soil phosphorus test for the Mid-Atlantic United States of America. *Soil Sci. Soc. Am. J.* 66:2016-2032.
- Standard Methods. 1995a. Method 4500-P. APHA 19th ed. Washington DC, USA.
- Standard Methods. 1995b. Method 4500-Si-D. APHA 19th ed. Washington DC, USA.
- Stevenson, F.J. 1994. Humus chemistry: genesis, composition, reactions. John Wiley and Sons Inc., New York, NY, USA.
- Stone, E.L., and P. J. Kalisz. 1991. On the maximum extent of tree roots. *Forest Ecol. Manag.* 46:59-102.
- Stumm, W., and J.J. Morgan. 1996. Aquatic chemistry. John Wiley and Sons, Inc., New York, NY, USA.
- Sun, G., S.G. McNulty, J.P. Shepard, D.M. Amatya, H. Riekerk, N.B. Comerford, W. Skaggs, and L. Swift, Jr. 2001. Effects of timber management on the hydrology of wetland forests in the southern United States. *Forest Ecol. Manag.* 143:227-236.
- Thomas, G.W. 1982. Exchangeable cations. p.159-165. *In* A.L. Page et al. (ed.) Methods of soil analysis, part 2 chemical and microbiological properties. 2<sup>nd</sup> ed., ASA-SSSA, Madison, WI, USA.
- Torrent, J. 1997. Interactions between phosphate and iron oxide. *Adv. GeoEcol.* 30:321-344.
- Towns, T. 1986. Determination of aqueous phosphate by ascorbic acid reduction of phosphomolybdic acid. *Anal. Chem.* 58:223-229.
- Turner, J., M.J. Lambert, and F.R. Humphreys. 2002. Continuing growth response to phosphate fertilizers by a *Pinus radiata* plantation over fifty years. *Forest Sci.* 48:556-568.
- USDA Soil Conservation Service. 1983. Soil taxonomy. Robert E. Krieger Pub. Co., Malabar, FL, USA.
- Walbridge, M.R., C.J. Richardson, and W.T. Swank. 1991. Vertical distribution of biological and geochemical phosphorus subcycles in two southern Appalachian forest soils. *Biogeochemistry* 13:61-81.
- Walker, L. C., and B. P. Oswald. 2000. The Southern Forest. CRC Press, Boca Raton, FL, USA.

- Walker, T.W., and J.K. Syers. 1976. The fate of phosphorus during pedogenesis. *Geoderma* 15:1-19.
- Wells, C., and L. Allen. 1985. A loblolly pine management guide, when and where to apply fertilizer. General Tech. Rep. SE-36, USDAFS, Southeastern For. Exp. St., Asheville, NC, USA.
- Wells, C.G., D.M. Crutchfield, N.M. Berenyi, and C.B. Davey. 1973. Soil and foliar guidelines for phosphorus fertilization of loblolly pine. Res. Paper SE-110, USDAFS, Southeastern For. Exp. St., Asheville, NC, USA.
- Wienand, K.T., and W.D. Stock. 1995. Long-term phosphorus fertilization effects on the litter dynamics of an age sequence of *Pinus elliottii* plantations in the southern cape of South Africa. *Forest Ecol. Manag.* 75:135-146.
- Willett, I.R. 1989. Causes and prediction of changes in extractable phosphorus during flooding. *Aust. J. Soil Res.* 27:45-54.
- Williams, J.D.H., J.K. Syers, and T.W. Walker. 1967. Fractionation of soil inorganic phosphate by a modification of Chang and Jackson's procedure. *Soil Sci. Soc. Am. Proc.* 31:736-739.
- Wolf, A.M., and D.E. Baker. 1990. Colorimetric method for phosphorus measurement in ammonium oxalate soil extract. *Commun. Soil Sci. Plan.* 21:2257-2263.
- Wood, T., F.H. Bormann, and G.K. Voigt. 1984. Phosphorus cycling in a northern hardwood forest: biological and chemical control. *Science* 223:391-393.
- Xu, Y.J., J.A. Burger, W.M. Aust, S.C. Patterson, M. Miwa, D.P. Preston. 2002. Changes in surface water table depth and soil physical properties after harvest and establishment of loblolly pine (*Pinus taeda* L.) in Atlantic coastal plain wetlands of South Carolina. *Soil Till. Res.* 63:109-121.
- Yuan, G., and L.M. Lavkulich. 1995. Colorimetric determination of phosphorus in citrate-bicarbonate-dithionite extracts of soils. *Commun. Soil Sci. Plan.* 26:1979-1988.
- Zhang, Y., X. Lin, and W. Werner. 2003. The effect of soil flooding on the transformation of Fe oxides and the adsorption/desorption behavior of phosphate. *J. Plant Nutr. Soil Sci.* 166:68-75.
- Zheng, Z., R.R. Simard, J. Lafond, and L.E. Parent. 2002. Pathways of soil phosphorus transformations after 8 years of cultivation under contrasting cropping practices. *Soil Sci. Soc. Am. J.* 66:999-1007.
- Zimmermann, C.F., and C.W. Keefe. 1997. Method 365.5 Determination of orthophosphate in estuarine and coastal waters by automated colorimetric analysis. National Exposure Research Laboratory Office of Research and Development U.S. Environmental Protection Agency Cincinnati, OH, USA.

Zinder, B., G. Furrer, and W. Stumm. 1986. The coordination chemistry of weathering:  
II. dissolution of Fe(III) oxides. *Geochim. Cosmochim. Acta* 50:1861-1869.

## VITA

Name: Amir Hass

Address: Forest Science Department, Texas A&M University College  
Station, TX 77843-2135.

Email Address: amirhass@neo.tamu.edu

Education: B.S. 1996, Soil Science, The Hebrew University of Jerusalem,  
Rehovot 76100 Israel  
M.S. 2003, Soil Science, The Hebrew University of Jerusalem,  
Rehovot 76100 Israel